

N64-23148

CODE-1

Cat. 26



**AN ANALYTICAL STUDY OF THE PROPAGATION OF PRESSURE
WAVES IN LIQUID HYDROGEN-VAPOR MIXTURES**

by

J. M. Clinch and H. B. Karplus

prepared for

NATIONAL AERONAUTICS AND SPACE ADMINISTRATION

CONTRACT NAS 3-2569

OTS PRICE

XEROX

MICROFILM

\$

11.50 ph

\$

none

IIT RESEARCH INSTITUTE

FINAL REPORT

AN ANALYTICAL STUDY OF THE PROPAGATION OF PRESSURE
WAVES IN LIQUID HYDROGEN-VAPOR MIXTURES

by

J. M. Clinch and H. B. Karplus

prepared for

NATIONAL AERONAUTICS AND SPACE ADMINISTRATION

May 1964

CONTRACT NAS 3-2569

Technical Management
NASA Lewis Research Center
Advanced Development and Evaluation Division
James J. Watt

IIT RESEARCH INSTITUTE
Chicago 16, Illinois

FOREWORD

"An Analytical Study of the Propagation of Pressure Waves in Liquid Hydrogen-Vapor Mixtures" was undertaken for NASA Lewis Research Center, Contract No. NAS 3-2569 by the IIT Research Institute, Project No. N6054 (originally A6054). Appendices A and B were written by Hugo Nielsen. Appendix H was written by Graham J. Walker. Verner J. Raelson contributed to the analysis of pressure pulses. Numerical computations were performed by Gale Hruska.

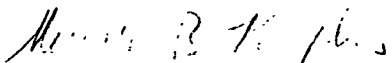
Computations are recorded in Notebooks C13821, C13822, C13828, C13846, C14132, and C14162.

Respectfully submitted,

IIT RESEARCH INSTITUTE

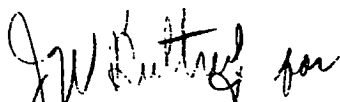


J. Michael Clinch
Research Physicist

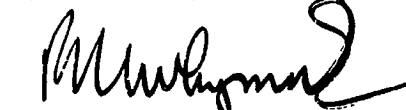


Henry B. Karplus
Research Physicist

APPROVED BY:



William C. Sperry, Manager
Acoustics Research



R. R. Whymark
Associate Director
Fluid Dynamics Research

AN ANALYTICAL STUDY OF THE PROPAGATION OF PRESSURE WAVES IN LIQUID HYDROGEN-VAPOR MIXTURES

by

J. M. Clinch and H. B. Karplus

ABSTRACT

23,48

The complex sound propagation constant is calculated for liquid-vapor mixtures. Sound velocity and attenuation, related to the real and imaginary components of this constant, are physically measurable quantities, governed by the state and structure of the mixture. Low frequency behavior is shown to be a function of the mixture quality or relative masses of the phases. At intermediate frequencies the propagation depends on the sound frequency and also on the size distribution of the discontinuous phase. At high frequency the propagation is essentially a function of the dominant phase. Early hopes of utilizing low frequencies to determine the quality in two-phase flow directly are circumscribed by effects such as noise, pipe wall heat transfer, standing waves, etc., which set limits to the lowest frequency which may be used. At intermediate frequencies the effects of size distribution and quality are difficult to separate. The high frequency velocity is likely to be useful in determining the flow velocity of one of the phases so that other parameters of interest in two-phase flow may be deduced.

authr

TABLE OF CONTENTS

<u>Section</u>		<u>Page</u>
I	INTRODUCTION	1
II	PROPAGATION OF PRESSURE FLUCTUATIONS IN A FLUID	3
III	RELAXATION	21
IV-A	VISCOSITY EFFECTS AT THE INTERFACE BETWEEN THE PHASES	36
IV-B	COMBINED EFFECTS OF HEAT CONDUCTION AND VISCOSITY ON SOUND PROPAGATION	46
IV-C	PRESSURE PULSE PROPAGATION IN THE TWO-PHASE HYDROGEN MIXTURE	60
V	SUMMARY	68
VI	CONCLUSION	71
	LIST OF REFERENCES	72

Appendices

A	TEMPERATURE AND DENSITY FLUCTUATIONS ASSOCIATED WITH SOUND WAVES IN TWO-PHASE FLUIDS	A-1
B	APPROXIMATE RELAXATION TIMES FOR LIQUID DROPS SURROUNDED BY VAPOR	B-1
C	DERIVATION OF THE WAVE EQUATION TAKING INTO ACCOUNT DRAG BETWEEN THE LIQUID AND VAPOR PHASES	C-1
D	COMPARISON OF PRESENT FORMULA FOR ATTENUATION DUE TO VISCOUS DRAG WITH THAT OF EPSTEIN AND CARHART	D-1
E	EVALUATION OF THE CRITICAL QUALITY FOR A TWO-PHASE FLUID	E-1

TABLE OF CONTENTS (Continued)

<u>Appendices</u>	<u>Page</u>
F EFFECT OF TUBE DIAMETER ON SOUND PROPAGATION CONSTANTS	F-1
G DERIVATION OF THE FORMULA USED TO CALCULATE THE HIGH FREQUENCY SOUND VELOCITY	G-1
H LITERATURE ON BOILING HEAT TRANSFER AND TWO-PHASE FLOW	H-1

LIST OF SYMBOLS

a_j	Fourier coefficient of j th component
A	cross-sectional area of tube = πr_T^2
c	sound velocity
c_0	sound velocity at very low frequencies
c_∞	sound velocity at very high frequencies
C_p	specific heat at constant pressure
C_v	specific heat at constant volume
E	internal energy per unit mass
f	sound frequency
H	enthalpy per unit mass
i	$\sqrt{-1}$
$I_{\eta E}$	viscosity frequency function defined by equation D.4
I_{nR_f}	heat conduction frequency function defined by equation 4.12
j	integer
J	mechanical equivalent of heat
k	thermal conductivity

LIST OF SYMBOLS (Continued)

l	pulse width
n	heat conduction frequency parameter $= \sqrt{\omega/2a_g}$
N	number of particles per unit volume
p	pressure
q	quality
q_c	critical quality (no phase change)
r	radial distance
r_T	tube radius
R	universal gas constant
R_g	radius of vapor shell
R_f	droplet radius
R_0	real part
s	condensation
S	entropy
t	time
T	absolute temperature

LIST OF SYMBOLS (Continued)

T_s	saturation temperature
ΔT	difference between actual temperature and that due to adiabatic pressure change
u	velocity
U	instantaneous velocity amplitude of sound wave
V	specific volume per unit mass = $1/\rho$
X	drag force on droplet defined by equation 4.1

GREEK SYMBOLS

α	amplitude attenuation coefficient
α_f	thermal diffusivity of liquid = $k_f/\rho_f C_{pf}$
α_g	thermal diffusivity of vapor = $k_g/\rho_g C_{pg}$
β	viscosity frequency parameter = $\sqrt{\omega/2\nu_g}$
γ	ratio of the principal specific heats = C_p/C_v
ϵ	angular phase difference between droplets and vapor
θ	viscous force coefficient = $\frac{9}{4} \frac{\rho_g}{\rho_f} \frac{1}{\beta R_f} \left(1 + \frac{1}{\beta R_f} \right)$ defined by equation 4.6
λ	sound wavelength

LIST OF SYMBOLS (Continued)

Λ	frequency parameter = $\sqrt{\omega/2a_f} R_f$
μ_g	absolute vapor viscosity
μ_H	absorption per wavelength due to heat conduction
μ_V	absorption per wavelength due to viscosity
ν_g	kinematic vapor viscosity
ρ	density
τ	time constant
τ_p	pulse repetition period
Φ	inertial force coefficient = $\frac{\rho_g}{\rho_f} \left(\frac{1}{2} + \frac{9}{4\beta R_f} \right)$ defined by equation 4.5
ω	angular sound frequency
Ω	complex frequency parameter = $\sqrt{i\omega/a_g}$

SUBSCRIPTS

f	liquid
g	vapor or gas
fg	difference between liquid and vapor, i.e. $V_{fg} = V_g - V_f $
eff	effective value of physical property
o	initial or zero conditions

LIST OF SYMBOLS (Continued)

S constant entropy conditons

∞ infinite conditions

μ micron ($1\mu = 10^{-4}$ cm)

I. INTRODUCTION

The flow of two-phase fluids has in the past been the subject of numerous investigations. Much of this work has been concerned with establishing the laws which govern the behavior of two-phase fluids under varying flow conditions. Among the flow properties of two-phase fluids to be measured, a knowledge of the relative masses of the phases or quality is of prime importance.

In principle the quality could be determined by measuring some fluid property which depends on it. One such fluid property which depends on the quality is the velocity of sound in the two-phase fluid. Under certain simplifying assumptions the velocity of sound in a two-phase fluid is related directly to the quality. These assumptions require that thermodynamic equilibrium exists between the phases during sound propagation. When equilibrium prevails the velocity of sound as a function of quality may be calculated from the known thermodynamic properties of the constituent phases. The equilibrium condition is reached only at very low sound frequencies.

It is shown in Section IV that there is a range of frequencies over which the sound velocity depends not only upon the quality but also upon the manner in which the phases are distributed in the mixture and also the frequency of the sound. Above this frequency range, the sound velocity becomes independent of the quality and assumes the value appropriate to that of the predominant phase. Thus to be able to predict the quality from measurements of the sound velocity some knowledge of the phase distribution is required. It is the object of this investigation to study analytically the feasibility of using acoustical techniques to measure the quality of two-phase fluid

flow. Whilst the particular requirement of the investigation was to consider the propagation of pressure waves, both continuous and shock waves, in a mixture of boiling liquid hydrogen and its saturated vapor, the approach is quite general and is applicable to any two-phase fluid.

The following analysis of pressure wave propagation in two-phase hydrogen has been restricted to a homogeneous mixture of vapor and liquid; the liquid being dispersed uniformly throughout the vapor phase in the form of very small droplets as for example in atmospheric fog. This working model of the two-phase fluid was chosen for two reasons; firstly, because there is some evidence that the fog flow regime will predominate over a wide range of flow conditions, and secondly, because the underlying physical processes which occur between the phases during wave propagation can be more readily understood.

II. PROPAGATION OF PRESSURE FLUCTUATIONS IN A FLUID

A. Definition

The concept of sound implies the propagation of a pressure disturbance of small amplitude which undergoes no significant change in form during propagation.

It is often convenient to represent pressure disturbances in the form of a Fourier series containing a large number of individual components. Thus a pressure disturbance in the fluid is given by:

$$p = p(x, t) \quad (2.1)$$

where $p(x, t)$ is the pressure associated with the disturbance at any point x and time t may be transformed to

$$p = \sum_j p_j \exp i\omega_j (t - x/c_j) \quad (2.2)$$

The propagation constant, c , may in general be complex.

This would imply wave attenuation

$$c^{-1} = c_r^{-1} (1 + i\mu') \quad (2.3)$$

In this case one component of the Fourier series or the propagation of a single progressive sinusoidal wave would be

$$p = p_0 \exp(-\alpha x) \exp i\omega(t - x/c_r) \quad (2.4)$$

where $\alpha = 2\pi\mu'/\lambda = \mu/\lambda$ and $\lambda = 2\pi c_r/\omega = c_r/f$, and c_r is the sound velocity

By solving the equations of fluid dynamics for the conservation of mass and momentum for an element of fluid which undergoes changes in pressure and density with time the pressure wave equation may be derived. This wave equation yields a value for the constant c which is defined by:

$$\frac{\partial^2 p}{\partial t^2} = c^2 \frac{\partial^2 p}{\partial x^2} \quad (2.5)$$

where

$$c = \sqrt{\frac{dp}{d\rho}} \quad (2.6)$$

The rate of change of pressure with density may be related to the thermodynamic properties of the fluid and the complex parameter, c , may be found from the measurable properties c_r and α as given by equation (2.4). Conversely, it is possible in principle to measure the sound velocity and attenuation and derive such properties as density and quality (if a two-phase fluid) upon which the measured values depend.

The complexity of the problem is related to the manner in which the rate of change of pressure with density depends on the speed with which the pressure changes take place. In other words, the sound velocity, c_r , and the attenuation per wavelength, μ , are frequency dependent. In a

two-phase fluid mixture this time or frequency dependence is a function of how the phases are distributed both in size and space. To provide a better understanding of the physical principles involved in pressure wave propagation consider the following problem: A fluid contained in a cylinder fitted at one end with a piston is compressed when the piston moves inward. The density increases and heat is generated. For a long cylinder a sudden motion of the piston would compress only the fluid in contact with it. The resulting pressure increase then compresses the adjacent element of fluid and a pressure disturbance is propagated. The speed of the propagation as defined by equation 2.6 is the ratio of the applied force to the fluid inertia.

Next the heat generated by compression affects the stiffness of the medium, that is the pressure required for a given change in density. In gases the heat generated is quite large since gases have a large coefficient of thermal expansion. In liquids and solids the effect is usually small. In a liquid-vapor mixture, however, the heat generated in the vapor is also transferred to the liquid. When the liquid and vapor are composed of the same chemical substance, the problem is complicated by the change of phase which can take place. In this case, liquid can evaporate and the vapor can condense producing large changes in density with very small changes in pressure. If the pressure fluctuations are slow enough then the mixture will at each instant be in equilibrium and the constant c in equation 2.2 becomes a real number with zero wave attenuation. However, when the pressure fluctuations occur more rapidly the heat of compression liberated in the vapor cannot be conducted to the liquid before the rarefaction part of the acoustic cycle appears. In the limit at very high frequencies the pressure fluctuations may be

too fast to permit both heat transfer and phase change to take place. Because of this it is necessary to distinguish between the different vapor and liquid flow regimes as well as different frequency regions.

B. Small Amplitude Pressure Waves - Low Frequency Approximation

The propagation of slowly varying (low frequency) pressure waves in an infinite medium consisting of a mixture of liquid and gas uniformly dispersed within each other is considered. The assumption is implicitly made that all changes of phase and temperature occurring at the interface between the two phases takes place rapidly compared with the rate at which the pressure is changing. It is further assumed that, as is the case for a single phased fluid, the increased wavelength or reduced frequency accounts for the isolation of the compressed and rarefied regions of the wave. Because of this it is permissible to neglect heat exchange between regions of compression and rarefaction. In other words, the process is adiabatic. Furthermore, as there is no loss of acoustic energy it is also reversible and adiabatic. The rate of change of pressure with density, therefore, takes place isentropically and $(\partial p / \partial \rho)_s$ at constant entropy will be required to calculate the sound velocity c defined by equation 2.6.

Calculations have previously been carried out by many authors (Refs. 1 and 2) for the equilibrium sound velocity in two-phase mixtures. Karplus (Ref. 1), for example, shows that the equilibrium sound velocity c is in general given by:

$$c^2 = (qV_{fg} + V_f)^2 \left[q \left(\frac{V_{fg}}{S_{fg}} \frac{dS_{fg}}{dp} - \frac{dV_{fg}}{dp} \right) + \frac{V_{fg}}{S_{fg}} \frac{dS_f}{dp} - \frac{dV_f}{dp} \right]^{-1} \quad (2.7)$$

The quantities V_{fg} , S_{fg} , V_f , and S_f are defined in the list of symbols. The actual values of these quantities as a function of pressure for both the saturated liquid and vapor were obtained from published thermodynamic data (Ref. 3) for 20.4°K equilibrium hydrogen. The slopes dV/dp and dS/dp were obtained by interpolation of thermodynamic data on the saturation line. The results of the calculations for the equilibrium low frequency sound velocity c , as a function of pressure and quality are shown graphically in Figs. II-1 and II-2. It is seen that the sound velocity c , is a marked function of quality q but is relatively independent of the ambient pressure.

At low values of the quality, the sound velocity increases monotonically with pressure. Above quality of 0.3, however, there appears to be a maximum which lies in the vicinity of 60 psi for qualities approaching unity. Also of interest is the product ρc , plotted in Fig. II-2. This quantity is equal to the mass flow per unit area of a fluid flowing through a pipe with a sonic velocity. Since this study was initiated values of ρc as a function of pressure and quality have been reported by Smith (Ref. 4) and also by Harry (Ref. 5). It is found that there is agreement between these and the present results within about 2%. Differences are attributed to the method of estimating the slopes of the entropy-pressure and specific volume-pressure curves.

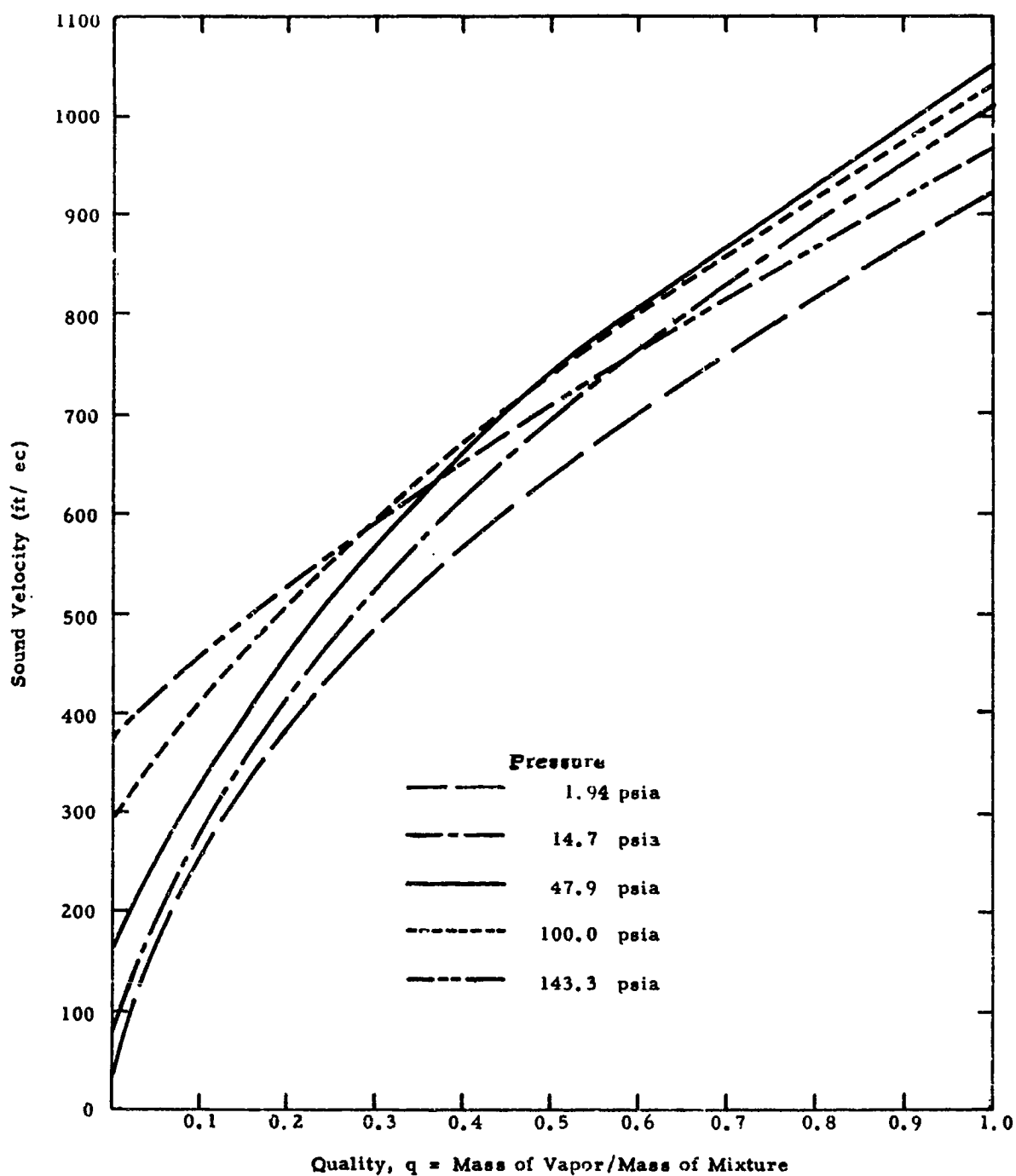


Fig. II-1 LOW FREQUENCY SOUND VELOCITY IN 20.4°K EQUILIBRIUM HYDROGEN PLOTTED AGAINST THE QUALITY FOR SEVERAL PRESSURES

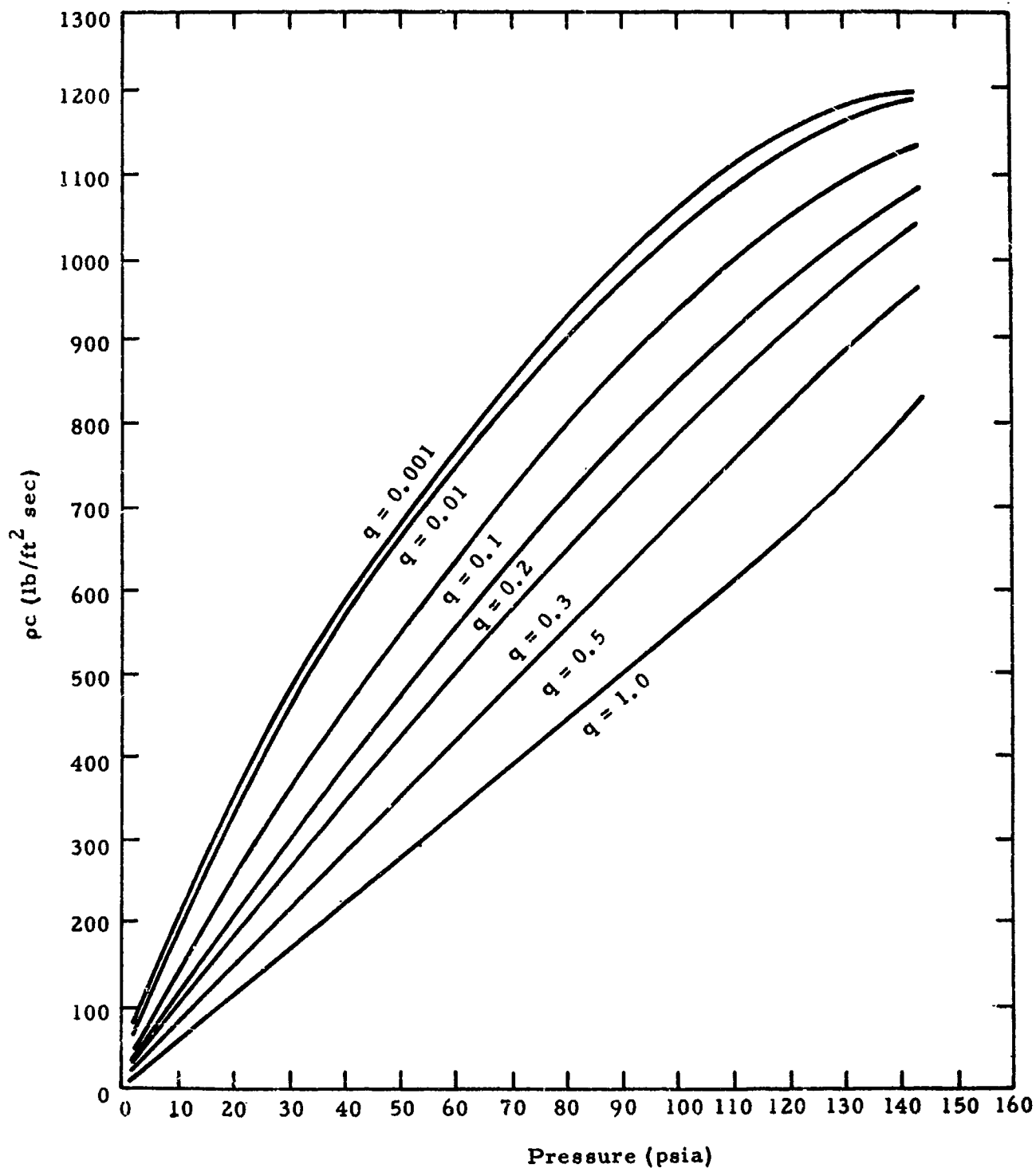


Fig. II-2 PLOT OF THE PRODUCT ρ_c AGAINST PRESSURE FOR VARIOUS QUALITIES IN THE HYDROGEN MIXTURE

C. Large Amplitude Pressure Waves--Shock Wave Approximation

The small amplitude approximation used up to this point implies very small changes in the state of the medium (pressure, density, temperature, etc.), and no change in its properties as, for example, the sound velocity. Changes in properties must be taken into account for large amplitude pressure disturbances.

In this section the propagation of a single large amplitude pressure step in a two-phase mixture is considered. The analysis utilizes the conventional Rankine-Hugoniot relations (Ref. 6) for shock waves even though it is well known that true shocks will degenerate into slowly rising steps in a two-phase fluid. The derivation of the Rankine-Hugoniot equations does not make any assumption concerning the rate of rise of the pressure but merely assumes continuity of mass and the proportionality of the acceleration to the applied pressure difference.

The change in the rate of rise of the pressure makes the definition of the propagation velocity of the wave front uncertain in that its separate components propagate at different velocities. The propagation velocity of the step will be an average velocity across a wave front whose profile is continually changing. However, the particle velocity and the state (density, temperature, enthalpy, etc.) of the two-phase mixture behind the step can be accurately predicted.

The Rankine-Hugoniot equations relate the enthalpy H , internal energy E , pressure p , velocity u , and specific volume V , in the two regions in front of and behind the step. It is convenient to choose a coordinate system fixed with respect to the step so that the velocity u_1 represents the relative velocity of the step with respect to the ambient medium and u_2 the relative

particle velocity of the medium behind the step. The particle velocity behind the step with respect to a coordinate fixed in the ambient medium is designated as $u_3 = u_2 - u_1$.

The Rankine-Hugoniot relations may be stated analytically as

$$H_2 - H_1 = (p_2 - p_1)(V_1 + V_2)/2 \quad (2.8a)$$

$$E_2 - E_1 = (p_2 + p_1)(V_1 - V_2)/2 \quad (2.8b)$$

$$u_1^2 = V_1^2 (p_2 - p_1)/(V_1 - V_2) \quad (2.9)$$

$$u_3^2 = (p_2 - p_1)(V_1 - V_2) \quad (2.10)$$

Suppose we consider a two-phase mixture of pressure, p_1 , and density, $1/V_1$, in which a pressure step, $p_2 - p_1$, is propagated. The specific volume behind the "shock" can be found since V_2 and H_2 are not independent variables but are given by

$$\underline{V}_2 = q_2 V_{2fg} + V_{2f} \quad \text{and} \quad \underline{H}_2 = q_2 H_{2fg} + H_{2f}$$

Now V_{2fg} , V_{2f} , H_{2fg} , H_{2f} are all fixed at the given pressure p_2 so that rearrangement of equation 2.8a gives

$$\underline{V}_2 = \frac{\underline{V}_1 (p_2 - p_1)/2J + H_{2fg} V_{2f}/V_{2fg} + \underline{H}_1 - H_{2f}}{- (p_2 - p_1)/2J + H_{2fg}/V_{2fg}} \quad (2.11a)$$

$$\underline{V}_2 = \frac{\underline{V}_1 (p_2 + p_1)/2J + E_{2fg} V_{2f}/V_{2fg} + \underline{E}_1 - E_{2f}}{(p_2 + p_1)/2J + E_{2fg}/V_{2fg}} \quad (2.11b)$$

and

$$q_2 = \frac{(\underline{V}_1 + V_{2f}) (p_2 - p_1)/2J + \underline{H}_1 - H_{2f}}{-V_{2fg} (p_2 - p_1)/2J + H_{2fg}} \quad (2.12a)$$

$$q_2 = \frac{(\underline{V}_1 - V_{2f}) (p_2 + p_1)/2J + \underline{E}_1 - E_{2f}}{+V_{2fg} (p_2 + p_1)/2J + E_{2fg}} \quad (2.12b)$$

Substituting in equation 2.9 gives

$$u_1^2 = \frac{\underline{V}_1^2 (H_{2fg} - V_{2fg} (p_2 - p_1)/2J) (p_2 - p_1)}{\underline{V}_1 (H_{2fg} - V_{2fg} (p_2 - p_1)/J) - V_{2fg} (\underline{H}_1 - H_{2f}) - V_{2f} H_{2fg}} \quad (2.13)$$

It is seen from Figs. II-4 and II-5 that the velocity of propagation for shocks is identically equal to the velocity of sound (see Section II-B) when the height of the pressure step, $p_2 - p_1$, approaches zero. The equivalence of equations 2.13 and 2.7 can also be demonstrated analytically.

The above derivation, of course, becomes invalid if the pressure step is sufficiently large to completely evaporate or condense one of the phases; which phase is reduced by the pressure step depends on the initial conditions. If the vapor concentration is initially high then a pressure increase causes the adiabatic temperature rise to evaporate some of the liquid. For high liquid concentration the large thermal capacity of the liquid reduces the temperature rise and vapor condenses. Figure II-6 shows the superpositi

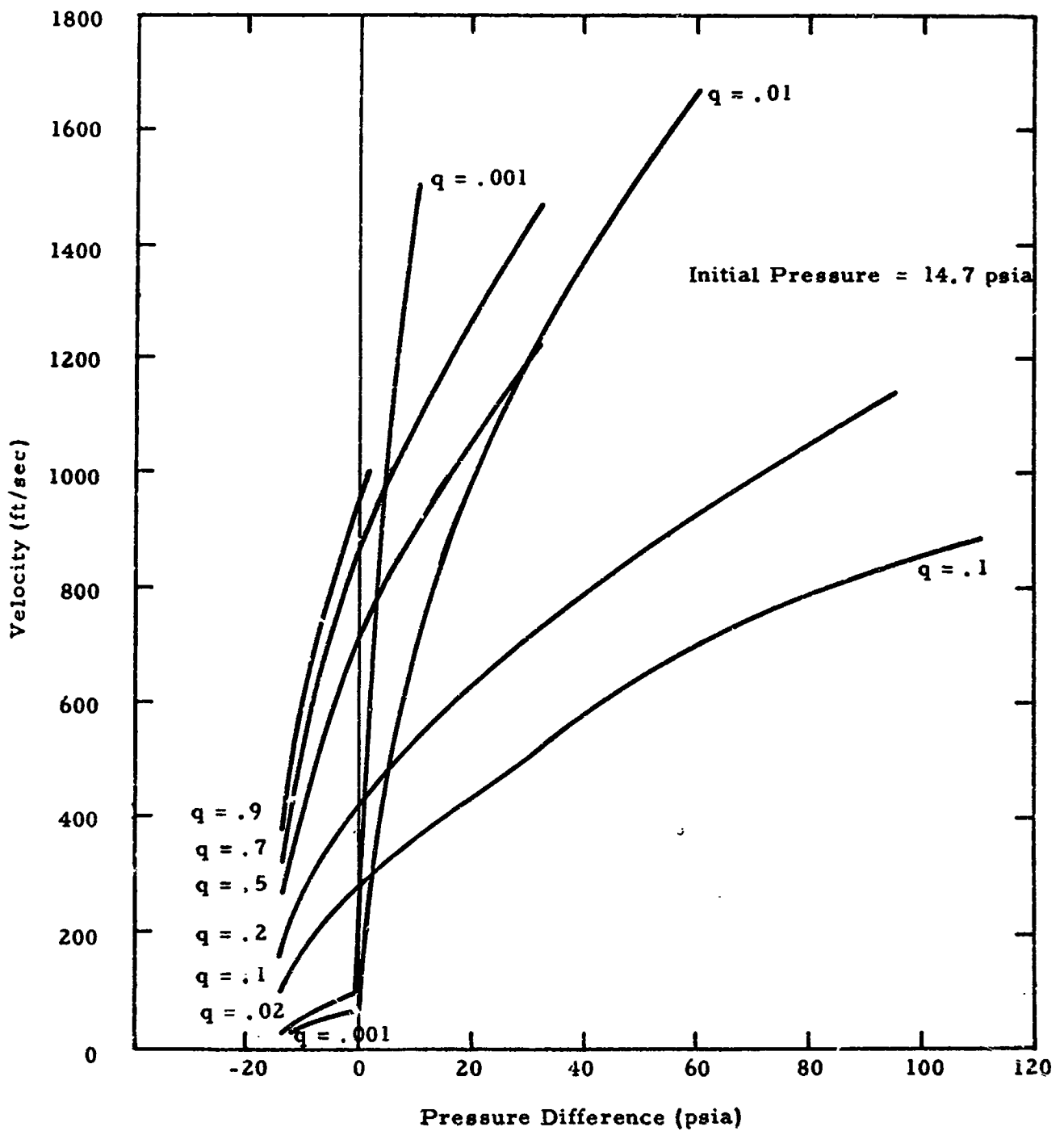


Fig. II-3 VELOCITY OF SHOCK WAVES IN HYDROGEN MIXTURE AGAINST PRESSURE DIFFERENCE FOR VARIOUS QUALITIES

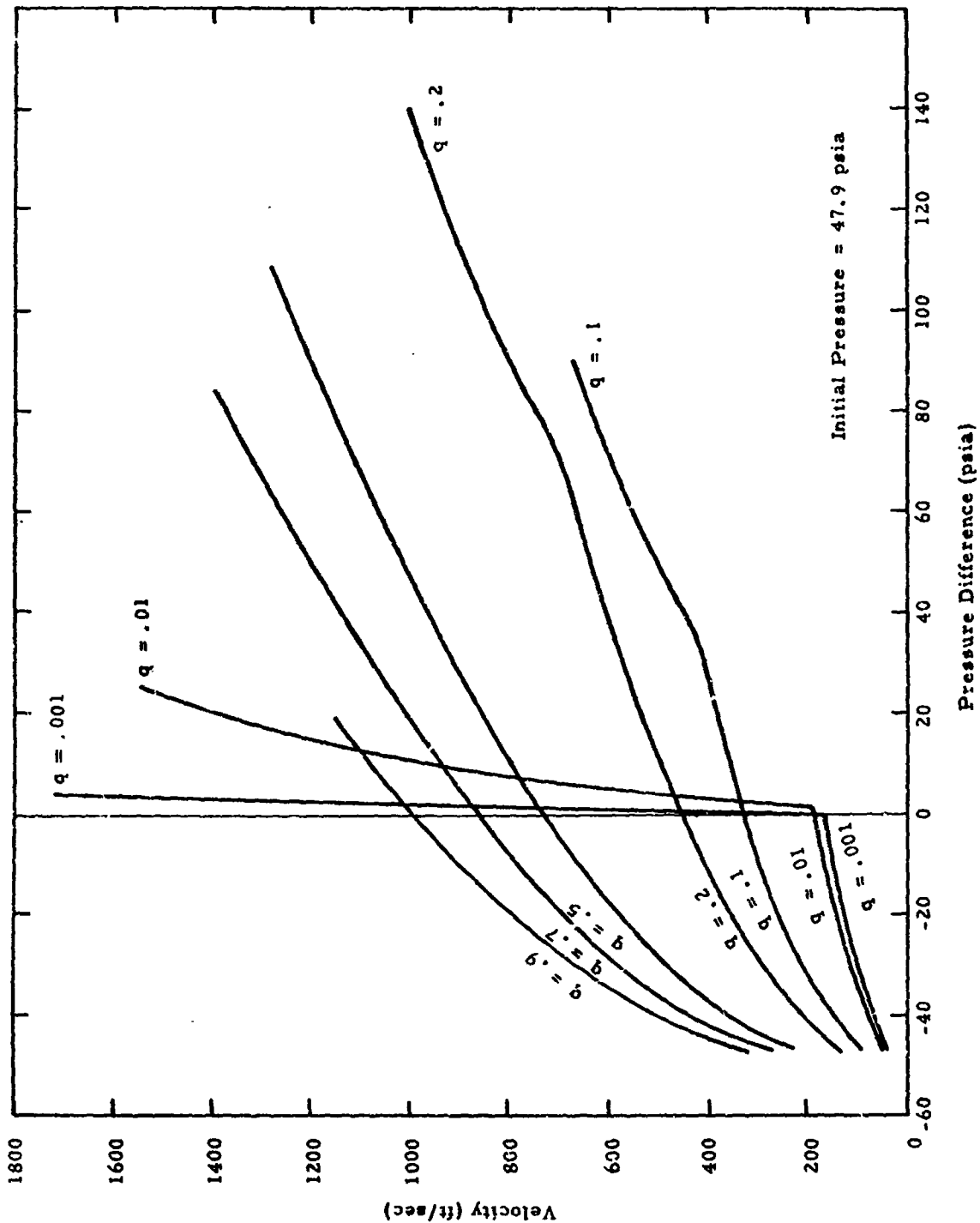


Fig. II-4 VELOCITY OF SHOCK WAVES IN HYDROGEN MIXTURE AGAINST PRESSURE DIFFERENCE FOR VARIOUS QUALITIES

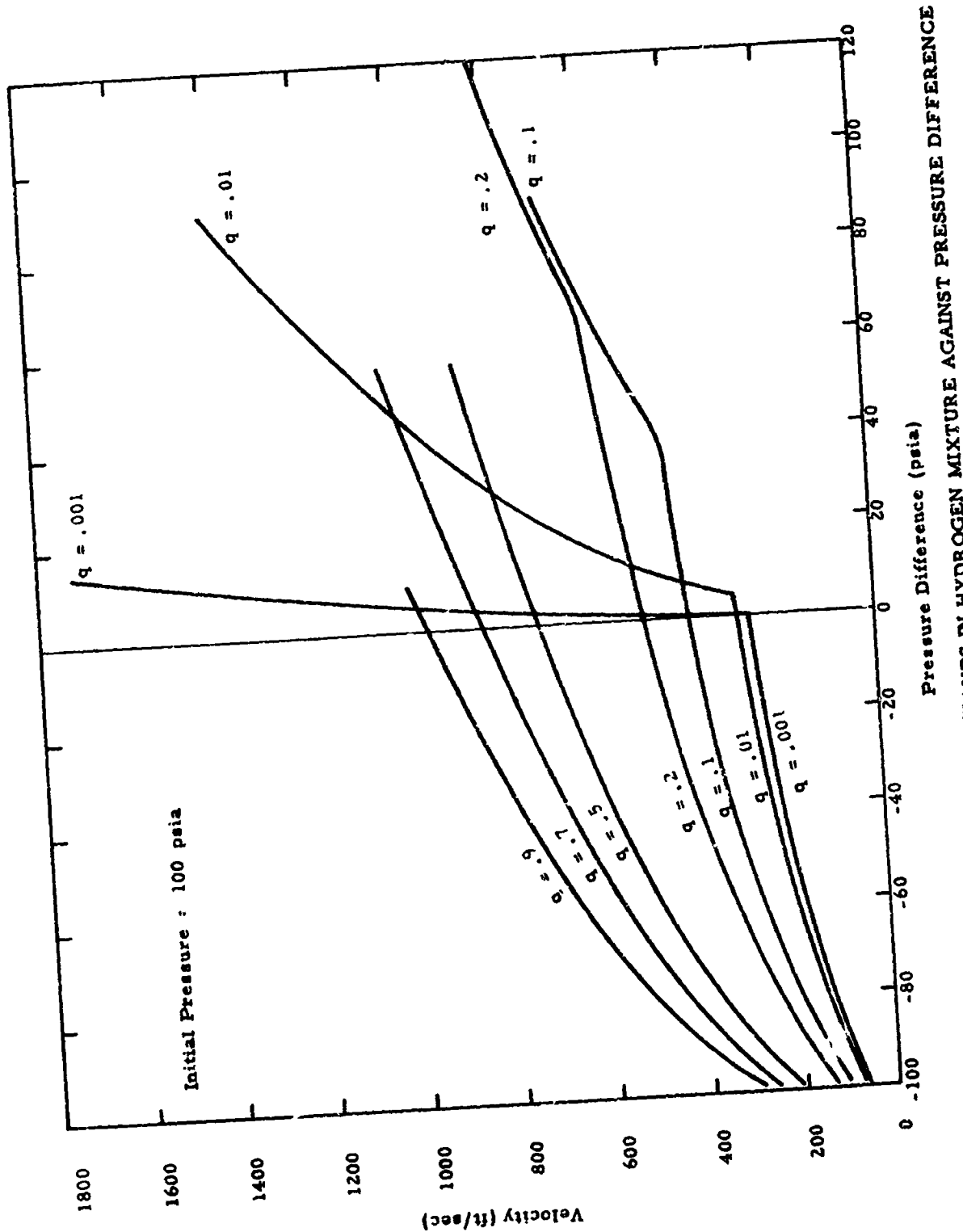


Fig. II-5 VELOCITY OF SHOCK WAVES IN HYDROGEN MIXTURE AGAINST PRESSURE DIFFERENCE FOR VARIOUS QUALITIES

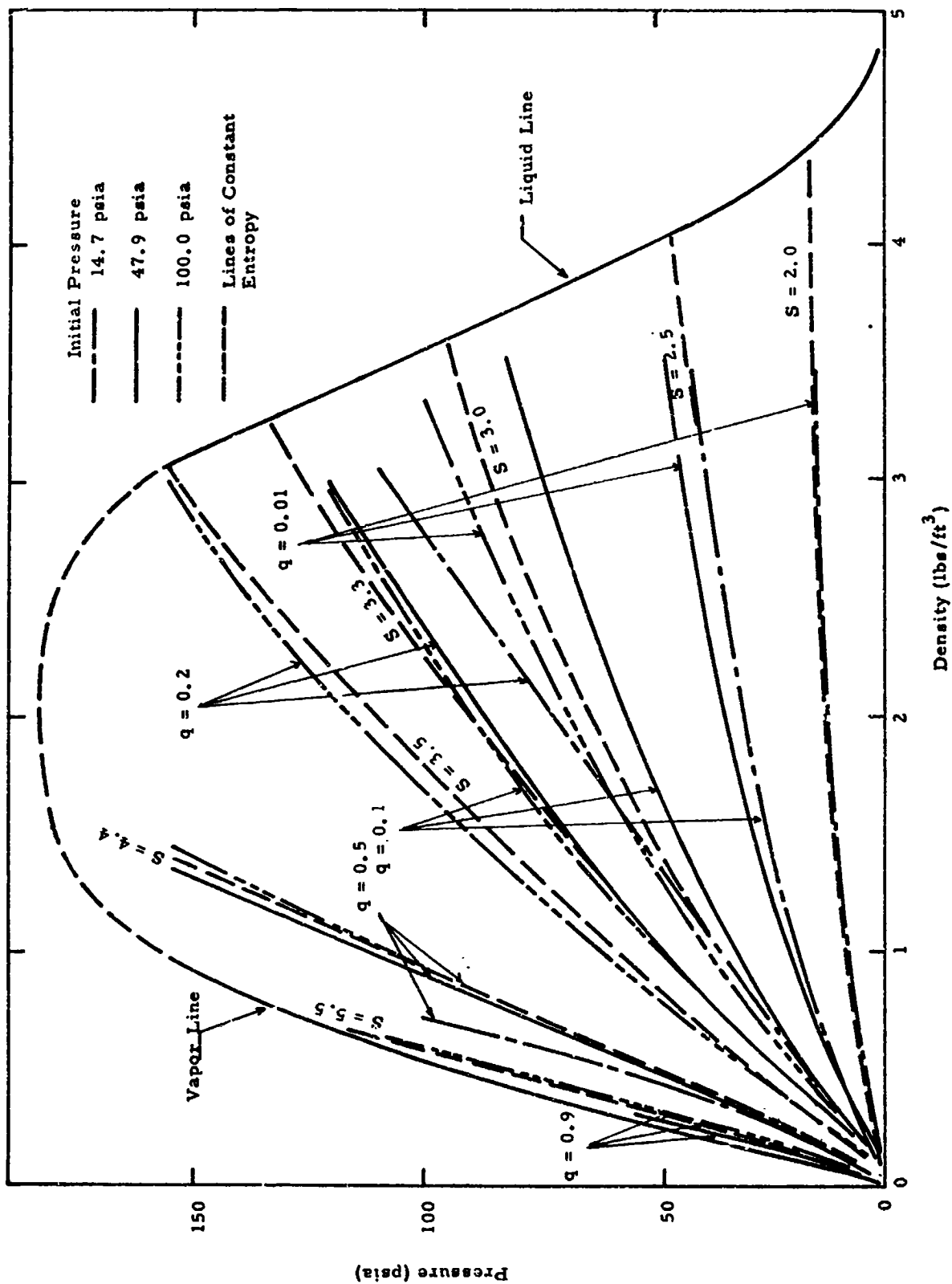


Fig. II-6 PRESSURE-DENSITY RELATION BEHIND "SHOCK" FOR VARYING INITIAL QUALITY AND AMBIENT PRESSURE. Lines of constant entropy are superimposed for comparison.

of initial and final pressures and densities after the passage of a shock. They are seen to lie fairly close to lines of equal entropy which are shown as solid lines.

For shocks which condense all the vapor the compressibility of the liquid is neglected, and it is assumed that $V_2 = V_{1f}$. Substitution in equation 2.9 leads to

$$u_1^2 = (p_2 - p_1) V_1^2 / q V_{1fg} \quad (2.14)$$

Equations 2.13 and 2.14 where applicable are plotted for different initial pressures, p_1 , in Figs. II-3 through II-5. The "shock" velocity is seen to increase with increasing positive pressure step and decreases if progressively larger negative steps are applied. The decreasing velocity with an applied negative step implies that the shape of the step cannot possibly be maintained as the small initial part of the step travels faster than the larger parts of the step. On the positive side conditions would appear to be better than for a pure gas for shock formation, because the rate of increase of velocity is much higher than in pure gases. Also seen on Figs. II-3 through II-5 are sharp kinks for the low quality initial condition. This is the point at which all the liquid has condensed and no appreciable further change of density takes place, transition from equation 2.13 to equation 2.14. In this region the rate of velocity increase becomes really large, and without further information one might expect particularly rapid shock formation. Experiments (Ref. 1) using boiling water disprove this idea. The exchange of heat between the phases delays the pulse rise and an incident shock is slowed to a gradually increasing pressure front also in this region.

D. Pressure Wave Propagation--High Frequency Approximation

Experimental data have been reported which indicate that the measured sound velocity in two-phase mixtures can be quite different from those calculated assuming equilibrium between the phases. Clinch (Ref. 2), for example, measured the sound velocity in high quality wet steam at ultrasonic frequencies. His results showed that the sound velocity is independent of the quality and remained at the value appropriate to the dry steam at the temperature and pressure at which the measurements were made. This result has recently been verified by Collingham (Ref. 7) who measured the propagation velocity of negative shock waves in steam-water mixtures.

To explain the disparity between the experimental data at high frequencies and the calculated low frequency equilibrium sound velocity, Clinch proposed a frequency dependence for the sound velocity. This frequency dependence is attributed to departures from equilibrium due to drag and heat and mass transfer between the phases. An analysis to include these effects as the reasons for the velocity dependence upon frequency, i.e. dispersion, is given in Section IV. In other words at high frequencies, the effect of phase drag and heat and mass transfer is to prevent equilibrium from being established in the period of the acoustic cycle. Thus the high frequency propagation velocity is essentially given by the thermodynamic properties of the dominant phase; the other phase making no contribution whatsoever to the velocity. For instance, in a mixture of liquid droplets suspended in a large volume of vapor, the high frequency sound velocity is that of the vapor phase alone. This concept is discussed further in Section IV.

Calculations were made of the sound velocity in pure hydrogen vapor close to the saturation line over a large pressure range. The thermodynamic properties of the vapor used to make these calculations were taken from Reference 3 for 20.4°K equilibrium hydrogen. To compute the high frequency sound velocity c_{∞} , the following relationship was used:

$$c_{\infty}^2 = \left(\frac{\partial p}{\partial \rho} \right)_S = \frac{p}{\rho} \left(\frac{\partial H}{\partial E} \right)_S = \frac{p}{\rho} \frac{H}{E} \left[1 + \frac{E^2}{H} \left(\frac{\partial (H/E)}{\partial E} \right)_S \right] \quad (2.15)$$

where H and E are the enthalpy and internal energy per unit mass of the hydrogen vapor. This relationship (2.15) for c_{∞} is derived in Appendix G. The function $E^2/H \left[\partial(H/E)/\partial E \right]_S$ is found to vary slowly and remains less than ± 0.15 over the range of interest.

By plotting this function and using graphical interpolation, fairly accurate values of the sound velocity in the pure vapor were obtained. The sound velocity c_{∞} , is shown plotted against the vapor pressure in Fig. II-7. The sound velocity is seen to increase rapidly with pressure in the low pressure range. Above 50 psia, there is little further change in velocity with pressure until the critical region is approached.

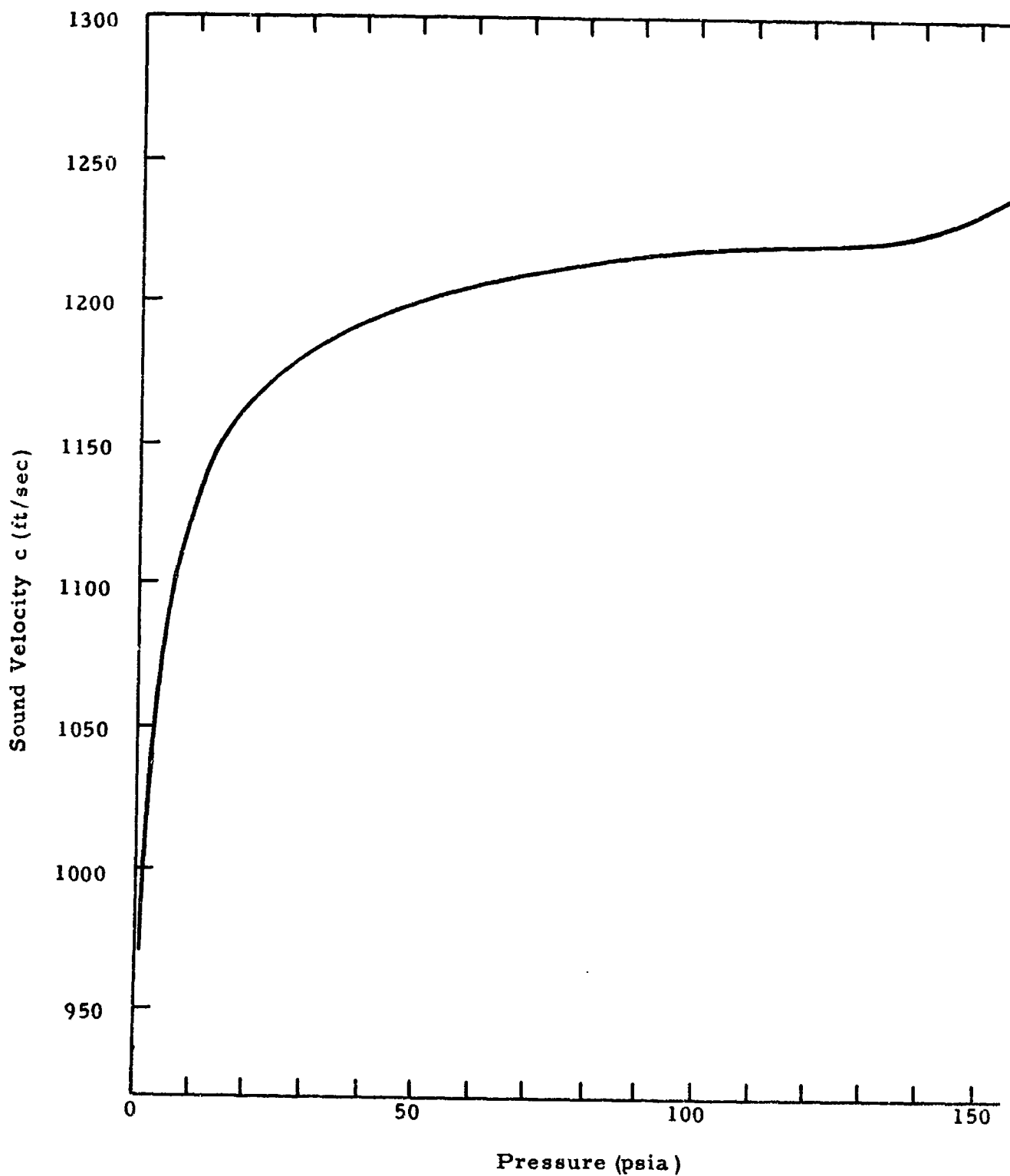


Fig. II-7 SOUND VELOCITY IN 20.4°K EQUILIBRIUM HYDROGEN VAPOR AGAINST PRESSURE

III. RELAXATION

A. Introduction

In a polyatomic gas the wave propagation constants are derived classically in terms of the internal and translational energies of the molecules, and the relaxation time required for equilibrium to be established between the internal and external energies.

For a two-phase mixture of liquid and vapor estimates of relaxation times for heat transfer between the vapor and liquid, together with the low and high frequency sound velocities, calculated in Section II-B and D respectively, yield approximate estimates of the sound velocity as a function of frequency. The dependence of sound velocity upon the frequency is shown further by taking into account drag and heat conduction between the phases. This is discussed in Section IV-A and B.

The initial approximation neglecting mass transfer are illustrated graphically. More complex functions are derived for mass transfer (Appendices A and B). These involve the temperature gradient in the vicinity of the interfaces and would require a computer program. This is beyond the scope of the present program.

B. Relaxation in Gases--Classical Approach

There is quite an extensive literature on wave propagation in fluids in which equilibrium conditions are not reached instantaneously. A

good summary is found in Herzfeld and Litovitz (Ref. 8). More general treatments are due to Meixner (Ref. 9) and others (Ref. 10).

The basic assumption in all these treatments involves the return to an equilibrium condition at a rate linearly proportional to the displacement from it. This assumption leads to a logarithmic approach to equilibrium in terms of a specific time constant. The classical treatment of relaxation cannot be applied very easily to two-phase fluids. Thus, in order to throw some light on the principles involved, the general case of relaxation in a polyatomic gas is given as an example.

In the treatment of relaxation in polyatomic gases account is taken of the following:

1. The rotational and vibrational modes of the atoms in the molecule
2. If the number n of molecules in the excited state differs from the equilibrium number n_0 , then the rate of change of n is linearly proportional to $(n - n_0)$

$$dn/dt = (n - n_0)/\tau$$

$$(n - n_0) = n_0 e^{-t/\tau} \quad (3.1)$$

τ is known as the time constant or relaxation time. This may be written in terms of an internal energy E_i and equilibrium internal energy E_{i0}

$$E_i - E_{i0} = E_{i0} e^{-t/\tau}$$

3. The equation of state relating pressure, density and temperature is a function of the temperature associated with the translation energy only and does not depend on the internal energy of the molecules. The specific heats of the gas are then defined in terms of the translational enthalpy, H_{tr} , and internal energy, E_i .

$$H = H_{tr} + E_i$$

$$(\partial H / \partial T) = C_{po}$$

$$(\partial H_{tr} / \partial T) = C_{p\infty}$$

$$(\partial E_i / \partial T) = C_i$$

then,

$$C_{po} = C_{p\infty} + C_i$$

also

$$C_{Vo} = C_{V\infty} + C_{Vi}$$

Combining these equations yields the complex propagation velocity c at angular frequency, ω , in terms of the zero frequency velocity and the specific heats of the gas:

$$(c_0/c)^2 = (1 + i\omega\tau C_{Vtr}/C_{Vo}) (1 + i\omega\tau C_{ptr}/C_{po})^{-1}$$

This gives the real component of velocity c_r and absorption per wavelength μ provided the latter is not too large.

$$c_r^2 = c_0^2 + (c_\infty^2 - c_0^2) (\omega \tau'')^2 / [1 + (\omega \tau'')^2] \quad (3.2)$$

and

$$\mu = 2\mu_m \omega \tau''' / [1 + (\omega \tau''')^2] \quad (3.3)$$

where

$$\mu_m = \pi (c_\infty / c_0 - c_0 / c_\infty) \quad (3.4)$$

μ_m is the maximum absorption per unit wavelength, c_0 is the sound velocity at very low frequencies, and c_∞ is the sound velocity at very high frequencies

$$\tau'' = (1 - C_i / C_{V0}) = \text{inflexion point on velocity curve}$$

$$\tau''' = (c_\infty / c_0) \tau'' = \text{maximum point on absorption curve}$$

It is seen from equation (3.2) that to obtain the sound velocity and attenuation at any given frequency, ω , a knowledge of the low and high frequency sound velocities as well as the relaxation time are required. This theory is, of course, valid only if one relaxation time is present. The general forms of these functions are plotted in Figs. III-1 and III-2.

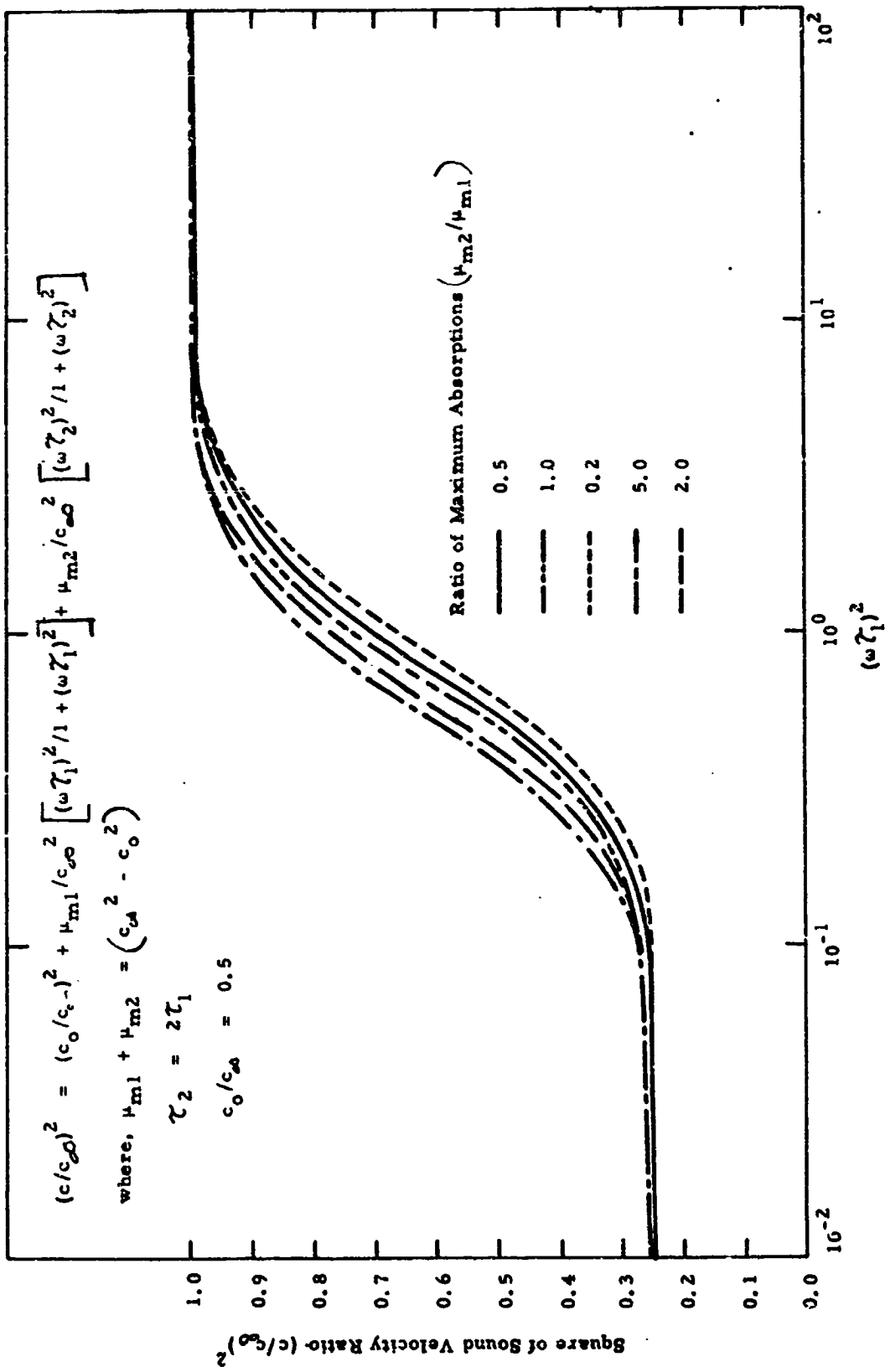


Fig. III-1 EFFECT OF VARYING MAXIMUM ABSORPTION RATIOS (μ_{m2}/μ_{m1}) ON THE SOUND VELOCITY-FREQUENCY FUNCTION FOR MULTIPLE RELAXATION TIMES, $\tau_2 = 2\tau_1$

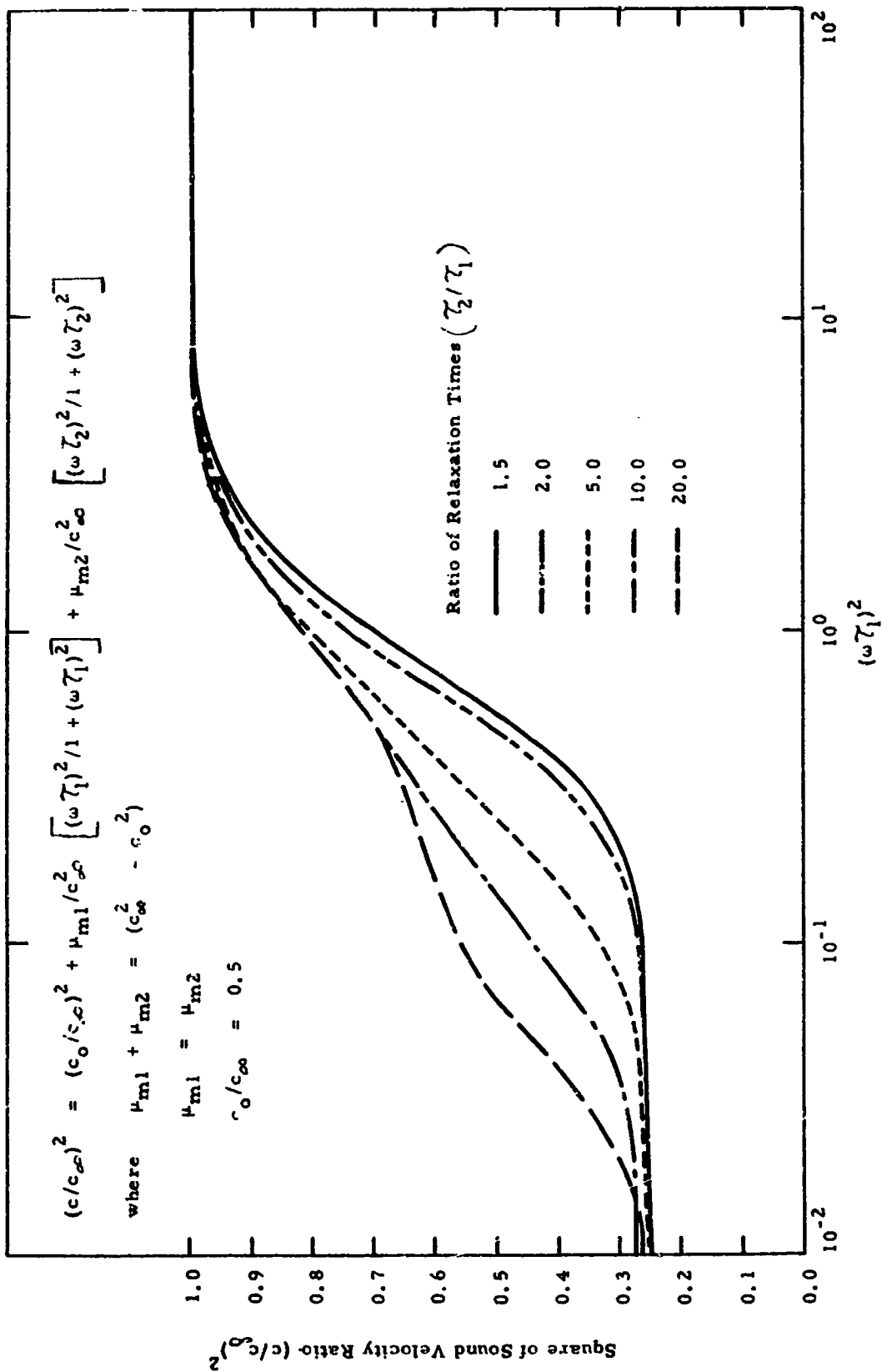


Fig. III-2 EFFECT OF VARYING RATIO OF TWO RELAXATION TIMES (τ_2/τ_1) ON THE SOUND VELOCITY-FREQUENCY FUNCTION FOR EQUAL MAXIMUM ABSORPTION, i.e. $\mu_{m1} = \mu_{m2}$

The existence of multiple relaxation times greatly complicates the picture; examples (for two relaxation times) of the velocity-frequency function are shown in Fig. III-2. The relative magnitude of the absorption due to the two processes is used as a parameter. These plots in Figs. III-1 and 2 are intended to illustrate the fact that with more than one relaxation time, it is very difficult to predict the limiting value of the low frequency sound velocity c_0 from a limited number of measurements at intermediate frequencies.

It has been shown in Section II-B that the low frequency velocity depends only on the quality; at intermediate frequency it depends on both the quality and the time constants.

C. Relaxation Processes in Two-Phase Mixtures

To illustrate the order of magnitude of the time constants involved, the mean temperature time functions of simple geometries subjected to step function temperature changes at the geometrical boundaries are analyzed. The geometries chosen are a sphere and a spherical shell. This may represent liquid droplets in vapor or spherical bubbles in liquid. In a model consisting of many uniformly spaced identical spherical droplets surrounded by the vapor, heat transfer occurs at each boundary.

In the vapor there exists a neutral plane across which there is no heat transfer. Attention may be focussed, therefore, on an individual droplet surrounded by a vapor shell whose boundary undergoes a sudden temperature change. The radii R_f and R_g of the droplet and vapor spheres are

chosen such that the volumes of the two regions are in the same ratio as in an arbitrary two-phase mixture of quality, q

$$(R_f/R_g)^3 = 1 + \rho_f/\rho_g (1 - 1/q) = M^3 \quad (3.5)$$

The mean temperature T_m of a droplet when subjected to a sudden surface temperature change from T_o to T_s is given by Appendix B, Equation B-5.

$$(T_m - T_s)/(T_s - T_o) = (6/\pi^2) \sum_{j=1}^{\infty} 1/j^2 \exp(-j^2 t/\tau_f) \quad (3.6)$$

$$\tau_f = R_f^2/\alpha_f \pi^2$$

This function is plotted in Fig. III-3. This is, of course, not simple relaxation, but may be considered to consist of an infinite number of relaxation times τ_f/j^2 , j being any integer. Figure III-3 shows that higher order relaxation times contribute very little after a time $t \approx \tau_f$.

This permits consideration of a single relaxation time τ_f for low frequencies, $f < 1/\tau_f$. For higher frequencies $f > 1/\tau_f$ the effects of several relaxation times have to be considered. At very high frequencies $f \gg 1/\tau_f$, there is very little heat transfer.

Appendix B-2 shows that if the spherical shell surrounding a sphere of infinite thermal capacity suddenly changes its temperature from T_o to T_s , then the mean temperature, T_m of the shell is

$$\frac{T_m - T_s}{T_o - T_s} = \frac{6M^2 (1 - M)^2}{1 - M^3} \sum_{j=1}^{\infty} \frac{\exp(-t/\tau_g)}{\omega_j^2 (\sin^2 \omega_j - M)} \quad (3.7)$$

where $M = R_f/R_g$ and $\tau_g = R_f^2 (M^{-2} - 1)/a_g \omega_j^2$ and ω_j is a root of the equation

$$\omega_j / \tan \omega_j = 1 - M$$

This function resembles that derived above for the sphere, but it has not been plotted separately. The effect of the higher order constants is somewhat smaller than in the case of the sphere.

The time constants are seen to depend upon the radius R_f of the droplet. Numerical values of the time constant τ_g in the vapor region were calculated for a fog of liquid droplets suspended in vapor. These values for the vapor shell may be compared with the relaxation times τ_f of the droplets shown in Table I. The ratio τ_f/R_f^2 is given for three temperatures and τ_g/R_f^2 is also given for these same temperatures and for different values of quality in Table II.

It is seen that the time constant for the vapor is generally longer than in the liquid. The thermal diffusivity is greater for the liquid and in most cases the distance between droplets is considerably larger than the droplet radius. An exception is noted for low quality-high temperature conditions. In that case $T_s = 54^\circ R$, $q = 0.1$, and R_g/R_f is only 1.16. Evidently the density of the two phases are approximately the same in this case, so that a quality of 0.1 does not conform to the basic assumption of well separated small droplets.

TABLE I

TIME CONSTANTS OF DROPLETS AND SURROUNDING VAPOR
IN TERMS OF THE DROPLET RADIUS R_f

(Microseconds per square micron)

or

(Seconds per square millimeter)

$T_s =$		25°	36°	54°
τ_f/R_f^2		0.5	0.51	1.06
τ_g/R_f^2	$q = 0.1$	1.94	0.65	0.01
τ_g/R_f^2	$q = 0.5$	22.9	11.5	0.61
τ_g/R_f^2	$q = 0.9$	231.0	137.3	11.4

TABLE II

TIME CONSTANTS FOR VARYING DROPLET DIAMETERS
IN A HYDROGEN MIXTURE AT A SATURATION
TEMPERATURE OF 36°R

		Diameter $2R_f$			
Quality q		2 μ	20 μ	200 μ	2 mm
τ_f	Independent	0.51 μ s	0.051 ms	5.1 ms	0.51 s
τ_g	0.1	0.65 μ s	0.065 ms	6.5 ms	0.65 s
τ_g	0.5	11.5 μ s	1.15 ms	115.0 ms	11.5 s
τ_g	0.9	137.3 μ s	13.7 ms	1370.0 ms	137.3 s

It is seen that small droplets rapidly equalize in temperature. If the droplets do not exceed a few microns in diameter it seems quite possible to select a measuring frequency of a few hundred cycles per second with full assurance of being below the velocity dispersion region up to qualities of about 0.9. As very high qualities are approached the separation of the droplets become so large that other mechanisms of heat exchange including that of convection and radiation must be included.

Droplets of several tens of microns in diameter have vapor relaxation times τ_g of a few milliseconds up to qualities of 0.5. At 0.9 quality the vapor relaxation time is already in the tens of milliseconds. Thus any measurement in the low frequency region where velocity dispersion is not evidenced would require frequencies with periods of hundreds of milliseconds, that is, frequencies well below 10 cycles/sec. From Appendix F it is seen that in this frequency region the effect of tube walls on sound propagation must be taken into account; unless, of course, the tube has a very large diameter. In other words the wall diameter must be large compared to the distance between droplets.

Other difficulties also present themselves for low frequency measurements in tubes of finite length. Reflections from the ends of a tube would be pronounced and measurements of a progressive wave in the presence of multiple tube reflections would be impossible. Of course, the velocity could be determined by measuring the length of the standing wave produced by the wave and its reflection. However, the resolution becomes inadequate; a half wavelength at 10 cycles/sec for a velocity of 500 ft/sec is 25 ft. Furthermore, standing waves of low frequencies would be difficult to interpret in regions less than a half wavelength.

It must be pointed out that the models used to obtain the vapor relaxation times (Appendix B-2) are somewhat limited and only indicate orders of magnitude. However the marked dependence on droplet radius shows that the uncertainty in knowing the precise droplet diameter would outweigh that of the relaxation time of the particular droplet size.

D. Conclusions

The difficulty of measuring the quality in fog flow by an acoustic technique may thus be related to the slowness with which the temperature fluctuation penetrates the droplets. Low frequency sounds capable of probing the individual droplets cannot be used for detailed analysis at distances small compared with a wavelength. In very long pipes plane progressive waves can be propagated and phase differences may be measured within limits set only by the noise accompanying the flow.

To determine the quality from an intermediate frequency measurement it might be possible to predict the velocity-frequency function accurately from the theory given in Appendix A and then extend this to a typical droplet size distribution. However, if the droplet size distribution is already known with sufficient accuracy there is no longer any need for a sound velocity measurement to determine quality.

Alternatively the sound velocity and attenuation measured over a wide frequency spectrum might be combined to yield data both on the quality and droplet size distribution. However, the nature of attenuation measurements does not permit measurements to be made over very small distances

and from what has already been stated low frequency standing waves measurements do not give adequate resolution.

Other acoustic techniques may find application, however, in two-phase fluid flow research. It is well known that heat flux data and total mass flow rate do not give all the information required to determine the flow rates of the individual phases, because the slip rate, that is the difference between liquid and gas velocity is not known.

It may, however, be possible to use acoustic techniques to measure the flow velocity of the continuous phase of a two-phase mixture because, at high frequencies, the velocity of sound is independent of the presence of the discontinuous phase. Ultrasonic flow meters have been constructed based on a measurement of the difference of the velocity of sound upstream and downstream in the fluid. This difference may be measured in terms of the phase of continuous waves or arrival time of pulses. Because high frequencies are used, good resolution is possible; moreover, reflections from the ends of the pipes can be overcome. In conclusion, it appears that acoustic techniques involving the direct measurement of quality have many serious drawbacks in spite of their apparent attractiveness. However, the measurement of the flow velocity of the continuous phase appears to be feasible and likely to be of considerable importance in two-phase flow research.

IV. A. VISCOSITY EFFECTS AT THE INTERFACE BETWEEN THE PHASES

1. Introduction

Much of the past work on sound propagation in two-phase fluids has been concerned with the attenuation of sound by particles suspended in gases and liquids. Attenuation is caused by several effects which occur at the phase boundaries. Basically these effects are due to viscous drag, heat conduction between the phases, and an additional loss mechanism due to mass transfer by condensation or evaporation of liquid. Rayleigh particle scattering can also occur, but this source of attenuation can be neglected when the sound wavelength is large compared to the particle dimensions. Several authors have calculated the sound attenuation by small spherical particles suspended in a viscous fluid. Sewell (Ref. 12), for example, considered the case where the particles did not move with the sound wave but were stationary in the fluid. Epstein (Ref. 13) in a more rigorous analysis examined the attenuation of oscillating particles in a viscous fluid. Epstein's theory is quite complicated, and consisted of setting up expressions for the particle velocity in the oscillating fluid in terms of vector and scalar potentials. Epstein considered both rigid and elastic particles and was able to derive Sewell's formula for the particle attenuation as a special case of the general theory.

Unfortunately, Epstein's theory fails to take into account the change of sound velocity of the mixture with frequency, i.e. dispersion, and the theory is valid only when the density of the gas to the density of the suspended particles is very small. In a later paper Epstein and Carhart (Ref.

14) treated the problem of sound attenuation by particles due to both viscosity and heat conduction. The effect of heat conduction will be considered in Section B of this chapter.

Zink and Delsasso (Ref. 15) used Epstein and Carhart's theory to calculate both the attenuation and sound velocity in several particle filled gases. The theory was compared with experimental data taken in the audio-frequency range. Zink and Delsasso assumed ideal gas conditions and used a step-by-step method to calculate the sound velocity in the mixture for each frequency and particle size. It was found that the agreement between theory and experiment was quite good over the limits of experimental error. The theory outlined below for the velocity dispersion and absorption due to viscous drag between phases is a different approach to that used by Epstein. A comparison between these two approaches (Appendix D) shows that the present theory is quite general in its application, and that Epstein's solution is valid only under certain circumstances.

2. Effect of Viscous Drag on Sound Propagation

The nature of the viscous drag process has been investigated by Lamb (Ref. 16) who considered the effect of viscosity on the period of a spherical pendulum oscillating in a viscous fluid. Lamb found that the force X exerted by the fluid on a sphere of radius, R_f , oscillating with angular frequency ω is

$$X = m_g \left(\frac{1}{2} + \frac{9}{4\beta R_f} \right) \frac{d}{dt} (U_g - U_f) + \frac{9}{4} m_g \omega \left(\frac{1}{\beta R_f} + \frac{1}{\beta^2 R_f^2} \right) (U_g - U_f) \quad (4.1)$$

where $(U_g - U_f)$ is the instantaneous relative velocity between the fluid and sphere, $\beta^2 R_f^2$ is the frequency parameter $\omega R_f^2 / 2\gamma_g$, and m_g is the mass of fluid displaced by the sphere. The first term on the right of equation (4.1) gives the correction to the inertia of the sphere while the second term gives the frictional or drag force proportional to the relative velocity. The equation of motion of a spherical droplet can be written as

$$\rho_f \frac{4}{3} \pi R_f^3 \frac{dU_f}{dt} = X + \rho_g \cdot \frac{4}{3} \pi R_f^3 \frac{dU_g}{dt} \quad (4.2)$$

where $\rho_g \cdot \frac{4}{3} \pi R_f^3 \frac{dU_g}{dt}$ is the external force produced by the sound wave. Assuming sinusoidal motion of the fluid of the form $U_g = U_{go} \exp i\omega t$ and that the droplet lags in general the fluid oscillation by phase angle ξ , where $U_f = U_{fo} \exp i(\omega t - \xi)$. The solution of equations 4.1 and 4.2 for the relative amplitude ratio $(U_{go} - U_{fo}/U_{go})$ and phase angle ξ between the motions is given by:

$$\frac{U_{go} - U_{fo}}{U_{go}} = \frac{(1 - \rho_g/\rho_f)}{\sqrt{\theta^2 + (1 + \Phi)^2}} \quad (4.3)$$

$$\xi = \tan^{-1} \left(\frac{\theta}{\Phi + 1} \right) \quad (4.4)$$

where

$$\Phi = \left(\frac{1}{2} + \frac{9}{4\beta R_f} \right) \frac{\rho_g}{\rho_f} \quad (4.5)$$

and

$$\theta = \frac{9}{4} \frac{1}{\beta R_f} \left(1 + \frac{1}{\beta R_f} \right) \frac{\rho_g}{\rho_f} \quad (4.6)$$

These functions have been calculated in a mixture of saturated hydrogen vapor containing liquid hydrogen droplets at several pressures. These plots are shown in Fig. IV-1 for relative amplitude and phase. It may be seen that when the parameter $\beta^2 R_f^2 < 10^{-3}$, the droplets and vapor move with equal amplitude and phase during sound propagation. Alternatively, when $\beta^2 R_f^2 > 10^2$, the relative velocity amplitude reaches a maximum, that is $U_{fo} \rightarrow 0$, and as a result the droplets remain stationary in the sound field. The effect of the drag force given by equation 4.1 on the sound velocity in the two-phase mixture can be seen by writing down the wave equation for the mixture.

$$\frac{\partial^2 U_g}{\partial t^2} = c_\infty^2 \frac{\partial^2 U_g}{\partial x^2} - \left(\frac{1-q}{q} \right) \frac{1}{(4/3) \pi R_f^3 \rho_f} \frac{\partial X}{\partial t} \quad (4.7)$$

Equation 4.7 is derived in Appendix C by considering the fluid forces acting on an elementary volume of vapor due to pressure, inertia, and phase drag. The second term on the right side of the above equation clearly takes into account the relative motion between the phases. For instance, as $\partial X / \partial t \rightarrow 0$, such as would be the case at high frequencies when $\beta^2 R_f^2 > 10^2$, the effective sound velocity will be that of the vapor. This is the situation when the droplet is large and/or when the frequency is high. Eliminating $\partial X / \partial t$ from

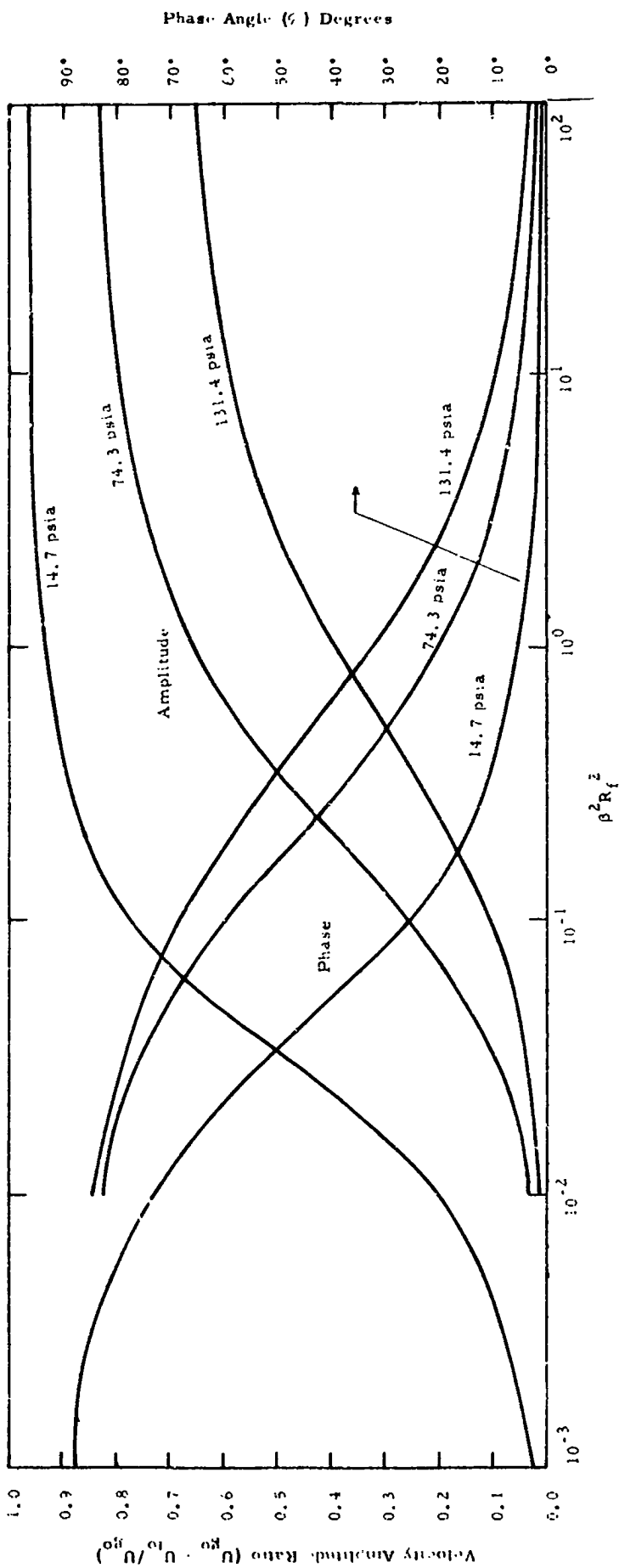


Fig. IV-1 RATIO OF RELATIVE VELOCITY AMPLITUDE BETWEEN VAPOR AND DROPLET AND RELATIVE PHASE ANGLE AGAINST FREQUENCY PARAMETER $\beta^2 R_f^2$ AT SEVERAL PRESSURES IN HYDROGEN MIXTURE

the wave equation by the relation between U_g and U_f at any instant, and by considering U_g to be of the form $U_g = U_{g0} \exp i(\omega t + kx)$, where $k = i\alpha_v - \omega/c$, c being the phase velocity and α_v the amplitude attenuation coefficient it can be shown that:

$$\left(\frac{c_\infty}{c}\right)^2 = 1 + \left(\frac{1-q}{q}\right) \frac{\Phi(1+\Phi) + \theta^2}{(1+\Phi)^2 + \theta^2} \left(1 - \frac{\rho_g}{\rho_f}\right) \quad (4.8)$$

and

$$\mu_v = \alpha_v \lambda_\infty = \pi \frac{c}{c_\infty} \left(\frac{1-q}{q}\right) \frac{\theta}{(1+\Phi)^2 + \theta^2} \left(1 - \frac{\rho_g}{\rho_f}\right) \quad (4.9)$$

where μ_v is the attenuation/wavelength λ_∞ due to viscous effects. If the apparent increase in the inertia of the droplet is neglected, i.e. $\Phi = 0$, the attenuation becomes:

$$\alpha_v = N \cdot \pi R_f^2 \left[\frac{3(2\gamma_g \omega)^{1/2}}{c_\infty} + \frac{6\gamma_g}{c_\infty R_f} \right] \quad (4.10)$$

This expression is identical to Sewell's formula for the viscous attenuation in a fluid containing N particles of radius R_f per unit volume. It is of interest to note that Sewell's formula gives a finite attenuation at the low frequency limit $\omega = 0$. The reason for this error is that Sewell assumed the droplets to be fixed in space which is only true at high frequencies. A comparison of the present expression for the viscous attenuation is made with Epstein's formula in Appendix D. It is noted in Appendix D that Epstein's

formula is an approximation of equation 4.8. This is because Epstein neglected to take into account velocity dispersion and higher values of the gas to particle density ratio as well as omitting certain coefficients above the fourth power in his formula.

Changes in the sound velocity and attenuation using the foregoing theory have been calculated for liquid hydrogen-vapor mixtures at several pressures and dryness fractions over the range of interest. These results are plotted in Figs. IV 2 through IV-4. It may be seen that the value of the frequency parameter $\beta^2 R_f^2$ determines the magnitude of the sound velocity ratio $(c/c_\infty)^2$ and attenuation per wavelength μ_v for a given pressure and quality q . For example, at a quality of 0.7 and a pressure of 74.3 lb/in², velocity dispersion occurs over the range $10^{-2} < \beta^2 R_f^2 < 10^2$. This means that at values of $\beta^2 R_f^2 < 10^{-2}$, the droplets and vapor are in dynamical equilibrium with little or no dissipation of sound energy occurring due to drag at the phase interfaces. In other words at very low frequencies and/or with very small droplets, the total mass of the liquid is effective during wave propagation. Thus under these conditions $c^2/c_\infty^2 = q$. As the frequency is raised or more specifically as $\beta^2 R_f^2$ increases, the droplets contribute less of their total mass to the vapor density. A terminal value of $\beta^2 R_f^2 > 10^2$ is therefore reached when the droplets remain stationary in the vapor thereby contributing none of their mass to the propagation. At values of $\beta^2 R_f^2 > 10^2$ the effective density of the mixture will be that of the vapor alone, and the propagation will be governed only by the thermodynamic properties of the vapor.

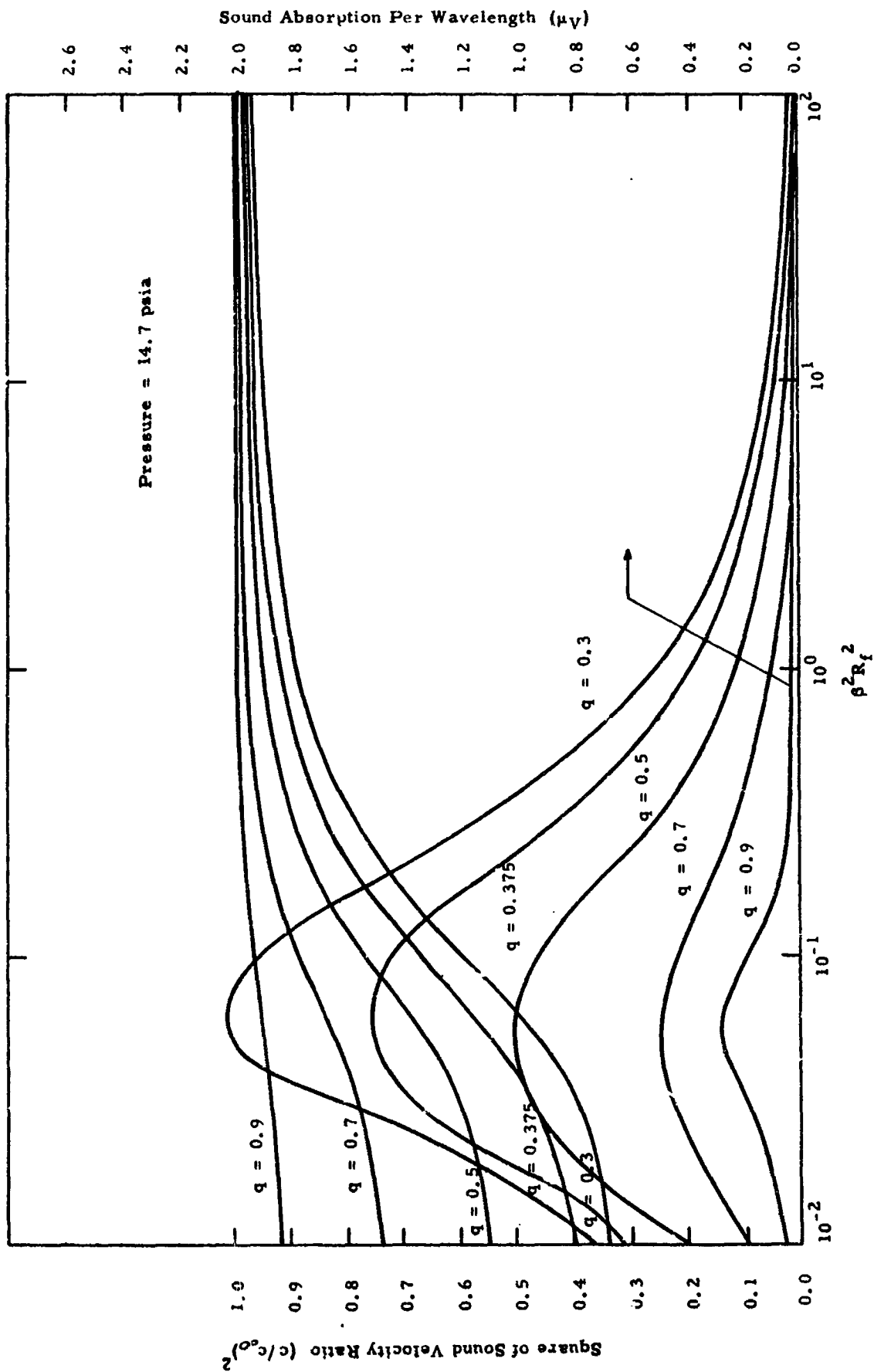


Fig. IV-2 SOUND VELOCITY DISPERSION RATIO AND ABSORPTION PER WAVELENGTH, μ_V , DUE TO VISCOUS DRAG PLOTTED AGAINST FREQUENCY PARAMETER $\beta^2 R_f^2$ FOR HYDROGEN MIXTURE

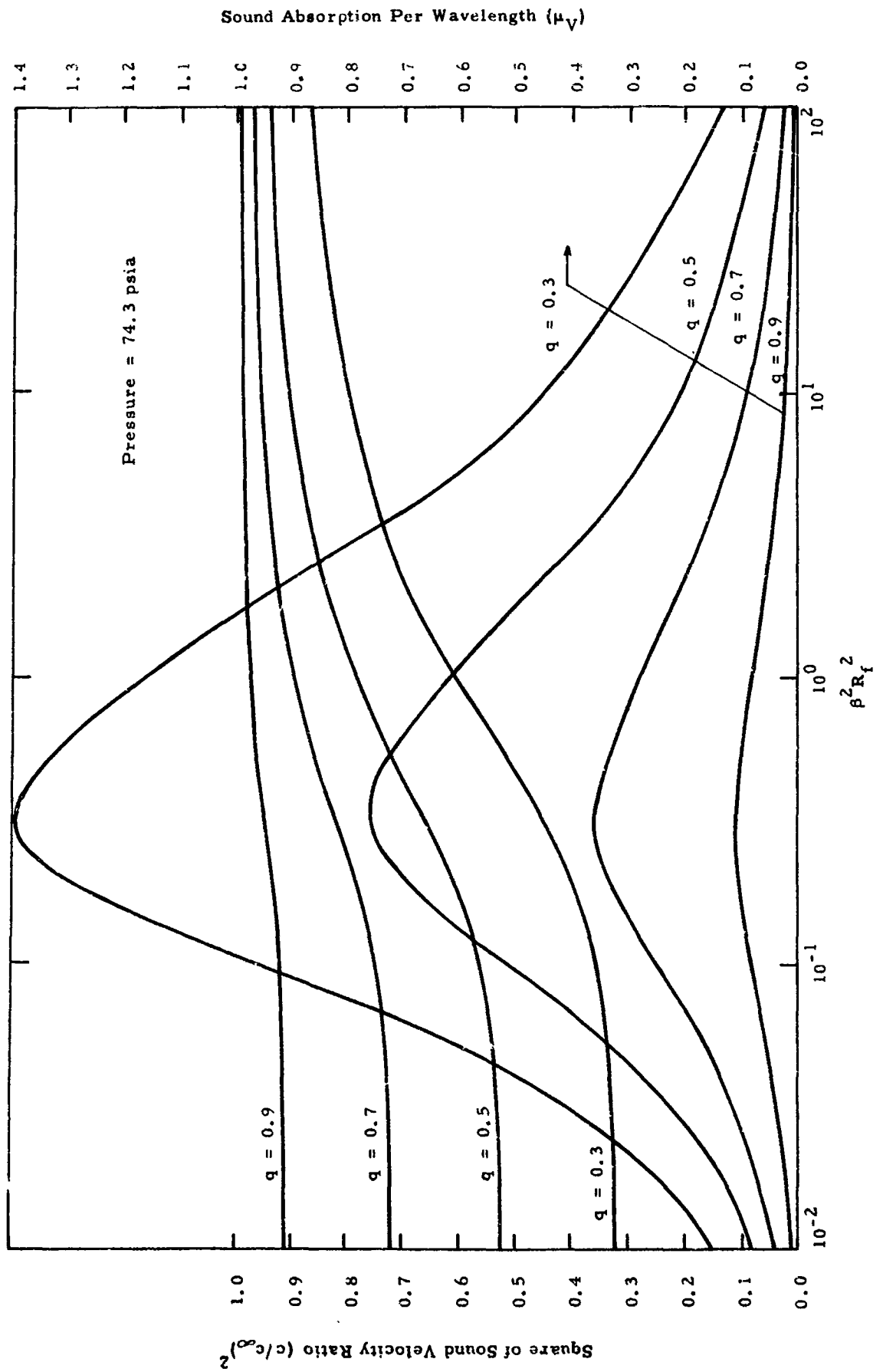


Fig. IV-3 SOUND VELOCITY DISPERSION RATIO AND ABSORPTION PER WAVELENGTH, μ_V DUE TO VISCOUS DRAG PLOTTED AGAINST FREQUENCY PARAMETER $\beta^2 R_f^2$ FOR HYDROGEN MIXTURE

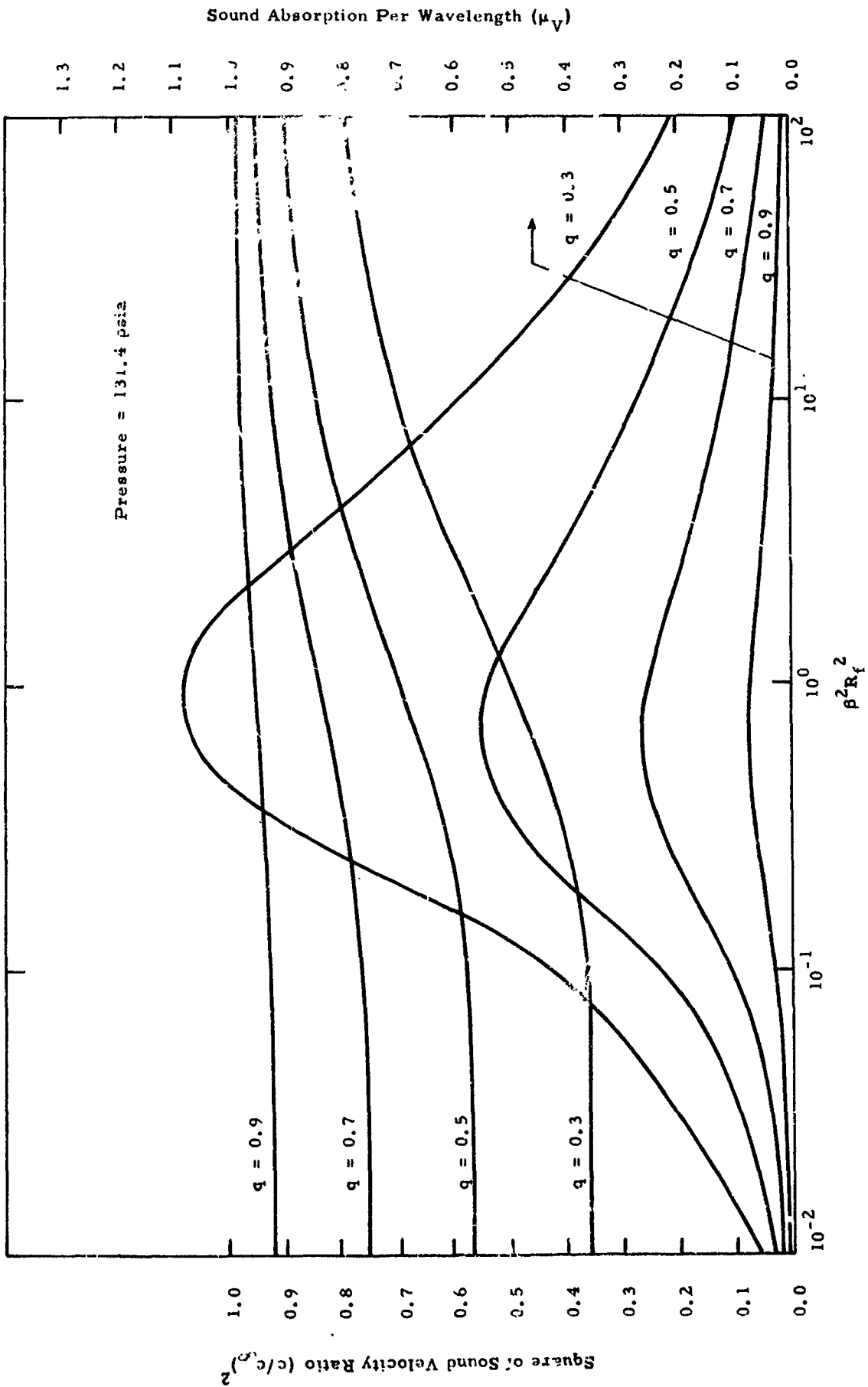


Fig. IV-4 SOUND VELOCITY DISPERSION RATIO AND ABSORPTION PER WAVELENGTH, μ_V DUE TO VISCOUS DRAG PLOTTED AGAINST FREQUENCY PARAMETER $\beta^2 R_f^2$ FOR HYDROGEN MIXTURE

IV. B. COMBINED EFFECTS OF HEAT CONDUCTION AND VISCOSITY ON SOUND PROPAGATION

1. Introduction

The problem of heat conduction between the phases during sound propagation has been examined by Epstein and Carhart (Ref. 14) for gas-particle mixtures. They derive an expression for the wave attenuation due to heat conduction between the gas and particles but no account is taken of the case of the evaporation and condensation of liquid when the particle is a droplet. In order to simplify the problem of heat exchange in the liquid hydrogen-vapor mixture it is assumed in this discussion that no phase change, i.e. mass transfer occurs during sound propagation; the only heat exchange taking place is that of conduction. This assumption is justified only under certain circumstances, namely that there is a critical value of the quality, q_c such that a pressure increase does not promote phase change, i.e. $dq/dp = 0$. Values of this critical quality q_c have been calculated for several pressures in Appendix E.

2. Effect of Heat Conduction on Sound Absorption

It has been shown by Epstein and Carhart that the sound attenuation due to heat conduction is given by

$$a_H = \frac{4\pi NR_f}{c_\infty} \frac{k_g}{\rho_g C_{pg}} \left(\frac{C_{pg}}{C_{vg}} - 1 \right) \left(1 + nR_f \right) I_{nR_f} \quad (4.11)$$

where

$$I_{nR_f}^{-1} = 1 + \frac{12\rho_g C_{pg}}{nR_f \rho_f C_{pfo}} + \frac{9\rho_g^2 C_{pg}^2}{n^4 R_f^4 \rho_f^2 C_{pfo}^2} \quad (4.12)$$

$n^2 R_f^2 = \omega R_f^2 / 2\alpha_g$, α_g is the gas diffusivity. The function I_{nR_f} determines to what extent temperature changes influence acoustic wave propagation. When $I_{nR_f} \rightarrow 1$, the frequency is too rapid to permit heat conduction into a liquid droplet. Alternatively, when $I_{nR_f} \rightarrow 0$, as at very low frequencies, complete heat exchange takes place between the phases in the acoustic time period. As a result of this the droplets remain in temperature equilibrium with the sound wave. Thus, over the range $0 < I_{nR_f} < 1$, sound dispersion and attenuation occurs due to heat conduction effects between the separate phases. The above formula (4.11) for the attenuation due to heat conduction may be written as

$$\mu_H = \alpha_H \lambda_\infty = \pi \rho_g / \rho_f \left(\frac{1 - q_c}{q_c} \right) (\gamma_\infty - 1) (1 + nR_f) \frac{1}{n^2 R_f^2} 3 I_{nR_f} \quad (4.11a)$$

This yields the absorption per unit wavelength μ_H , due to heat conduction in terms of the frequency parameter $n^2 R_f^2$ and critical quality q_c . A plot of μ_H , against $n^2 R_f^2$ for a liquid hydrogen-vapor mixture at atmospheric pressure is shown in Fig. IV-5. It is to be noted that the value of the critical quality for the mixture under these conditions is 0.375 (See Appendix E).

A comparison of the absorption curves for the combined effects of viscous drag and heat conduction is shown in Fig. IV-6. As the viscous

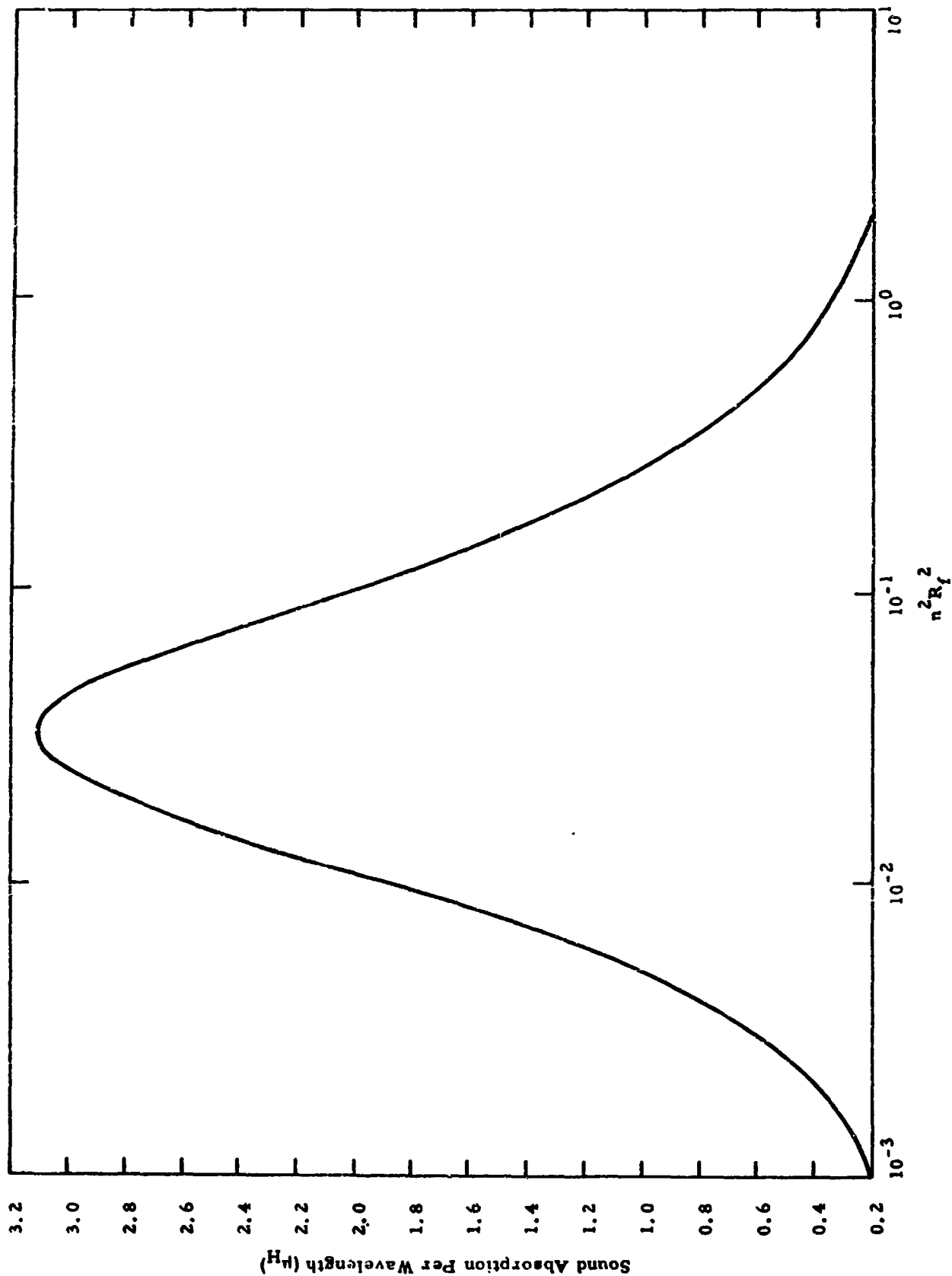


Fig. IV-5 SOUND ABSORPTION PER WAVELENGTH μ_H DUE TO HEAT CONDUCTION PLOTTED AGAINST FREQUENCY PARAMETER $n^2 R_f^2$ FOR HYDROGEN MIXTURE AT ATMOSPHERE PRESSURE ($q_c = 0.375$)

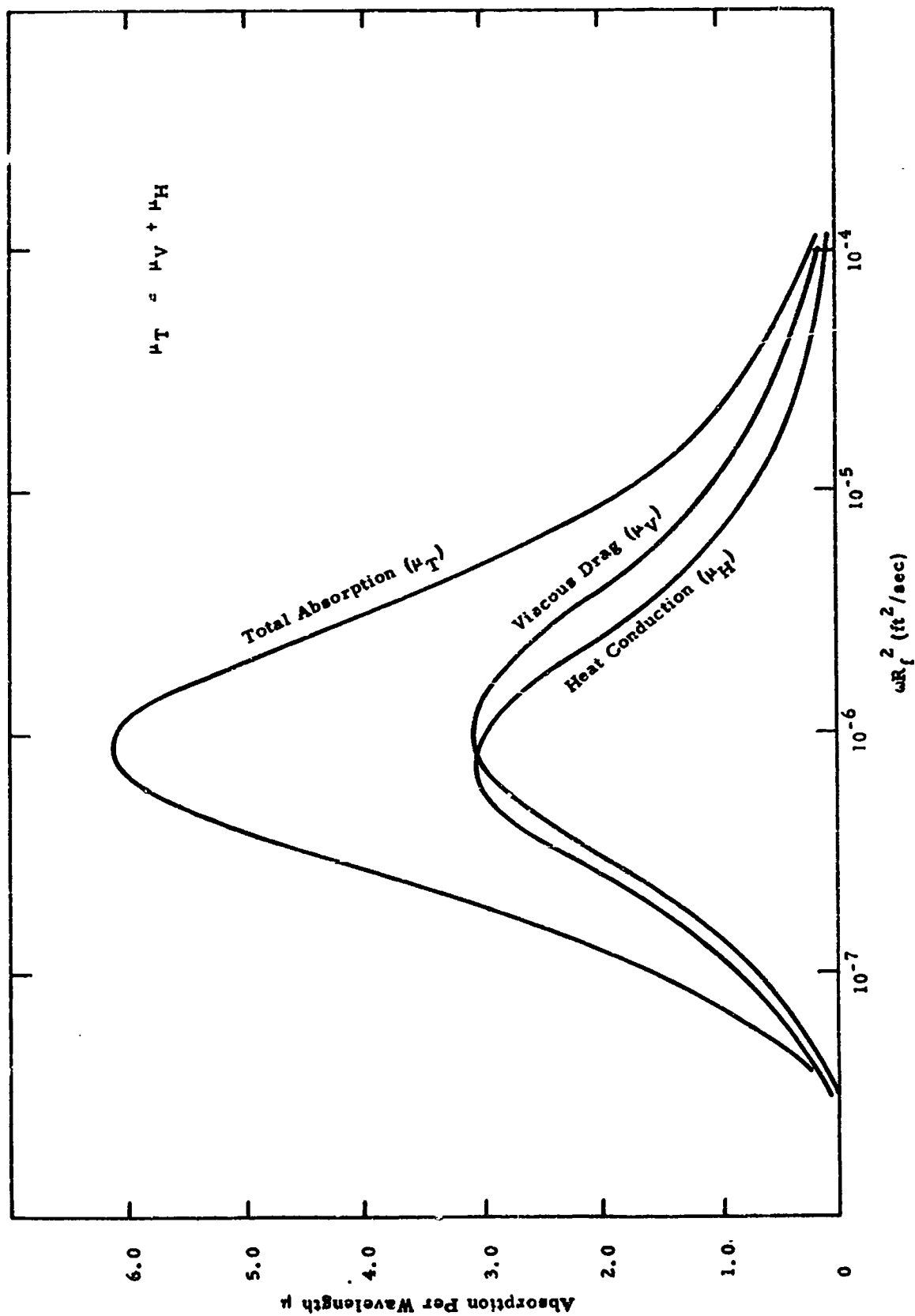


Fig. IV-6 ABSORPTION PER UNIT WAVELENGTH FOR HYDROGEN MIXTURE AGAINST ωR_f^2 AT ATMOSPHERIC PRESSURE ($q_c = 0.375$)

drag depends upon the parameter $\beta^2 R_f^2$ and the heat conduction upon $n^2 R_f^2$, the absorption is plotted ωR_f^2 for both effects. It may be seen that both absorption curves follow a similar trend over the range of dispersion for the mixture. In particular, the peak absorption is seen to occur at approximately the same frequency. For a droplet radius of 10μ , the frequency at which maximum absorption occurs is of the order of 160 cycles/sec. It must be pointed out, however, that the frequency at which peak absorption occurs is in this approximation independent of the quality, q , and does not in itself provide a means of measuring quality by sound absorption techniques. This may be demonstrated by referring to Figs. IV-2 through IV-4 for the absorption due to viscous drag in which the absorption peaks for various qualities all lie close to the same value of $\beta^2 R_f^2$.

Figure IV-6 shows drag effects to predominate at high frequencies. The peak absorption due to this effect occurs at a slightly higher frequency than that of heat conduction. Below the peak region of the curves absorption due to heat conduction slightly dominates that of viscous drag, on the other hand, above peak absorption the converse is true, and the viscous drag absorption is greater (than that caused by heat transfer) by at least 50 % over a wide range of frequencies.

3. Effect of Heat Conduction on Sound Velocity

To calculate the sound velocity change with frequency due to heat conduction between the phases in liquid hydrogen-vapor mixtures the following simplified analysis is proposed. It is assumed that the mixture contains

equally sized droplets distributed homogeneously throughout the vapor which is considered an ideal gas. At the cryogenic temperatures under consideration, hydrogen behaves like a monatomic gas whose ratio of specific heats, γ_{∞} is 1.667. This is because both the rotational and vibrational degrees of freedom of the diatomic molecule remain inactive below about 60°K and only the translational energy contributes to the specific heat of the gas. At low frequencies, there will be a specific heat ratio for the mixture, γ_0 , when the total heat capacity of the droplets and vapor will be effective during wave propagation. This results from the time period of the wave being larger than the time required to distribute the heat generated during an acoustic period uniformly throughout the liquid and vapor. Since the specific heats of the gas and liquid are extensive properties, then for a homogeneous mixture at very low frequencies

$$C_{po} = q_c C_{pg} + (1 - q_c) C_{pfo} \quad (4.13)$$

and

$$C_{vo} = q_c C_{vg} + (1 - q_c) C_{vfo} \quad (4.14)$$

Furthermore, since $C_{pg}/C_{vg} = \gamma_{\infty}$ for the gas,

$$\gamma_0 = \frac{C_{po}}{C_{vo}} = \frac{q_c \gamma_{\infty} + (1 - q_c) \frac{C_{pfo}}{C_{vg}}}{q_c + (1 - q_c) \frac{C_{vfo}}{C_{vg}}} \quad (4.15)$$

where γ_0 is the low frequency specific heat ratio for the mixture, and C_{pfo} is the low frequency specific heat at constant pressure for a droplet. The values of C_{pfo} and C_{vg} may be found listed under the physical properties of hydrogen. It is assumed for the purposes of calculation that $C_{pfo} = C_{vfo}$. This is approximately true for any liquid. Thus, both the low and high frequency specific heat ratios may be calculated for the two phase mixture since the effective value of specific heat of the liquid at high frequencies is zero. In the intermediate frequency range over which velocity dispersion occurs due to a quasi-relaxation of the droplet specific heat, we may define an effective heat capacity for the droplet and an effective ratio of specific heats of the mixture both dependent upon the frequency.

$$C_{p \text{ eff}} = q_c C_{pg} + (1 - q_c) C_{pf \text{ eff}} \quad (4.16)$$

and

$$C_{v \text{ eff}} = q_c C_{vg} + (1 - q_c) C_{pf \text{ eff}} \quad (4.17)$$

The variation of $(C_{pf})_{\text{eff}}$ with frequency may be found by considering the function I_{nR_f} in equation 4.12 for the attenuation due to heat conduction. The meaning of I_{nR_f} may be interpreted as follows: For N droplets of equal size I_{nR_f} represents the effective number of droplets not absorbing any heat from the gaseous phase. The effective heat capacity of a droplet at a given frequency is the difference between the total heat capacity of the droplet (zero frequency), C_{vfo} , and the fraction of its heat capacity not absorbing any heat for the gas, $C_{vfo} I_{nR_f}$, i.e.:

$$(C_{vf})_{eff} = C_{vfo} - C_{vfo} I_{nR_f}$$

also,

$$(C_{pf})_{eff} = C_{pfo} - C_{pfo} I_{nR_f}$$

Substituting this expression for $(C_{vf})_{eff}$ and $(C_{pf})_{eff}$ in equations 4.16 and 4.17 and dividing by C_{vg}

$$\left(\frac{C_p}{C_v}\right)_{eff} = \gamma_{eff} = \frac{q_c \gamma + \frac{(1 - q_c)}{C_{vg}} C_{pfo} (1 - I_{nR_f})}{q_c + \frac{(1 - q_c)}{C_{vg}} C_{pfo} (1 - I_{nR_f})} \quad (4.18)$$

This expression for γ_{eff} is plotted in Fig. IV-7 against the frequency parameter $n^2 R_f^2$ for a hydrogen mixture of critical quality 0.375 at atmospheric pressure. It is seen that γ_{eff} increases very slowly with $n^2 R_f^2$ from about 1.19 for the low frequency specific heat ratio (γ_o) to 1.67 at high frequencies (γ_{∞}). Thus over the range $6 \times 10^{-3} < n^2 R_f^2 < 10^2$, velocity dispersion is seen to occur due to the thermal lag in the heat capacity of the droplet.

For droplets radius of 10μ , this frequency range varies from about 30 cycles/sec to about 365 Kc/sec. It is of interest to compare this frequency range for dispersion due to heat conduction with that for viscous drag under the same physical conditions. For viscous drag it may be seen from Fig.

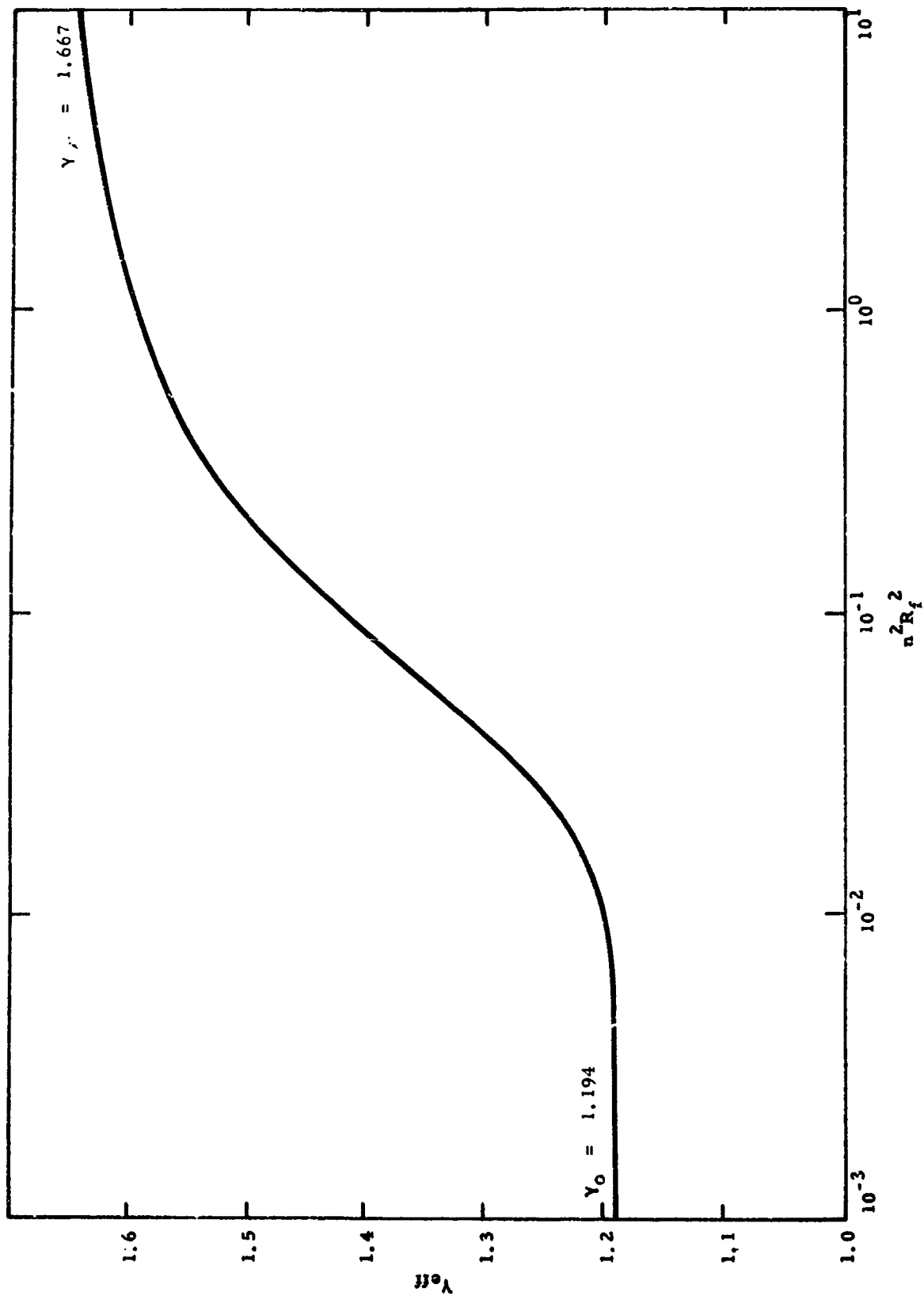


Fig. IV-7 PLOT OF EFFECTIVE SPECIFIC HEAT RATIO (γ_{eff}) AGAINST FREQUENCY PARAMETER $n^2 R_f^2$ FOR HYDROGEN MIXTURE AT ATMOSPHERIC PRESSURE ($q_c = 0.375$)

IV-2 that the dispersion ranges from $6 \times 10^{-3} < \beta^2 R_f^2 < 10^2$. This range corresponds to frequencies from about 15 cycles/sec to 260 Kc/sec for droplets of 10μ radius.

4. Combined Effects of Heat Conduction and Viscosity on Sound Velocity

In order to calculate the sound velocity change with frequency it is necessary to combine the effects of drag and heat conduction. By assuming the mixture to be an ideal gas, the sound velocity c is

$$c^2 = \frac{\gamma_{\text{eff}} p}{\rho_{\text{eff}}} \quad (4.19)$$

The effective value of the specific heat ratio from equation 4.18 is

$$\gamma_{\text{eff}} = \frac{q_c \gamma_{\infty} + \frac{(1 - q_c)}{C_{vg}} C_{pfo} (1 - I_{nR_f})}{q_c + \frac{(1 - q_c)}{C_{vg}} C_{pfo} (1 - I_{nR_f})}$$

and for viscous drag dispersion (see Section A, equation 4.8) by:

$$\left(\frac{c_{\infty}}{c} \right)^2 = 1 + \left(\frac{1 - q_c}{q_c} \right) \frac{\Phi (1 + \Phi) + \theta^2}{(1 + \Phi)^2 + \theta^2} \left(1 - \frac{\rho_g}{\rho_f} \right)$$

in this case

$$c_{\infty}^2 = \frac{\gamma_{\infty} p}{\rho_g} \quad \text{and} \quad c^2 = \frac{\gamma_{\infty} p}{\rho_{\text{eff}}}$$

since the above dispersion equation is derived on assumption of no heat exchange between phases, i. e. $\gamma_{\text{eff}} = \gamma_{\infty}$ for all frequencies. Thus, the above expression yields the effective density change with frequency in the mixture:

$$\rho_{\text{eff}} = \rho_g \left[1 + \left(\frac{1 - q_c}{q_c} \right) \frac{\Phi (1 + \Phi) + \theta^2}{(1 + \Phi)^2 + \theta^2} \left(1 - \frac{\rho_g}{\rho_f} \right) \right] \quad (4.20)$$

Combining the above formulae for γ_{eff} and ρ_{eff} in equation 4.19 the sound velocity in the mixture c , may be calculated as a function of the product ωR_f^2 . These results are plotted in Figs. IV-8 and IV-9. It is seen that for values of $\omega R_f^2 < 10^{-7}$, thermodynamic equilibrium exists between the phases during sound propagation. This corresponds to frequencies less than about 15 cycles/sec for droplets of 10μ radius, and yields a value of 600 ft/sec for the equilibrium sound velocity, c_0 . This value is in excellent agreement with that calculated from the thermodynamic properties of the hydrogen mixture for a quality of 0.375 at atmospheric pressure (see Section II-B). At values of $\omega R_f^2 > 10^{-3}$ the high frequency sound velocity of 1150 ft/sec is approached. This checks very well with that calculated from the properties of the hydrogen gas (see Section II-D).

This agreement lends support to the validity of this theory of velocity dispersion due to both drag and heat conduction. It must be emphasized, however, that the heat conduction theory is only applicable at values

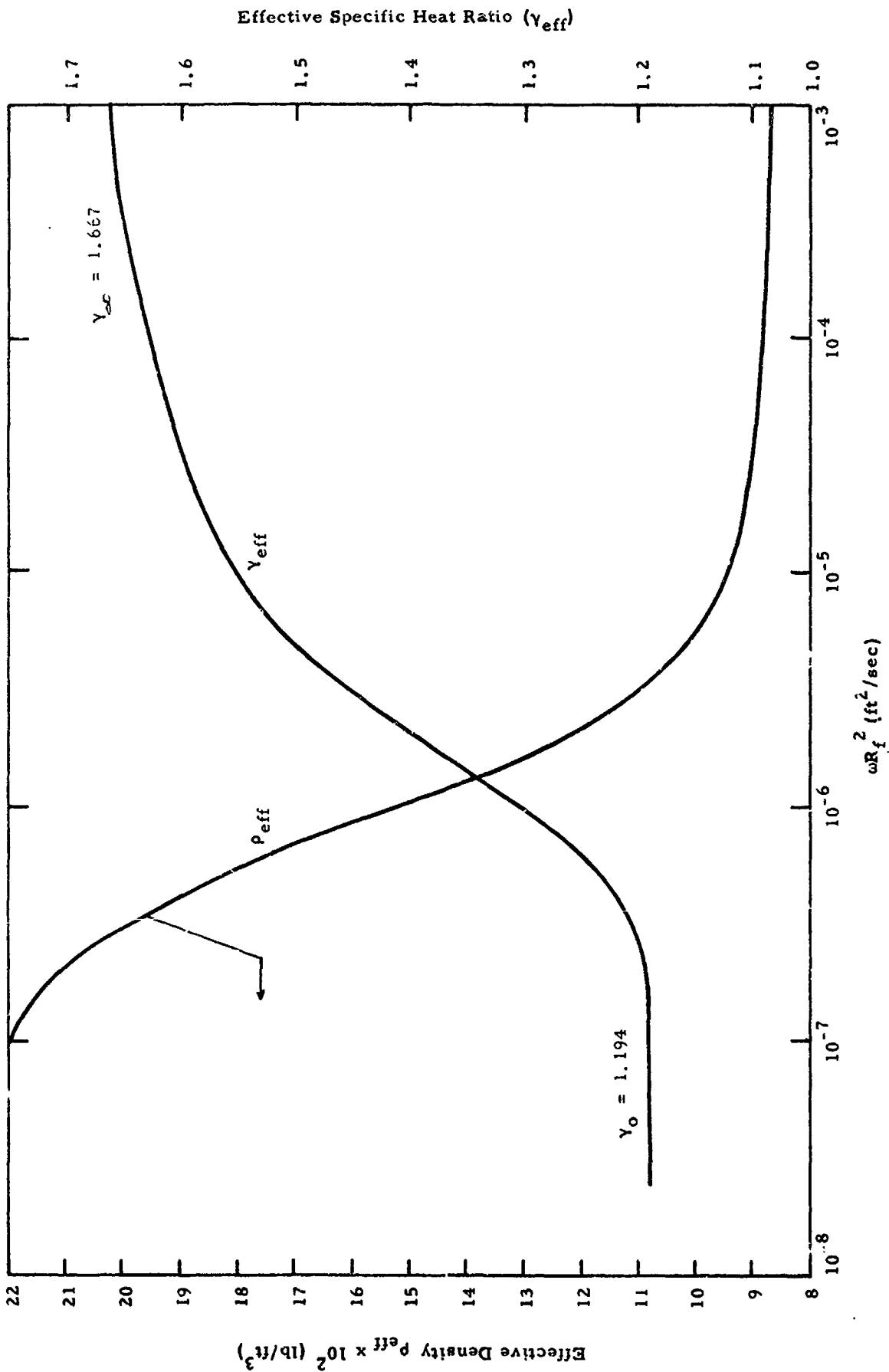


Fig. IV-8 EFFECTIVE DENSITY (ρ_{eff}) AND SPECIFIC HEAT RATIO (γ_{eff}) AGAINST ωR_f^2 FOR HYDROGEN MIXTURE AT ATMOSPHERIC PRESSURE ($q_c = 0.375$)

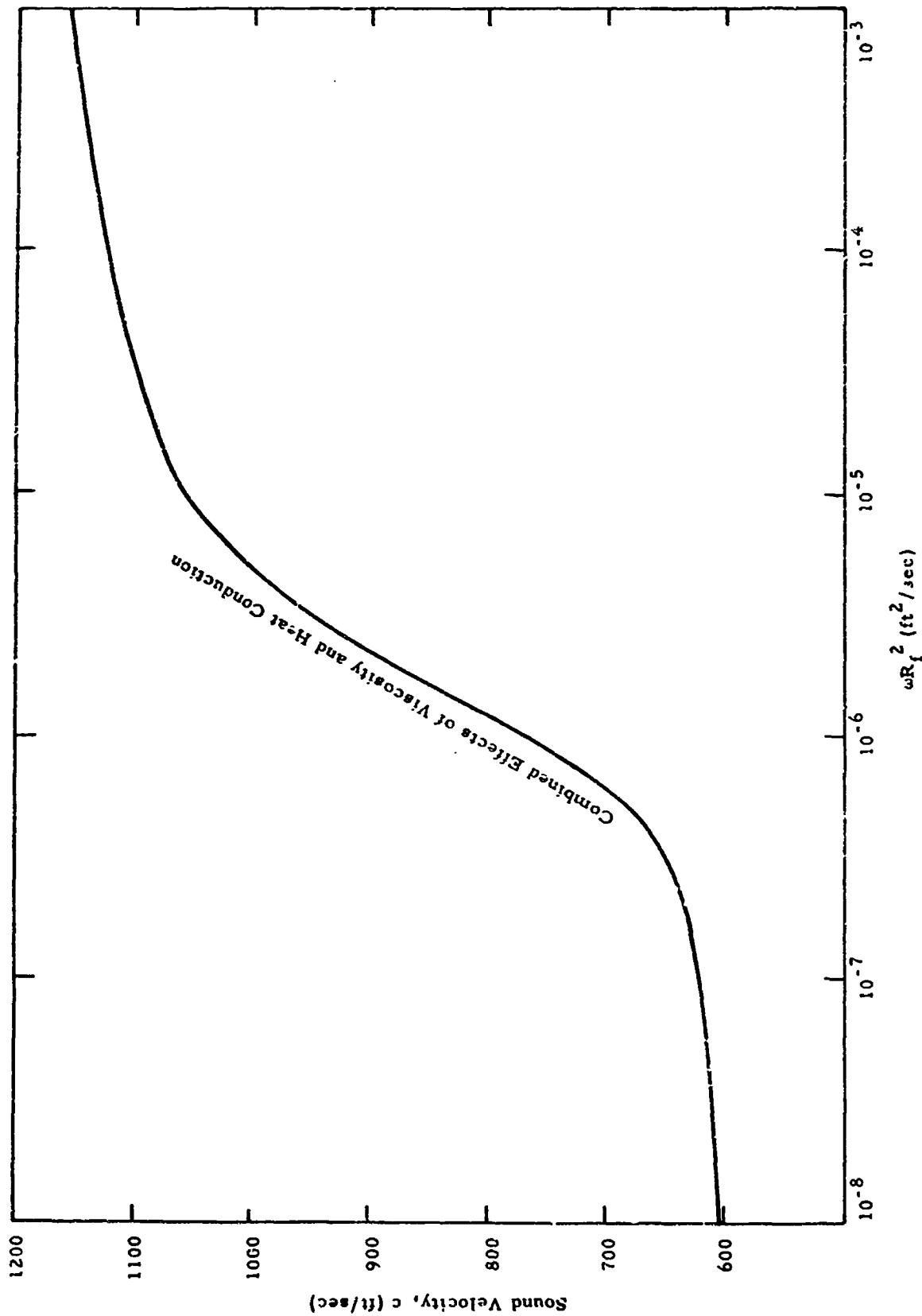


Fig. IV-9 SOUND VELOCITY IN HYDROGEN MIXTURE AGAINST ωR_f^2 AT ATMOSPHERIC PRESSURE
($q_c = 0.375$)

of the critical quality q_c when no evaporation or condensation of liquid occurs at the phase interfaces. For all other qualities account must be taken of mass transfer. This is considered in Appendices A and B.

IV. C. PRESSURE PULSE PROPAGATION IN THE TWO-PHASE HYDROGEN MIXTURE

In this section the problem of the propagation of a pressure pulse in a mixture of hydrogen vapor containing liquid droplets in suspension is considered in relation to the dispersion and absorption properties of the mixture. It is assumed that the amplitude absorption coefficient as well as the phase velocity are known functions of the frequency and quality. These functional relationships have already been established in Section IV-A for the velocity dispersion and absorption in the mixture due to drag effects. These results will be used in the following analysis. The object here is to provide an analytical description of the propagation of varying pressure pulses through the mixture, and attempt to relate this description to the quality. Such a description may be expected to reveal the changing pressure pulse shape both in space and time and to suggest some quantitative means by which the quality could be determined experimentally.

Several abortive attempts were made to analyze the propagation of a single pressure pulse of arbitrary form in the hydrogen mixture. The following approach was, however, found to be quite successful: A series of pulses of a given shape and having a periodicity τ_p or repetition rate $1/\tau_p$ is assumed. Such a series of pulses may be represented by a Fourier series of which a finite number of the initial terms in the series represent an adequate physical description of the pulse. This implies that a good approximation of the pulse at any instant is given by a finite number of appropriate sine and cosine terms, namely

$$p(x,t) = \frac{a_0}{2} + \sum_{j=1}^m A_j(x) \cos B_j(x,t) \quad (4.21)$$

where $p(x,t)$ is the pressure associated with the pulse at any point x and time t as the pulse propagates through the dispersive media. It is assumed that the amplitude attenuation of each component is of the form:

$$A_j(x) = a_j \exp \left[-\alpha_v(\omega_j) x \right] \quad (4.22)$$

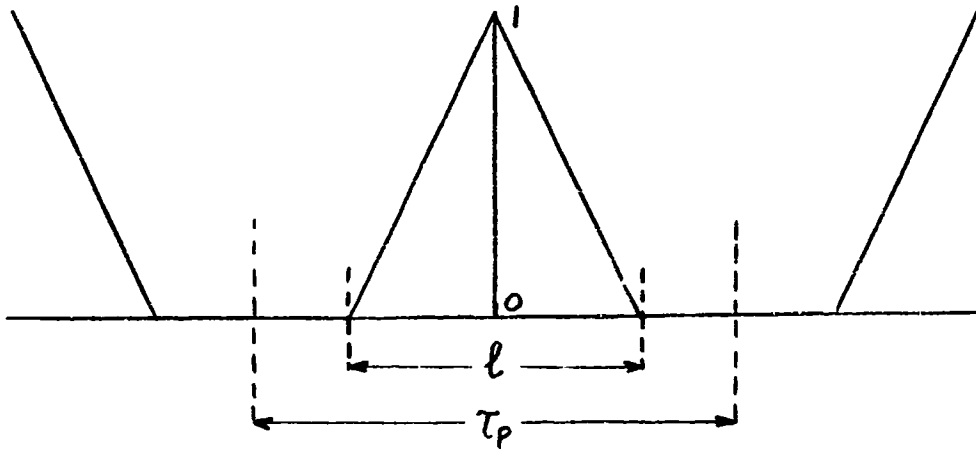
a_j is the Fourier coefficient of the j th component at $x = x_0$, the reference point. The phase $B_j(x,t)$ will be of the form:

$$\frac{\omega_j x}{c(\omega_j)} - \omega_j t \quad (4.23)$$

Each component represents a progressive sinusoidal wave whose amplitude is decreasing exponentially according to the frequency dependent amplitude attenuation coefficient $\alpha_v(\omega_j)$ and whose phase velocity is given by the frequency dependent term $c(\omega_j)$. At any position x and time t the components of the Fourier series may then be calculated and combined algebraically to obtain the pulse wave form at a particular point.

A wide variety of pulse shapes were considered and the triangular pulse shown below was selected for detailed analysis:

Triangular Pulse



The Fourier series description of such a pulse is given by

$$a_0 = l/\tau_p \quad (4.24)$$

$$a_n = \frac{2\tau_p}{l\pi^2 j^2} \left(1 - \cos \frac{j\pi l}{\tau_p} \right) \quad (4.25)$$

To start the pulse at time $t = 0$, equation 4.21 has to be modified so that

$$p(x, t) = \frac{a_0}{2} + \sum_{j=0}^m a_j \exp \left[-\alpha_v(\omega_j) x \right] \cos \omega_j \left[\frac{x}{c(\omega_j)} - (t - l/2) \right] \quad (4.26)$$

To evaluate $\alpha_v(\omega_j)$ and $c(\omega_j)$ for each frequency to account for both absorption and velocity dispersion reference may be made to Fig. IV-3 in which the velocity dispersion ratio $(c/c_\infty)^2$ and the absorption per wavelength $\mu_v = \alpha_v(\omega)/\lambda_\infty(\omega)$ are shown plotted against the frequency parameter

$\beta^2 R_f^2$. It must be emphasized, however, that these graphs account for only viscous drag between the hydrogen vapor and liquid droplets and do not include other dispersion mechanisms such as heat and mass transfer between the phases. Consequently in this analysis of pulse propagation only the contribution of viscous drag to the dispersion is considered. It is also noted that the sound velocity c_∞ refers to the high frequency nondispersive vapor velocity. This is calculated in Section II-D from the known thermodynamic data for hydrogen vapor.

To analyze the propagation of the triangular pulse the following calculations are made

1. A duty cycle, $l/\tau_p = 1/4$ is assumed.
2. A gas pressure of 74.3 lb/in^2 and a quality of 0.5 are selected to represent the physical conditions of the liquid hydrogen-vapor mixture. This permits both the velocity dispersion and absorption to be calculated under these conditions from Fig. IV-3.
3. The pulse repetition frequency $1/\tau_p$ is chosen such that the value $\omega_1 = 2\pi/\tau_p$ lies in the range of frequencies in Fig. IV-3 where the dispersion is pronounced and where the absorption reaches a maxima. This frequency ω_1 is selected from the value of $\omega_1 = \beta^2 R_f^2 \times 2v_g/R_f^2$.
4. Two values of ω are selected: $\omega_1 = 1.07 \times 10^3$ and $\omega_1 = 0.25 \times 10^3$ radians/sec which lie on either side of the absorption maxima shown in Fig. IV-3 for $q = 0.5$.

5. Five harmonics of ω_1 are taken to be representative of the frequency components of the triangular pulse.
6. The Fourier coefficients a_1, a_2, \dots, a_5 corresponding to $\omega_1, \omega_2, \dots, \omega_5$ are calculated from equation 4.25.
7. Two points $x = 0$ and $x = 4.0$ inch are selected as the points at which the pulse shape is to be calculated.
8. The amplitude attenuation coefficient $a_v(\omega_j)$ is calculated from

$$a_v(\omega_j) = \frac{\mu_v(\omega_j) \omega_j}{2\pi c(\omega_j)}$$

9. The phase velocity $c(\omega_j)$ is calculated from

$$c(\omega_j) = c_\infty \sqrt{\frac{c^2(\omega_j)}{c_\infty^2}}$$

10. Finally, the pulse pressure distribution at $x = 0$ and $x = 4.0$ inch is obtained as a function of time t from equation 4.26.

The results of these calculations are shown plotted in Figs. IV-10 and IV-11. It may be seen that taking the first six terms of the Fourier series gives a very good approximation to a triangular pulse. On comparing the pulse shapes at $x = 0$ and $x = 4.0$ inch it is seen that for $\omega_1 = 2.5 \times 10^2$ rad/sec there is little difference in shape or displacement but for $\omega_1 = 1.07 \times 10^3$ rad/sec a marked phase shift and change of pulse shape is apparent.

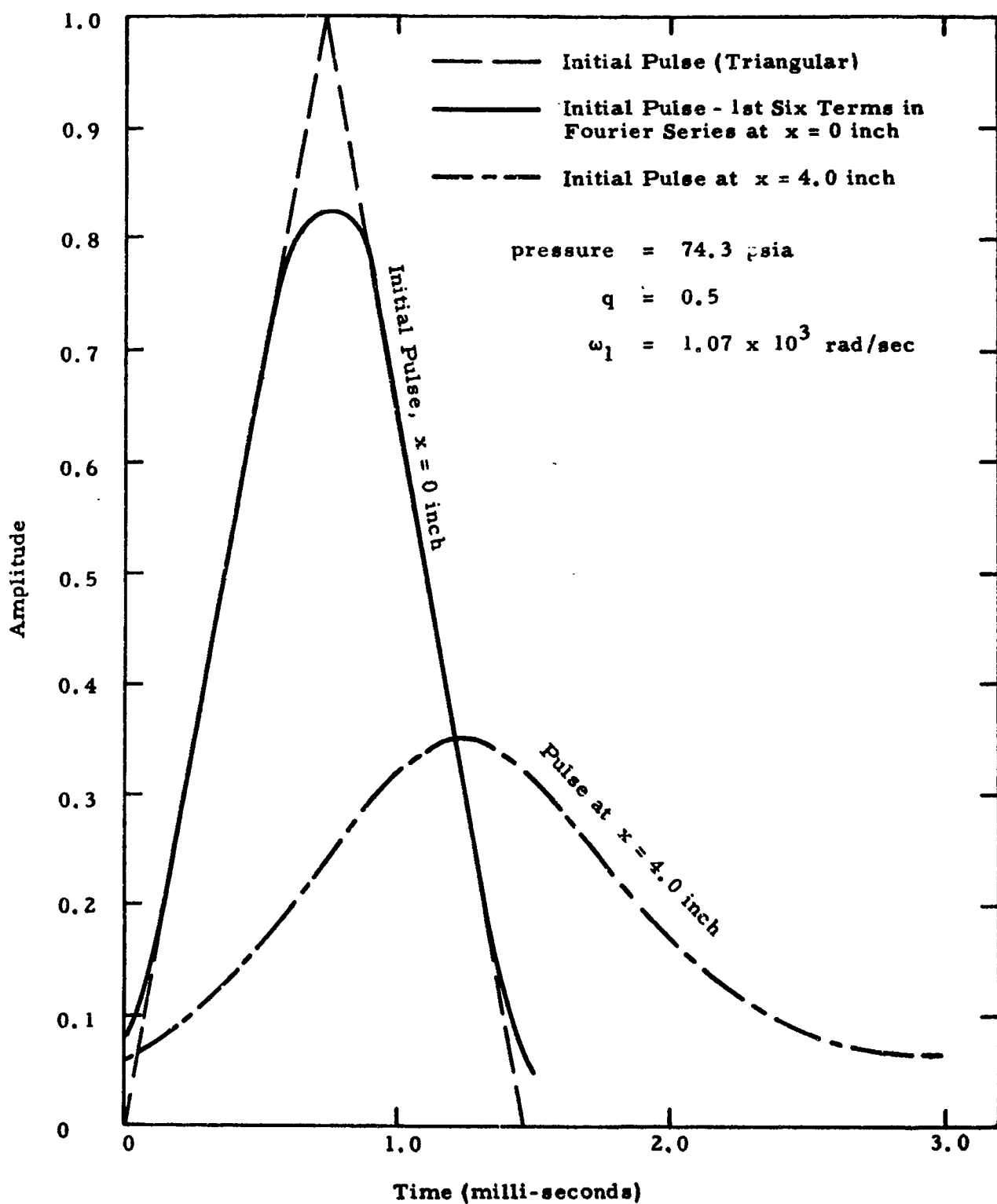


Fig. IV-10 PROPAGATION OF A TRIANGULAR SHAPED PULSE IN HYDROGEN MIXTURE

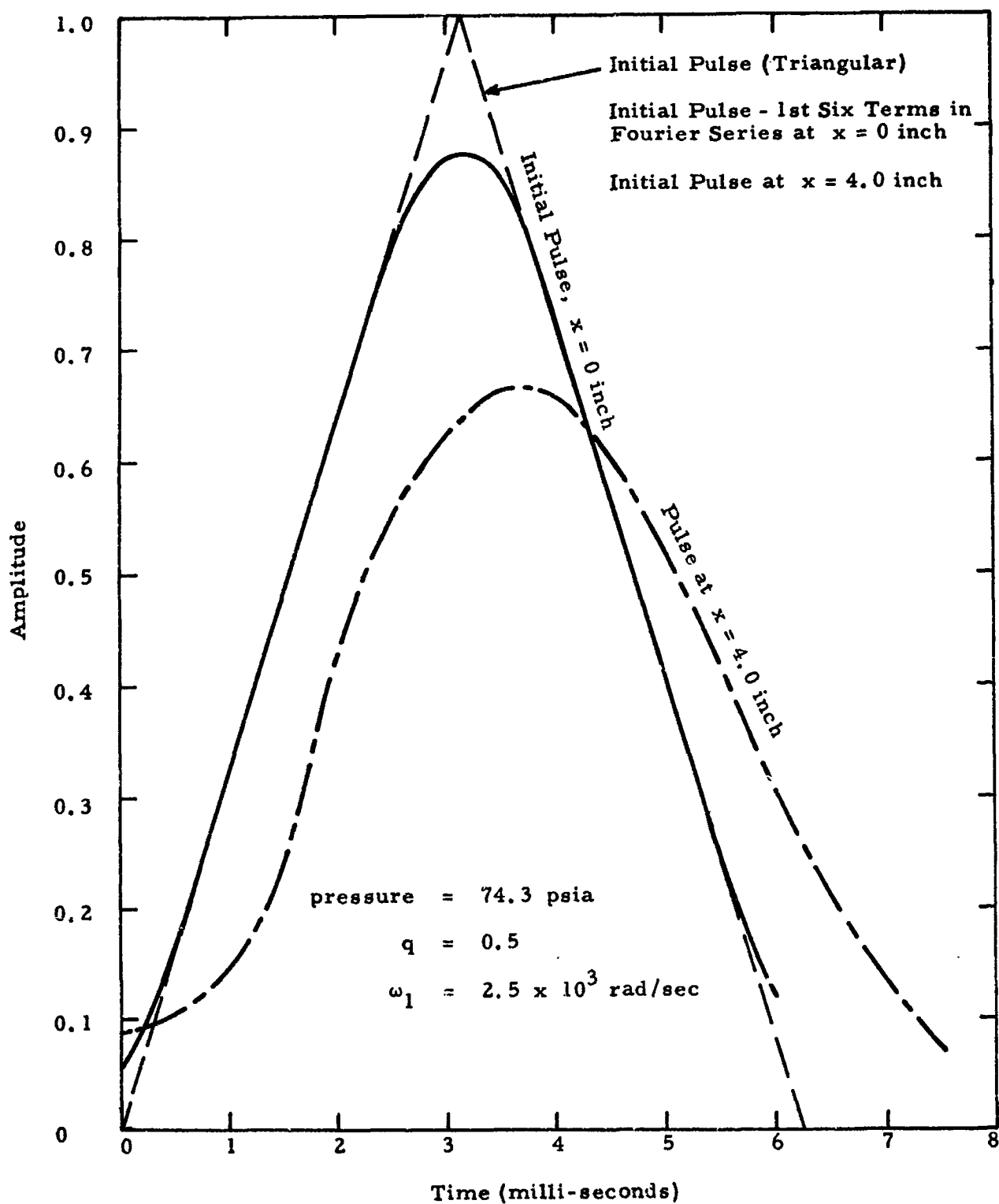


Fig. IV-11 TRIANGULAR SHAPED PULSE IN HYDROGEN MIXTURE

It may be tentatively suggested from the results that any small change in quality is unlikely to significantly affect the shapes of these pulse curves. In view of the limited time available it was decided not to pursue any further the problem of pulse propagation.

V. SUMMARY

Sound propagation in a two-phase fluid depends not only upon the relative masses of the phases, that is the quality, but also upon the size and spatial distribution of the constituent phases.

The propagation velocity is shown to increase with sound frequency. At very low frequencies the velocity depends only upon the quality, whereas at intermediate frequencies, the velocity is a complicated function of both the quality and aggregate phase sizes. At high frequencies the velocity approaches a fixed value, which is related directly to the properties of the predominant phase in the mixture.

Calculations for the low frequency velocity agree with those reported by other workers. Experimental data for the high frequency velocity in other two-phase fluids support the view that the propagation is governed by the dominant phase alone. This assumption is used in calculating the high frequency velocity in the liquid hydrogen-vapor mixture.

Calculations at intermediate frequencies lead to complicated expressions for the wave propagation constants. This is true even for an idealized two-phase fluid as, for example, a vapor fog containing uniformly spaced droplets of equal size.

Simplified expressions taking into account drag and heat transfer between the phases yield estimates of the relaxation times or time constants associated with these processes. These time constants determine the region of frequency and aggregate sizes of the individual phases in which these parameters have little effect on the propagation constants.

The sound velocity and absorption have been calculated using a simplified model. This model is valid only for one particular value of the quality (critical quality). At the critical quality no evaporation or condensation of liquid takes place for adiabatic pressure changes.

At qualities greater than the critical value, the calculated time constants due to heat conduction are further increased because of the additional heat transfer needed to evaporate the liquid. For qualities less than critical, adiabatic pressure increases produce condensation which increase the effective heat transfer. The detailed computation accounting for the mass transfer rate between the phases (in addition to simple heat conduction) involved estimates of the temperature gradients in the vicinity of the phase boundaries.

The precise meaning of the terms low, intermediate, and high frequencies used in the text is relative and their magnitude and range is determined by the droplet size and quality of the two-phase mixture. To illustrate the dependence of the frequency ranges on droplet size Table I has been constructed for a mixture of liquid hydrogen and vapor of critical quality at atmospheric pressure.

Application of the analysis given in this report to a direct measurement of quality in two-phase flow are limited to situations where the aggregates, i. e. droplets in fog or vapor bubbles in liquid, are exceedingly small. For normal droplet distributions working sound frequencies would, of convenience, lie in the intermediate range where the propagation velocity depends on the aggregate size as well as the quality. Methods of separating the unknown variables, that is the aggregate size and quality are, as far as is known, beyond the frontiers of present knowledge. Using low frequency

TABLE I

DEPENDENCE OF FREQUENCY ON DROPLET SIZE FOR HYDROGEN
MIXTURE OF CRITICAL QUALITY AT ATMOSPHERIC PRESSURE

<u>Droplet</u> <u>Diameter $2Rf$</u>	<u>Low Frequency</u> <u>Range</u>	<u>Intermediate</u> <u>Frequency Range</u>	<u>High Frequency</u> <u>Range</u>
2μ	$< 1500 \text{ c/s}$	$1500 \text{ c/s} - 36.5 \text{ Mc/s}$	$> 36.5 \text{ Mc/s}$
20μ	$< 15 \text{ c/s}$	$15 \text{ c/s} - 365 \text{ kc/s}$	$> 365 \text{ kc/s}$
200μ	$< 0.15 \text{ c/s}$	$0.15 \text{ c/s} - 3650 \text{ c/s}$	$> 3650 \text{ c/s}$
2mm	$< 0.0015 \text{ c/s}$	$0.0015 \text{ c/s} - 36.5 \text{ c/s}$	$> 36.5 \text{ c/s}$

It is to be noted that the low and high frequency sound velocities in the mixture are approached asymptotically (see Fig. IV-9). Because of this the low and high frequencies given in Table I are calculated to be those corresponding to the case when the sound velocity is within 3 % of its final value.

sound waves in aggregates of droplets or bubbles of moderate size involves difficulties of measuring very small phase differences in a progressive wave in the presence of turbulent noise and multiple reflected waves.

Calculations of the change of the shape of pulses propagating through the liquid hydrogen-vapor mixture are illustrated with examples. It is found that in the dispersion region the changing pulse shape is too rapid to permit any precise measurement to be made of the complex propagation velocity.

In the presence of more complex two-phase flow regimes as for example, annular or slug flow, the sound propagation will be unpredictable both in space and time. Under these conditions coupling between closely spaced sound transducers could perhaps indicate whether the fluid between them is, at any particular instant, predominantly liquid or vapor. The relative duration of the passage of liquid or vapor at any location could provide basic information on the phase distribution.

The result that at high frequencies the sound velocity is a function only of the simply connected phase and not of dispersed droplets or bubbles may be utilized in two-phase flow research to measure the flow velocity of the dominant phase. This would permit the slip velocity between the phases to be determined provided the velocity of the dispersed phase is independently known.

VI. CONCLUSION

Acoustic techniques have a specific, though limited application for supplementing the more conventional experimental methods used in two-phase flow research.

Useful data could be obtained by measuring the flow velocity of the dominant phase either in fog or bubble flow using an acoustic Doppler method. In the more complex flow regimes it may be possible to resolve the spatial phase distribution by the differences in acoustic coupling when the fluid flows between sound transducers

The original idea of determining the quality of a two-phase fluid by measuring the sound propagation constants has been shown to be subject to many difficulties; the exception being the special case of exceeding sr all flow aggregates.

Further development of instrumentation along the former lines is recommended.

LIST OF REFERENCES

1. Karplus, H. B., Armour Research Foundation, Report No. ARF 4132-12, January 1961.
2. Clinch, J. M., M.Sc. Thesis, London University, February 1962.
3. Shaffer, A., and Rousseau, J., ASD Technical Report 61-360, October 1961.
4. Smith, R. V., NBS Technical Note 179, August 1963.
5. Harry, D. P., Private Communication.
6. Courant, R., and Friedrichs, O., "Supersonic Flow and Shock Waves," Interscience Publications, Inc., New York, 1948.
7. Collingham, R. E., I and EC Design and Development, Vol. 2, p. 197, July 1963.
8. Herzfeld, K. F., and Litovitz, T. A., "Absorption and Dispersion of Ultrasonic Waves," Academic Press, New York, 1959.
9. Meixner, J., Ann Physik, (5), Vol. 43, p. 470, 1943.
10. Kneser, H. O., Ann Physik, (5), Vol. 16, p. 337, 1933.
11. Hiedemann, E., and Spence, R., Z. Physik, Vol. 133, p. 109, 1952.
12. Sewell, C. J. F., Phil. Trans. Roy. Soc., London, A210, p. 239, 1910.
13. Epstein, P. S., "Theodore von Karman Anniversary Volume," Cal. Inst. Tech., p. 162, 1941.
14. Epstein, P. S., and Carhart, R. R., J. Acoust. Soc. Am., Vol. 25, p. 553, 1953.
15. Zink, J. W., and Delsasso, L. P., J. Acoust. Soc. Am., Vol. 30, p. 8, 1958.
16. Lamb, H., "Hydrodynamics," p. 657, Dover, 6th Edition, 1932.
17. Carslaw, H., and Jaeger, J., "Conduction of Heat in Solids," Clarendon Press, Oxford, 1959.

LIST OF REFERENCES (Continued)

18. Goodwin, R. D., et al, NBS Report 6791, August 1961.
19. Lord Rayleigh, "Theory of Sound," Dover Publications, New York, Vol. 2, p. 321, 1945.
20. Henry, P.S.H., Proc. Phys. Soc., London, Vol. 43, p. 340, 1931.
21. Hilsenrath, J., et al, "Tables of Thermal Properties of Gases," NBS Circular 564, November 1955.

APPENDIX A

TEMPERATURE AND DENSITY FLUCTUATIONS ASSOCIATED WITH SOUND WAVES IN TWO-PHASE FLUIDS

1. INTRODUCTION

The periodic fluctuations in pressure involved in the transmission of sound waves in a gas, produce fluctuations in the gas temperature and density in accordance with the laws governing isentropic change. For an ideal gas, this leads to the following equation for the temperature and density of the gas associated with its pressure at any instant.

$$\left(\frac{T}{T_o}\right)^{\frac{\gamma}{\gamma-1}} = \left(\frac{\rho}{\rho_o}\right)^{\gamma} = \frac{p}{p_o} \quad (A-1)$$

The speed of sound c , is determined by the well known equation

$$c^2 = \left(\frac{\partial p}{\partial \rho}\right)_S \quad (A-2)$$

where S denotes isentropic changes in the gas. From equations 1 and 2 the speed of sound in an ideal gas is readily found to be:

$$c^2 = \gamma p / \rho \quad (A-3)$$

In a two-phase medium the pressure fluctuations produce negligible changes in the temperature of the liquid phase due to the relative incompressibility of the liquid compared with the compressibility of the vapor. The resulting fluctuation temperature difference between the vapor and liquid causes heat transfer to take place between the phases and reduces the amplitude of the temperature fluctuations in the vapor from what they would be if a liquid phase were not present. The temperature fluctuations are no longer in phase with the pressure fluctuations since time is required for the transfer of finite amounts of heat, and the fluctuations in the vapor temperature, therefore, lead the pressure fluctuations.

To perform an analysis of heat transfer between the phases it is required that the geometry of the phase boundaries be idealized to a simple shape. This appears to be physically justifiable for two kinds of two-phase flow; droplet or dispersed flow and bubble flow. Other types of two-phase flow are described in Appendix H and do not seem to permit this same kind of idealization. Dispersed or droplet flow is shown in Appendix H to exist over a wider range of quality than other types of two-phase flow. For this reason, and because the assumptions required in the analysis seem physically justifiable, two-phase droplet flow is selected for the following detailed analysis.

2. THEORETICAL MODEL

In droplet two-phase flow the droplets of liquid are dispersed uniformly in the vapor. Heat transfer phenomena take place in the liquid

droplet and in the region of vapor in the neighborhood of each droplet. It seems reasonable to idealize the actual geometry of the regions involved in the transfer of heat to one that is spherically symmetric. In this idealization the vapor space is treated as a spherical shell about a droplet of liquid as shown in Fig. A-1.

If all the droplets of liquid can be assumed to be of the same size, the temperature fluctuations at corresponding points in the vapor about each droplet will be the same, and heat will not flow between the vapor associated with one droplet and that associated with neighboring droplets. The outer spherical shell of the vapor, R_g , in the assumed model is therefore taken as insulated. Dimensions of the droplet and spherical shell are chosen so that the proportion of vapor and liquid is the same in the model as in the flow case under consideration.

$$\frac{R_g}{R_f} = \sqrt[3]{1 - \frac{q}{1 - q} \cdot \frac{\rho_f}{\rho_g}} \quad (A-4)$$

a. Boundary Conditions

A sound wave of angular frequency, ω , is considered to be passing through the two-phase medium. The wavelength over the frequency range of interest will be large with respect to the size of the heat transfer model and the pressure in the model can be considered to be uniform at any instant.

$$p = \bar{p} (\bar{p} + p' e^{i\omega t}) \quad (A-5)$$

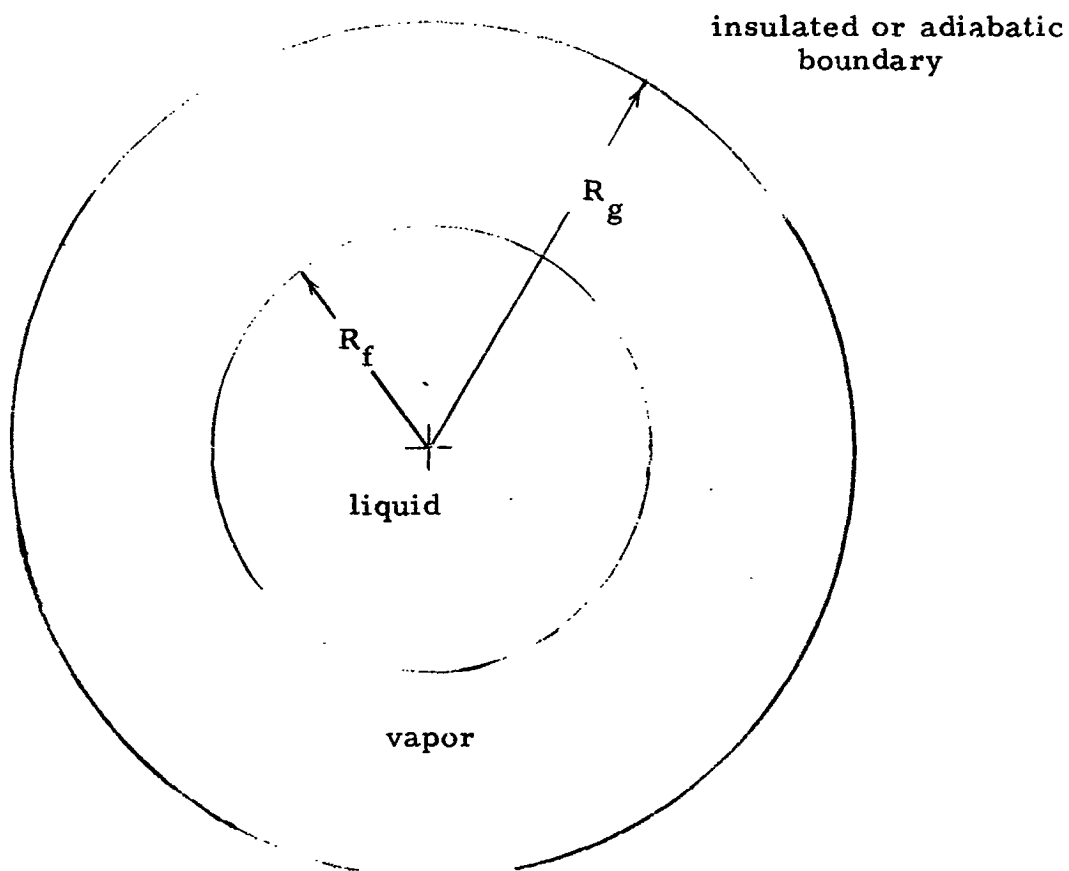


FIG. A-1 SKETCH OF MODEL ASSUMED FOR
HEAT TRANSFER ANALYSIS

(i) Interface Temperature

Since each phase consists of the same component, diffusion processes do not occur and the rate of evaporation or condensation is controlled by the transfer of heat. The temperature at the liquid-vapor interface is the saturation temperature corresponding to the pressure at any instant. The saturation temperature is conveniently found from the empirical relation shown below:

$$\ln p = A - B/T_s \quad (A-6)$$

If the amplitude of the pressure fluctuations is small, a linear relation can be assumed for the resulting fluctuation in the saturation temperature. The saturation temperature is also a harmonic function in this case.

$$T_s = \Re (\bar{T}_s + T_s' e^{i\omega t}) \quad (A-7)$$

where

$$T_s' = \frac{dT_s}{dp} \cdot p' = \frac{\bar{T}_s^2}{B\bar{p}} p' \quad (A-8)$$

(ii) Evaporation or Condensation at Interface

Evaporation or condensation will cause the radius of the drop to be time dependent and the principles of mass and energy conservation have to be applied at the liquid-vapor interface in terms of the velocity of the fluid relative to that of the boundary.

For mass conservation

$$-\rho_f \frac{dR_f}{dt} = \rho_g \left[U_g(R_f) - \frac{dR_f}{dt} \right] \quad (A-9)$$

For energy conservation

$$-H_f \rho_f \frac{dR_f}{dt} - k_f \left. \frac{\partial T_f}{\partial r} \right|_{R_f} = H_g \rho_g \left[U_g(R_f) - \frac{dR_f}{dt} \right] - k_g \left. \frac{\partial T_g}{\partial r} \right|_{R_f} \quad (A-10)$$

Employing the definition of the latent heat of vaporization,

$$H_{fg} = H_g - H_f$$

the velocity of the vapor U_g at the interface becomes

$$U_g = \frac{\left(1 - \frac{\rho_g}{\rho_f}\right)}{\rho_g H_{fg}} \left[k_g \left. \frac{\partial T_g}{\partial r} \right|_{R_f} - k_f \left. \frac{\partial T_f}{\partial r} \right|_{R_f} \right] \quad (A-11)$$

It will be shown later in this Appendix that the temperature gradient will also be a harmonic function with time for the case where the interface temperature is harmonic. In view of this the mass flow between phases is also harmonic if the density, thermal conductivity and latent heat of vaporization can be regarded as constant over the range of temperature and density fluctuation.

$$U_g' = \frac{\left(1 - \frac{\rho_g}{\rho_f}\right)}{\rho_g H_{fg}} \left[k_g \frac{dT_g'}{dr} \Big|_{R_f} - k_f \frac{dT_f'}{dr} \Big|_{R_f} \right] \quad (A-12)$$

where

$$U_g = U_g' e^{i\omega t}$$

$$T(r, t) = \Re \left[\bar{T} + T'(r) e^{i\omega t} \right]$$

(iii) Insulated Outer Shell

To satisfy the condition of no heat flow across the outer spherical shell the temperature gradient must be zero at this point.

$$\frac{\partial T}{\partial r} \Big|_{R_g} = \frac{dT'}{dr} \Big|_{R_g} = 0 \quad (A-13)$$

3. TEMPERATURE DISTRIBUTION IN THE DROPLET

Heat conduction in a sphere with a uniformly varying surface temperature is governed by the equation

$$\frac{1}{r^2} \frac{\partial \left(r^2 \frac{\partial T}{\partial r} \right)}{\partial r} = \frac{1}{\alpha_f} \frac{\partial T}{\partial t} \quad (A-14)$$

A solution to this equation which satisfies the harmonic temperature variation at the interface has the form of a product of two functions, one of the space co-ordinates only, the other a harmonic function of time.

$$T(r, t) = \mathcal{R} \left[\bar{T}_s + T'(r) e^{i\omega t} \right] \quad (\text{A-15})$$

Substituting equation 15 into equation 14 gives,

$$\frac{1}{r^2} \frac{d \left(r^2 \frac{dT}{dr} \right)}{dr} = \frac{i\omega}{a_f^2} T' \quad (\text{A-16})$$

which can be simplified to

$$\frac{d^2 F}{dr^2} = \frac{i\omega}{a_f^2} F \quad (\text{A-17})$$

by the substitution,

$$T' = F/r \quad (\text{A-18})$$

A general solution for equation 17 is

$$F = A \sinh \sqrt{\frac{i\omega}{a_f^2}} r + B \cosh \sqrt{\frac{i\omega}{a_f^2}} r \quad (\text{A-19})$$

From equation 18

$$\lim_{r \rightarrow 0} F = 0$$

and the constant β , therefore, must be zero to satisfy this condition.

$$F = A \sinh \sqrt{\frac{i\omega}{a_f}} r \quad (\text{A-20})$$

The other constant, A , is evaluated from the condition that

$$T'(R_f) = T'_s$$

This leads to

$$T' = T'_s \frac{R_f}{r} \frac{\sinh \sqrt{\frac{i\omega}{a_f}} r}{\sinh \sqrt{\frac{i\omega}{a_f}} R_f} \quad (\text{A-21})$$

To determine the gradient at the interface the above equation is differentiated and evaluated at $r = R_f$.

$$\left. \frac{dT'}{dr} \right|_{R_f} = \frac{T'_s}{R_f} \left[\sqrt{\frac{i\omega R_f^2}{a_f}} \coth \sqrt{\frac{i\omega R_f^2}{a_f}} - 1 \right] \quad (\text{A-22})$$

Alternative forms of this expression can be obtained by separating the real and imaginary parts.

$$\left. \frac{dT'}{dr} \right|_{R_f} = \frac{T_s'}{R_f} \left[(1 + i) \Lambda \frac{\sinh 2\Lambda - i \sin 2\Lambda}{\cosh 2\Lambda - \cos 2\Lambda} - 1 \right] \quad (\text{A-23})$$

where

$$\Lambda = \sqrt{\frac{\omega R_f^2}{2 \alpha_f}}$$

4. TEMPERATURE DISTRIBUTION IN THE VAPOR

Due to the compressibility of the vapor, the equations governing heat transfer in the vapor are not the same as in the liquid. In this case the governing equations are obtained by applying the conservation laws of mass and energy.

The mass flow into any region of the vapor space is equal to the rate of accumulation of mass in that region.

$$\frac{d}{dt} \int_r^{R_g} r^2 \rho \, dr = r^2 \rho U \quad (\text{A-24})$$

The rate at which internal energy is accumulated involves three effects; the internal energy carried in by the moving vapor, the work done by compression, and the energy loss by conduction.

$$\frac{d}{dt} \int_r^{R_g} r^2 \rho E dr = r^2 \left(\rho U E + p U - k_g \frac{\partial T}{\partial r} \right) \quad (A-25)$$

Differential equations which correspond to these integral equations are obtained by simple differentiation.

Conservation of mass:

$$\frac{1}{r^2} \frac{\partial (r^2 \rho U)}{\partial r} + \frac{\partial \rho}{\partial t} = 0 \quad (A-26)$$

Conservation of energy:

$$\frac{k_g}{r^2} \frac{\partial \left(r^2 \frac{\partial T}{\partial r} \right)}{\partial r} = \frac{\partial (\rho E)}{\partial t} + \frac{1}{r^2} \frac{\partial (r^2 \rho U H)}{\partial r} \quad (A-27)$$

where

$$H = E + p/\rho \quad (A-28)$$

It will be assumed here that the vapor can be treated as an ideal gas.

$$\rho = p/RT \quad (A-29)$$

$$E = C_V T \quad (A-30)$$

$$H = C_p T \quad (A-31)$$

Employing these relations the energy equation becomes

$$\frac{k_g}{r^2} \frac{\partial \left(r^2 \frac{\partial T}{\partial r} \right)}{\partial r} = \frac{C_V}{R} \frac{dp}{dt} + \frac{C_p}{R} \frac{p}{r^2} \frac{\partial (r^2 U)}{\partial r} \quad (A-32)$$

The pressure appears here as a total derivative since it is assumed to be uniform in the model and therefore not a function of the space co-ordinate.

To eliminate the velocity term in the above equation, the mass conservation equation (equation 26) is expanded as shown below.

$$\frac{1}{r} \frac{\partial (r^2 U)}{\partial r} = - \frac{1}{\rho} \frac{\partial \rho}{\partial t} - \frac{U}{\rho} \frac{\partial \rho}{\partial r} \quad (A-33)$$

Substituting equation 29 into the above equation gives,

$$\frac{1}{r} \frac{\partial (r^2 U)}{\partial r} = - \frac{1}{p} \frac{dp}{dt} + \frac{1}{T} \frac{\partial T}{\partial t} - \frac{U}{p} \frac{\partial T}{\partial r} \quad (A-34)$$

Substituting this expression for the velocity term into equation 32, gives the following for the energy equation.

$$\frac{k_g}{r^2} \frac{\partial \left(r^2 \frac{\partial T}{\partial r} \right)}{\partial r} = \frac{\partial T}{\partial t} - \frac{U}{R p} \frac{\partial T}{\partial r} - \frac{1}{\rho C_p} \frac{dp}{dt} \quad (A-35)$$

where

$$\alpha_g = \frac{k_g}{\rho C_p}$$

It is quite evident that the velocity is not eliminated by these substitutions. However, it now appears in a second degree term. The magnitude of the velocity is shown in equation 11, to be proportional to the temperature gradients. Consequently if one considers pressure waves of decreasing intensity, the magnitude of the product $U \partial T / \partial r$ decreases in proportion to the square of the pressure fluctuations, whereas the other terms decrease as the first power. For small amplitude pressure waves, or for sound waves, the term involving the velocity can be neglected and one has the form shown below as the governing equation in the vapor.

$$\frac{\alpha_g}{r^2} \frac{\partial \left(r^2 \frac{\partial T}{\partial r} \right)}{\partial r} = \frac{\partial T}{\partial t} - \frac{1}{\rho C_p} \frac{dp}{dt} \quad (A-36)$$

This equation can be solved by methods similar to those used in the liquid. Substituting equations 5 and 15 into equation 35 gives,

$$\frac{\alpha_g}{r^2} \frac{d \left(r^2 \frac{dT'}{dr} \right)}{dr} = i\omega T' - \frac{i\omega p'}{\rho C_p} \quad (A-37)$$

The general solution to this equation is

$$T' = \frac{p'}{\rho C_p} + \frac{C}{r} e^{\Omega r} + \frac{D}{r} e^{-\Omega r} \quad (\text{A-38})$$

where

$$\Omega = \sqrt{\frac{i\omega}{\alpha_g}} \quad (\text{A-39})$$

Applying the condition that the temperature gradient must be zero at the outer radius of the spherical shell (equation 13), leads to the following relation between the coefficients.

$$C = D \frac{\Omega R_g + 1}{\Omega R_g - 1} e^{-2\Omega R_g} \quad (\text{A-40})$$

Equation 35 can now be expressed as

$$T' = \frac{p'}{\rho C_p} + \frac{D e^{-\Omega R_g}}{r (\Omega R_g - 1)} \left[(\Omega R_g + 1) e^{\Omega (r - R_g)} + (\Omega R_g - 1) e^{-\Omega (r - R_g)} \right] \quad (\text{A-41})$$

Satisfying the condition that the temperature fluctuations at the interface match those of the saturation temperature (equation 7) defines the coefficient D.

$$D = \left(T_s' - \frac{p'}{\rho C_p} \right) \frac{R_f (\Omega R_g - 1) e^{\Omega R_g}}{(\Omega R_g - 1) e^{\Omega (R_g - R_f)} + (\Omega R_g + 1) e^{-\Omega (R_g - R_f)}} \quad (A-42)$$

The final expression for the temperature distribution is then,

$$T' = \frac{p'}{\rho C_p} + \left(T_s' - \frac{p'}{\rho C_p} \right) \frac{R_f}{r} \cdot \frac{(\Omega R_g - 1) e^{\Omega (R_g - r)} + (\Omega R_g + 1) e^{-\Omega (R_g - r)}}{(\Omega R_g - 1) e^{\Omega (R_g - R_f)} + (\Omega R_g + 1) e^{-\Omega (R_g - R_f)}} \quad (A-43)$$

Differentiating with respect to r and setting $r = R_f$ gives the temperature gradient in the vapor at the vapor-liquid interface.

$$\left. \frac{dT'}{dr} \right|_{R_f} = - \frac{\left(T_s' - \frac{p'}{\rho C_p} \right)}{R_f} \cdot \frac{(\Omega R_g - 1)(\Omega R_f - 1) - (\Omega R_g + 1)(\Omega R_f + 1) e^{-2\Omega (R_g - R_f)}}{\Omega R_g - 1 + (\Omega R_g + 1) e^{-2\Omega (R_g - R_f)}} \quad (A-44)$$

5. VOLUME FLUCTUATION

Two factors are involved in the volume fluctuation of the assumed model. The density of the vapor fluctuates due to the changing temperature and pressure, and the mass of vapor also fluctuates due to the alternate evaporation and condensation occurring at the interface. An appropriate expression relating these factors is

$$\frac{d}{dt} \int_{R_f}^{R_g} r^2 \rho_g dr = R_f^2 \rho_g (R_f) \left[U_g (R_f) - \frac{dR_f}{dt} \right] \quad (A-45)$$

The fluctuation of the outer radius is obtained by taking the derivative on the left hand side of the above equation inside the integral.

$$\frac{1}{R_g} \frac{dR_g}{dt} = \left(\frac{R_f}{R_g} \right)^3 \frac{\rho_g (R_f)}{\rho_g (R_g)} \frac{U_g (R_f)}{R_f} - \frac{1}{R_g^3 \rho_g (R_g)} \int_{R_f}^{R_g} r^2 \frac{\partial \rho}{\partial t} dr \quad (A-46)$$

If only small disturbances are considered the vapor density may be regarded as the same at R_f and R_g and the equation may be simplified to,

$$\frac{1}{R_g} \frac{dR_g}{dt} = \left(\frac{R_f}{R_g} \right)^3 \frac{U_g (R_f)}{R_f} - \frac{1}{R_g^3 \rho_g} \int_{R_f}^{R_g} r^2 \frac{\partial \rho}{\partial t} dr \quad (A-47)$$

The volume fluctuation is then obtained from the relation,

$$\frac{1}{V} \frac{dV}{dt} = \frac{3}{R_g} \frac{dR_g}{dt} \quad (\text{A-48})$$

$$\frac{1}{V} \frac{dV}{dt} = 3 \left(\frac{R_f}{R_g} \right)^3 \frac{U_g(R_f)}{R_f} - \frac{3}{R_g^3 f_g} \int_{R_f}^{R_g} r^2 \frac{\partial \rho}{\partial t} dr \quad (\text{A-49})$$

Equations 12, 23 and 44 give the contribution to the volume fluctuation due to evaporation and condensation. To determine the contribution due to the density variation, the integral on the right hand side of the above equation is expressed in terms of the temperature and pressure.

Differentiating equation 29 gives

$$\frac{1}{\rho} \frac{\partial \rho}{\partial t} = \frac{1}{p} \frac{dp}{dt} - \frac{1}{T} \frac{\partial T}{\partial t} \quad (\text{A-50})$$

The derivative of temperature with respect to time may be eliminated through equation 36.

$$\frac{1}{\rho} \frac{\partial \rho}{\partial t} = \frac{1}{p} \left(1 - \frac{R}{C_p} \right) \frac{dp}{dt} - \frac{1}{T} \frac{a_g}{r^2} \frac{\partial \left(r^2 \frac{\partial T}{\partial r} \right)}{\partial r} \quad (\text{A-51})$$

This equation may be used to evaluate the integral in equation 49 if only small disturbances are considered.

$$\frac{1}{\rho_g} \int_{R_f}^{R_g} r^2 \frac{\partial \rho}{\partial t} dr = \frac{1}{\gamma p} \frac{dp}{dt} \frac{1}{3} (R_g^3 - R_f^3) - \frac{1}{T} a_g R_f^2 \left. \frac{\partial T_g}{\partial r} \right|_{R_f} \quad (A-52)$$

where

$$1 - \frac{R}{C_p} = 1 - \frac{C_p - C_v}{C_p} = \frac{1}{\gamma}$$

The volume fluctuation is then

$$\begin{aligned} \frac{1}{V} \frac{dV}{dt} &= 3 \left(\frac{R_f}{R_g} \right)^3 \frac{U_g(R_f)}{R_f} - \frac{1}{\gamma p} \left[1 - \left(\frac{R_f}{R_g} \right)^3 \right] \frac{dp}{dt} \\ &\quad - \frac{3}{T} a_g \left(\frac{R_f}{R_g} \right)^3 \frac{1}{R_f} \left. \frac{\partial T_g}{\partial r} \right|_{R_f} \end{aligned} \quad (A-53)$$

Since the volume is a harmonic function, the above equation may be expressed as

$$\frac{V'}{\bar{V}} = - \frac{3i}{\omega} \left(\frac{R_f}{R_g} \right)^3 \frac{U_g'(R_f)}{R_f} - \left[1 - \left(\frac{R_f}{R_g} \right)^3 \right] \frac{p'}{\gamma \bar{p}} - \frac{3}{T} a_g \left(\frac{R_f}{R_g} \right)^3 \frac{1}{R_f} \left. \frac{dT_g'}{dr} \right|_{R_f} \quad (A-54)$$

where

$$V = \bar{V} + V' e^{i\omega t}$$

6. SOUND VELOCITY

The sound velocity in a single phase fluid is given by equation

2. In a two-phase fluid, the vapor may not be compressed or expanded isentropically because of the effects of heat transfer. However, if equation 2 is interpreted in terms of the spatial mean pressure and density over a volume containing a large number of droplets, the vapor and liquid taken in aggregate would be isentropic. This interpretation should be valid if the sound wavelength is large with respect to the mean distance between the droplets.

The sound velocity may be expressed in terms of the equation obtained for the volume fluctuations in the following way.

$$C^2 = \left(\frac{\partial p}{\partial \rho} \right)_S = \frac{\frac{dp}{dt}}{\frac{d\bar{\rho}}{dt}} = - \frac{\frac{dp}{dt}}{\bar{\rho} \frac{1}{V} \frac{dV}{dt}} = - \frac{\bar{V} p'}{\bar{\rho} V'} \quad (\text{A-55})$$

where

$$\bar{\rho} = \rho_g + (\rho_f - \rho_g) q \quad (\text{A-56})$$

The sequence of steps required to compute the velocity of sound are as follows. From the quality of the mixture the ratio of radius of the vapor shell to that of the drop is first computed.

$$\frac{R_g}{R_f} = \sqrt[3]{1 - \frac{q}{1 - q} \frac{\rho_f}{\rho_g}} \quad (\text{A-4})$$

The amplitude of the pressure fluctuation is arbitrarily assumed and used to calculate the fluctuation in the interface temperature.

$$T_s' = \frac{T_s^2}{B\bar{p}} p' \quad (\text{A-4})$$

$$\left. \frac{dT_f'}{dr} \right|_{R_f} = \frac{T_s'}{R_f} \left[(1 + i)\Lambda \frac{\sinh 2\Lambda - i \sin 2\Lambda}{\cosh 2\Lambda - \cos 2\Lambda} - 1 \right] \quad (\text{A-22})$$

where

$$\Lambda = \sqrt{\frac{\omega R_f^2}{2\alpha_f}}$$

$$\left. \frac{dT_g'}{dr} \right|_{R_f} = - \frac{T_s' - \frac{p'}{\rho C_p}}{R_f} .$$

$$\frac{(\Lambda R_g - 1)(\Lambda R_f + 1) - (\Lambda R_g + 1)(\Lambda R_f - 1) e^{-2\Lambda(R_g - R_f)}}{\Lambda R_g - 1 + (\Lambda R_g + 1) e^{-2\Lambda(R_g - R_f)}} \quad (\text{A-43})$$

where

$$\Omega = \sqrt{\frac{i\omega}{a_g}}$$

$$U_{g'}(R_f) = \frac{\left(1 - \frac{\rho_g}{\rho_f}\right)}{\rho_g H_{fg}} \left[k_g \frac{dT_g'}{dr} \Big|_{R_f} - k_f \frac{dT_f'}{dr} \Big|_{R_f} \right] \quad (A-12)$$

$$\begin{aligned} \frac{V'}{\bar{V}} = & - \frac{3i}{\omega} \left(\frac{R_f}{R_g} \right)^3 \frac{U_{g'}(R_f)}{R_f} - \left[1 - \left(\frac{R_f}{R_g} \right)^3 \right] \frac{p'}{\gamma \bar{p}} \\ & - \frac{3a_g}{\bar{T}} \left(\frac{R_f}{R_g} \right)^3 \frac{1}{R_f} \frac{dT_g'}{dr} \Big|_{R_f} \end{aligned} \quad (A-54)$$

$$C^2 = - \frac{p'}{\frac{V'}{\bar{V}} \left[\rho_g + (\rho_f - \rho_g) q \right]} \quad (A-55)$$

The sound velocity obtained this way is a complex number, and, as explained in this report includes the attenuation as well as the speed of propagation.

Unfortunately the results of this analysis require extensive computations. The above list of equations would not present much difficulty if only real numbers were involved. However, many of the variables

are complex (real and imaginary). The intricacy of the equations seems to preclude rationalizing them into separate expressions for the real and imaginary parts. Instead most of the arithmetic operations have to be performed in complex arithmetic.

As many digital computers now have the capability of performing computations in complex arithmetic, use of such computers would appear necessary for performing the required computations. The IIT Research Institute, has such a computer which could well perform these calculations. However, owing to limitations of time and funds, etc., its use is not anticipated at present. Instead approximate relaxation times are evaluated from solutions to the differential equation for the case of a unit step change in interface temperature. The details of this work are described in Appendix B.

APPENDIX B

APPROXIMATE RELAXATION TIMES FOR LIQUID DROPS SURROUNDED BY VAPOR

Relaxation times are an indication of the time required for a system to restore its equilibrium after an initial disturbance. The model in Appendix A is assumed to have a uniform temperature distribution initially and is then submitted to a sudden expansion or compression. In the liquid the temperature is at first unaffected. The temperature at the liquid-vapor interface is the new saturation temperature corresponding to the changed pressure. The temperature in the vapor is initially that obtained from an adiabatic pressure change (Eq. A-1).

Approximate estimates of the subsequent time-temperature histories in the liquid and vapor are given in the following calculations.

1. RELAXATION TIME OF THE LIQUID

The equation governing radial heat conduction in the liquid, Eq. A-14, is transformed to that for a flat slab by the transformation,

$$\phi = r (T - T_0) \quad (B-1)$$

After applying this transformation, Eq. A-14 becomes

$$\frac{\partial^2 \phi}{\partial x^2} = \frac{1}{a_f} \frac{\partial \phi}{\partial t} \quad (\text{B-2})$$

Boundary conditions after the transformation become,

$$\phi(r, 0) = 0$$

$$\phi(0, t) = 0$$

$$\phi(R_f, t) = R_f(T_s - T_o)$$

A solution to Eq. B-2 for these boundary conditions may be found in Ref. 17.

$$\phi = R_f(T_s - T_o) \left[\frac{r}{R_f} + \frac{2}{\pi} \sum_{j=1}^{\infty} \frac{(-1)^j}{j} \sin\left(j\pi \frac{r}{R_f}\right) e^{-\frac{a_f t j^2 \pi^2}{R_f^2}} \right] \quad (\text{B-3})$$

The average temperature in a droplet is then found from Eqs. B-1 and B-3 and the integral shown below

$$\bar{T} = \frac{3}{R_f^3} \int_0^{R_f} r^2 T dr \quad (\text{B-4})$$

The result obtained is

$$\bar{T} = T_s + (T_s - T_o) \frac{6}{\pi^2} \sum_{j=1}^{\infty} \frac{1}{j^2} e^{-\frac{\alpha_f t j^2 \pi^2}{R_f^2}} \quad (B-5)$$

Terms in this series with j greater than unity decrease with increasing time much more rapidly than the initial term. For practical purposes the relaxation time can be obtained by considering only the first term in the series. The relaxation time is by the usual definition the time required for the disturbance to decay by the factor, $1/e$. Considering only the first term, this occurs when the exponent is equal to unity. The relaxation time is, therefore,

$$\tau_f = \frac{R_f^2}{\alpha_f \pi^2} \quad (B-6)$$

To solve for the temperature distribution in the vapor, the governing equation (Eq. A-36) is put into the same form as the equation for the liquid. This is done by replacing the temperature by a new variable which is the difference between the temperature of the vapor and the temperature the vapor would have if the pressure changes took place adiabatically.

$$\Delta T = T - T_o \left(\frac{p}{p_o} \right)^{\frac{\gamma - 1}{\gamma}} \quad (B-7)$$

For small pressure changes this may be linearized to

$$\Delta T = T - \frac{\gamma - 1}{\gamma} \frac{T_o}{p_o} (p - p_o)$$

Since

$$\frac{\gamma - 1}{\gamma} = \frac{R}{C_p} = \frac{p_o}{C_p \rho_o T_o}$$

$$\Delta T = T - T_o - \frac{1}{\rho C_p} (p - p_o) \quad (B-8)$$

Substituting Eq. B-8 in Eq. A-36 gives

$$\frac{a_g}{r^2} \frac{\partial \left(r^2 \frac{\partial \Delta T}{\partial r} \right)}{\partial r} = \frac{\partial \Delta T}{\partial t} \quad (B-9)$$

This equation may now be transformed to that for a flat slab.

$$\psi = r (\Delta T - \Delta T_o) \quad (B-10)$$

The result is

$$\frac{\partial^2 \psi}{\partial r^2} = \frac{1}{a_g} \frac{\partial \psi}{\partial t} \quad (\text{B-11})$$

The boundary conditions for the transformed variable are,

$$\psi(r, 0) = 0 \quad (\text{B-12})$$

$$\psi(R_f, t) = R_f \Delta T_s \quad (\text{B-13})$$

where

$$\Delta T_s = T_s - T_o \left(\frac{p}{p_o} \right)^{\frac{\gamma - 1}{\gamma}} \quad (\text{B-14})$$

At the outer radius of the vapor shell, the insulated surface boundary condition transforms as shown below.

$$\left. \frac{\partial T}{\partial r} \right|_{R_g} = 0 \longrightarrow R_g \left. \frac{\partial \psi}{\partial r} \right|_{R_g} = \psi(R_g) \quad (\text{B-15})$$

Equation B-10 may be solved by the method of Fourier series.

A general solution is

$$\psi = A + Br + \sum_{j=1}^{\infty} \left[C_j \sin \lambda_j (r - R_f) + D_j \cos \lambda_j (r - R_f) \right] e^{-a_g \lambda_j^2 t} \quad (B-16)$$

Evaluating the coefficients from the boundary conditions gives

$$\psi = \Delta T_s \left[r - 2R_f \sum_{j=1}^{\infty} \frac{\sin \lambda_j (r - R_f) e^{-\lambda_j^2 a_g t}}{\lambda_j [R_g \sin^2 \lambda_j (R_g - R_f) - R_f]} \right] \quad (B-17)$$

where

$$R_g \lambda_j = \tan \lambda_j (R_g - R_f) \quad (B-18)$$

The average temperature in the vapor is then obtained from the expression below.

$$\overline{\Delta T} = \frac{3}{(R_g^3 - R_f^3)} \int_{R_f}^{R_g} r^2 \Delta T dr \quad (B-19)$$

Performing the integration gives,

$$\overline{\Delta T} = \Delta T_s - (\Delta T_s - \Delta T_o) \frac{6R_f^2}{(R_g^3 - R_f^3)} \sum_{j=1}^{\infty} \frac{e^{-a_g t \lambda_j^2}}{\lambda_j^2 [R_g \sin \lambda_j (R_g - R_f) - R_f]} \quad (B-20)$$

For computational purposes it is advantageous to put this equation in a dimensionless form. A new variable is defined as

$$\omega_j = \lambda_j (R_g - R_f) \quad (\text{B-21})$$

Substituting in Eq. B-20 and rearranging terms gives finally,

$$\overline{\Delta T} = \Delta T_s - (\Delta T_s - \Delta T_o) \frac{6 \left(\frac{R_g}{R_f} - 1 \right)^2}{\left(\frac{R_g}{R_f} \right)^3 - 1} \sum_{j=1}^{\infty} \frac{e^{-\frac{\alpha_g \omega_j^2 t}{R_f^2 \left(\frac{R_g}{R_f} - 1 \right)^2}}}{\omega_j^2 \left(\frac{R_g}{R_f} \sin \omega_j - 1 \right)} \quad (\text{B-22})$$

where

$$\omega_j \cot \omega_j = \frac{1}{1 - \frac{R_f}{R_g}} \quad (\text{B-23})$$

As in the equation for the liquid, the first term in the series decreases with time much more slowly than the others. For practical purposes only the first term in the series needs to be considered. The time constant is the time for which the first term has decreased by the factor $1/e$, or where the exponent is equal to minus one:

$$\tau_g = \frac{R_f^2 \left(\frac{R_g}{R_f} - 1 \right)^2}{\alpha_g \omega_1} \quad (\text{B-24})$$

The constant ω_1 , is the first root of Eq. B-23.

APPENDIX C

DERIVATION OF THE WAVE EQUATION TAKING INTO ACCOUNT DRAG BETWEEN THE LIQUID AND VAPOR PHASES

It has been shown in Section IV-A that when a sound wave is propagated through a homogeneous mixture of saturated hydrogen vapor and droplets, the relative velocity between the phases is dependent upon the value of the frequency parameter $\beta^2 R_f^2$. From what has been stated, each droplet opposes the vapor acceleration by the force X given by equation 4.1 Section IV-A. Because of this body force the dynamical equilibrium for an elementary volume of vapor undergoing pressure fluctuations in the sound wave must be modified. The following analysis is used to derive the wave equation taking into account this force.

Consider unit mass of a mixture of liquid hydrogen and vapor and assume there are N droplets each of mean radius R_f suspended uniformly in the vapor. Then the number of droplets per unit mass of vapor is N/q , where q is the quality.

Each droplet opposes the vapor acceleration by the force X . Therefore, the total reaction force on the vapor caused by N/q droplets per unit mass of vapor is $-NX/q$. The problem now reduces to determining the effect of this extraneous force on the wave equation.

Consider the equilibrium of unit volume of vapor of density ρ_0 at rest and bounded by sections x and $x + \delta x$ at time t .

*Elsewhere the vapor density is referred to as ρ_g .

Condensation of element δx is:

$$\rho \delta x = \rho_0 (1 + s) \delta x \quad (C.1)$$

where

$$s = \frac{\rho - \rho_0}{\rho} = \frac{\Delta \rho}{\rho}$$

and

$$\frac{\partial \rho}{\partial x} = \rho_0 \frac{\partial s}{\partial x}, \quad \frac{\partial \rho}{\partial t} = \rho_0 \frac{\partial s}{\partial t}$$

The continuity equation for the elementary volume is

$$\frac{\partial \rho}{\partial t} + \frac{\partial}{\partial x} (\rho U_g) = 0 \quad (C.2)$$

where

$$U_g = U_{g0} \exp i(\omega t + kx) \quad (C.3)$$

where

$$k = i\alpha_v - \frac{\omega}{c}$$

c being the phase velocity and α_v the attenuation coefficient due to drag.

The dynamical (Euler) equation for the forces acting on the element is

$$\rho \left(\frac{\partial U_g}{\partial t} + U_g \frac{\partial U_g}{\partial x} \right) \delta x = - \frac{\partial p}{\partial x} \delta x - \frac{N}{q} \rho X \delta x \quad (C.4)$$

Since the velocity amplitude is very small, $U_g \partial U_g / \partial x$ can be neglected in equation C.4, then,

$$\frac{\partial U_g}{\partial t} = - \frac{1}{\rho} \left(\frac{dp}{d\rho} \right)_S \frac{\partial \rho}{\partial x} - \frac{N}{q} X \quad (C.5)$$

The suffix S denotes an isentropic process in the vapor. Since,

$$\frac{\partial \rho}{\partial x} = \rho_o \frac{\partial s}{\partial x} \quad \text{and} \quad \rho_o \frac{\partial s}{\partial x} \quad (\text{small density fluctuations})$$

Equation C.5 becomes,

$$\frac{\partial U_g}{\partial t} = - \frac{1}{\rho} \left(\frac{dp}{d\rho} \right)_S \rho_o \frac{\partial s}{\partial x} - \frac{N}{q} X = - \left(\frac{dp}{d\rho} \right)_S \frac{\partial s}{\partial x} - \frac{N}{q} X \quad (C.6)$$

From equation C.2

$$\rho \frac{\partial U_g}{\partial x} = - \frac{\partial \rho}{\partial t} \quad (\text{since } U_g \text{ is small}) \quad (C.7)$$

and since,

$$\frac{\partial p}{\partial t} = \rho_o \frac{\partial s}{\partial t} \quad , \quad \frac{\partial U_g}{\partial x} = - \frac{\partial s}{\partial t} \quad (C.8)$$

Differentiating equations C.6 and C.8 with respect to t and x gives

$$\frac{\partial^2 U_g}{\partial t^2} = - \left(\frac{dp}{d\rho} \right)_S \frac{\partial}{\partial t} \left(\frac{\partial s}{\partial x} \right) - \frac{N}{q} \frac{\partial x}{\partial t} \quad (C.9)$$

and

$$\frac{\partial^2 U_g}{\partial x^2} = - \frac{\partial}{\partial x} \left(\frac{\partial s}{\partial t} \right) \quad (C.10)$$

Combining equations C.9 and C.10 the wave equation is obtained

$$\frac{\partial^2 U_g}{\partial t^2} = \left(\frac{dp}{d\rho} \right)_S \frac{\partial^2 U_g}{\partial x^2} - \frac{N}{q} \frac{\partial x}{\partial t} \quad (C.11)$$

In the case of a mixture of liquid hydrogen and vapor, the mass of liquid per unit mass of mixture is

$$(1 - q) = N \cdot \frac{4}{3} \pi R_f^3 \rho_f$$

where ρ_f is the density of liquid hydrogen. Accordingly, the wave equation C.11 for the two-phase mixture may be written as

$$\frac{\partial^2 U_g}{\partial t^2} = c_\infty^2 \frac{\partial^2 U_g}{\partial x^2} - \left(\frac{1-q}{q} \right) \frac{1}{\frac{4}{3} \pi R_f^3 \rho_f} \frac{\partial X}{\partial t}$$

where

$$c_\infty = \sqrt{\left(\frac{dp}{d\rho} \right)_S}$$

is the sound velocity in saturated hydrogen vapor (high frequency value).



APPENDIX D

COMPARISON OF PRESENT FORMULA FOR ATTENUATION DUE TO VISCOUS DRAG WITH THAT OF EPSTEIN AND CARHART

In Section IV-A it has been shown that the attenuation due to viscous drag, a_v as a function of the frequency parameter $\beta^2 R_f^2$, and quality q , is given by:

$$a_v = \frac{\omega}{c_\infty} \frac{(1 - q)}{q} \left(1 - \frac{\rho_g}{\rho_f} \right) \frac{\theta}{(1 + \theta)^2 + \theta^2} \frac{c}{c_\infty} \quad (D.1)$$

where

$$\frac{c_\infty}{c} = \left[1 + \frac{(1 - q)}{q} \left(1 - \frac{\rho_g}{\rho_f} \right) \frac{\theta (1 + \theta) + \theta^2}{(1 + \theta)^2 + \theta^2} \right]^{1/2} \quad (D.2)$$

Epstein and Carhart (Ref. 14) on the other hand quote the formula for the attenuation due to viscous drag as

$$a_E = \frac{6\pi N R_f}{c_\infty} \cdot \nu_g (1 + \beta R_f) I_E \quad (D.3)$$

where

$$I_E = \frac{16\beta^4 R_f^4}{16\beta^4 R_f^4 + 72 \frac{\rho_g}{\rho_f} \beta^3 R_f^3 + 81 \left(\frac{\rho_g}{\rho_f} \right)^2 \left[1 + 2\beta R_f + 2\beta^2 R_f^2 \right]} \quad (D.4)$$



The problem here is to show that under certain circumstances both the present theory and that of Epstein and Carhart represent alternative ways of describing the same phenomenon; that is, $a_v \stackrel{?}{=} a_E$. In equation D.3, N is the number of particles per unit volume

$$N = \frac{\rho_g}{\rho_f} \frac{(1 - q)}{q} \frac{1}{\frac{4}{3} \pi R_f^3} \quad (\text{in terms of the quality})$$

Substituting for N in equation D.3,

$$a_E = \frac{9}{2} \frac{\rho_g}{\rho_f} \frac{(1 - q)}{q} \frac{\nu_g}{R_f^2 c_\infty} (1 + \beta R_f) I_E \quad (\text{D.3a})$$

Rearranging equation D.1

$$a_v = \frac{2\pi}{c_\infty} f \frac{(1 - q)}{q} \left(1 - \frac{\rho_g}{\rho_f}\right) \theta \left[\frac{c}{c_\infty} \frac{1}{(1 + \Phi)^2 + \theta^2} \right]$$

$$a_v = \frac{2\pi}{c_\infty} f \frac{(1 - q)}{q} \frac{\rho_g}{\rho_f} \frac{9}{4} \frac{(1 + \beta R_f)}{\beta^2 R_f^2} \left(1 - \frac{\rho_g}{\rho_f}\right) \left[\frac{c}{c_\infty} \frac{1}{(1 + \Phi)^2 + \theta^2} \right]$$

since

$$\beta^2 R_f^2 = \frac{\omega R_f^2}{2\nu_g}$$

$$a_v = \frac{9}{2} \frac{\rho_g}{\rho_f} \frac{(1-q)}{q} \frac{\rho_g}{R_f^2 c_\infty} (1 + \beta R_f) D_v \quad (D.1)$$

where

$$D_v = \frac{c}{c_\infty} \frac{\left(1 - \frac{\rho_g}{\rho_f}\right)}{(1 + \Phi)^2 + \theta^2}$$

On comparing equations D.1a and D.3a, it is seen that $a_v = a_E$ provided $D_v = I_E$. Consider the expansion of $\left[(1 + \Phi)^2 + \theta^2\right]^{-1}$ in D_v

$$\begin{aligned} \frac{1}{(1 + \Phi)^2 + \theta^2} &= \frac{1}{\left[1 + \frac{\rho_g}{\rho_f} \left(\frac{1}{2} + \frac{9}{4\beta R_f}\right)\right]^2 + \left(\frac{\rho_g}{\rho_f}\right)^2 \frac{81}{16 \beta^4 R_f^4} (\beta R_f + 1)^2} \\ &= \frac{1}{1 + 2 \frac{\rho_g}{\rho_f} \left(\frac{1}{2} + \frac{9}{4\beta R_f}\right) + \left(\frac{\rho_g}{\rho_f}\right)^2 \left[\frac{1}{4} + \frac{9}{4\beta R_f}\right] + \left(\frac{\rho_g}{\rho_f}\right)^2 \frac{81}{16 \beta^4 R_f^4} +} \\ &\quad \left(\frac{\rho_g}{\rho_f}\right)^2 81 (\beta^2 R_f^2 + 2\beta R_f + 1) \end{aligned}$$

multiplying throughout by $16\beta^4 R_f^4$

$$\frac{1}{(1 + \Phi)^2 + \Theta^2} = \frac{16\beta^4 R_f^4}{16\beta^4 R_f^4 + 16 \frac{\rho_g}{\rho_f} \beta^4 R_f^4 + 72 \frac{\rho_g}{\rho_f} \beta^3 R_f^3 + \left(\frac{\rho_g}{\rho_f}\right)^2 \left[4\beta^4 R_f^4 + 9\beta^3 R_f^3 \right] + \left(\frac{\rho_g}{\rho_f}\right)^2 81 \left[1 + 2\beta R_f + 2\beta^2 R_f^2 \right]} \quad (D.5)$$

Comparing equation D.5 and D.4 it is seen that provided powers above the fourth are neglected in D.5, then:

$$\frac{1}{(1 + \Phi)^2 + \Theta^2} = I_E$$

$$a_v \frac{c}{c_\infty} \left(1 - \frac{\rho_g}{\rho_f} \right) a_E \quad (D.6)$$

Thus Epstein's and Carhart's theory fails to take into account

1. Dispersion in the sound velocity due to drag between the phases in the mixture.
2. Higher values of the gas to particle density ratio (ρ_g/ρ_f). Epstein considered only the case where $\rho_g/\rho_f \ll 1$, as for water droplets in air.



3. Coefficient greater than the fourth power in his function

I_E

4. Value of the frequency parameter $\beta^2 R_f^2 \sim 1$ when the frequency is high and/or when the droplet size is large.

It would appear therefore that provided the density ratio and velocity dispersion is small and the frequency low such that powers above the fourth in equation D.5 may be neglected, the two independent formulae for the wave attenuation due to phase drag are in good agreement.

APPENDIX E

EVALUATION OF THE CRITICAL QUALITY FOR A TWO-PHASE FLUID

During sound propagation in a two-phase fluid there is a unique value of the quality when the heat generated by an adiabatic compression in the vapor is not used in evaporating or condensating liquid. In other words none of the heat transferred by conduction in the vapor or liquid is used to promote phase change at the liquid-vapor boundaries. This critical quality can be evaluated in the following manner. Entropy per unit mass of mixture, $S = qS_{fg} + S_f$. For an isentropic change

$$dS = qdS_{fg} + S_{fg}dq + dS_f = 0$$

For small pressure changes,

$$S_{fg} \frac{dq}{dp} + q \frac{dS_{fg}}{dp} + \frac{dS_f}{dp} = 0$$

$$\frac{dq}{dp} = - \left[\frac{q \frac{dS_{fg}}{dp} + \frac{dS_f}{dp}}{S_{fg}} \right]$$

When there is no phase change during the isentropic process, $dq/dp = 0$, and $q = q_c$, is the critical quality. Therefore,

$$q_c = - \frac{(dS_f/dp)}{(dS_{fg}/dp)}$$

The value of q_c as a function of pressure has been calculated from the slopes of the entropy-pressure curves for liquid and vapor hydrogen. The results of these calculations are shown in Fig. E.1 for both equilibrium and para hydrogen. Thermodynamic data for the para hydrogen was taken from Ref. 18. It is seen from Fig. E.1 that for pressures below about 30 psia, the critical quality q_c increases rapidly with pressure. Above 30 psia, however, q_c reaches a constant value of about 0.42, although a slight variation is apparent. The reasons for this variation are not known.

The total change in the sound velocity due to viscous drag and heat conduction in the liquid hydrogen-vapor mixture is calculated in Section IV-B at one particular value of the critical quality. The effect of mass transfer on sound propagation is, of course, neglected in this case.

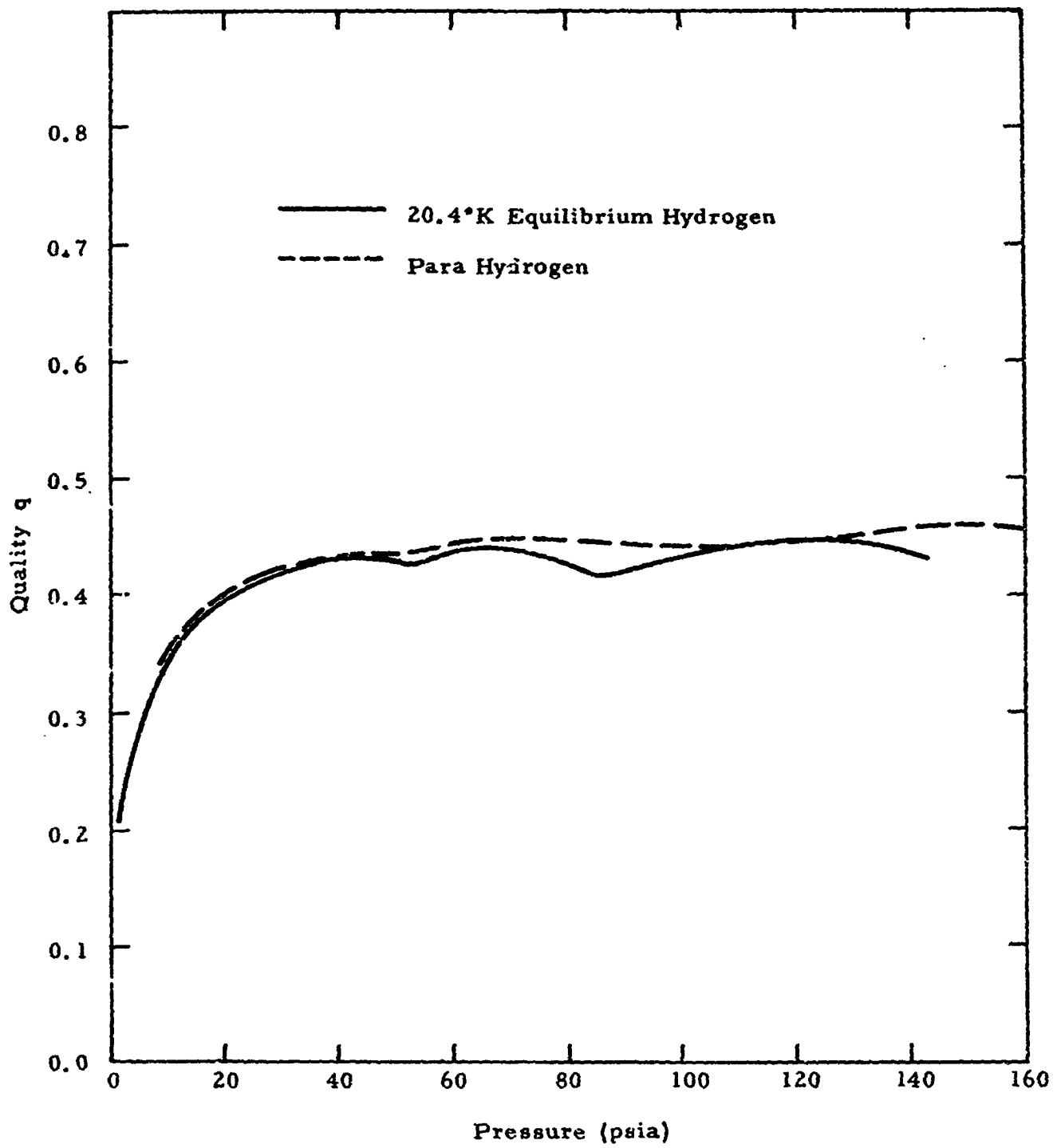


Fig. E1 PLOT OF CRITICAL QUALITY q_c AGAINST PRESSURE FOR HYDROGEN MIXTURE

APPENDIX F

EFFECT OF TUBE DIAMETER ON SOUND PROPAGATION CONSTANTS

The absorption and velocity dispersion of acoustic waves in fluids contained in narrow tubes due to viscosity and heat conduction has been analyzed by Kirchhoff (Ref. 19) and extended by other authors (Ref. 20). In general this effect is negligible, but for narrow tubes whose diameter is small compared to the wavelength, the viscous drag in the boundary layer at the tube walls influences wave propagation. An additional correction also has to be made for the heat conduction between the walls and fluid.

Analytical expressions for the corrected sound velocity c' , and attenuation constant α' , due to the effects of viscosity and heat conduction at the tube walls have been derived by Kirchhoff. These expressions are given by:

$$c' = c \left(1 - \frac{1}{2r_T} \sqrt{\frac{2\nu'_g}{\omega}} \right) \quad (F.1)$$

where ν'_g is the corrected kinematic viscosity, ν_g , and r_T is the tube radius, and

$$\nu'_g = \nu_g \left[1 + \left(\sqrt{\gamma_0} - \frac{1}{\sqrt{\gamma_0}} \right) \frac{k_g}{C_{pg}\mu_g} \right] \quad (F.2)$$

where γ_0 is the ratio of the specific heats of the fluid. Also, for the attenuation constant:

$$\alpha' = \frac{\alpha}{r_T c} \sqrt{\frac{\gamma_g' \omega}{2}} \quad (\text{F.3})$$

Equation F.2 gives the correction to the kinematic viscosity due to heat conduction between the tube walls and fluid. It may be seen from the above equations that at high frequencies and with tubes of large diameter, the corrected sound velocity c' approaches the free space velocity c . On the other hand for tubes of very small diameter, the effect of viscosity and heat conduction is to lower the sound velocity and increase the absorption in the fluid. It is of interest to note that for very fine capillary tubes such that $r_T \ll \sqrt{\gamma_g' / \omega}$, the wall temperature governs the fluid temperature and the process of sound propagation becomes isothermal rather than adiabatic. This source of velocity dispersion will be neglected in the present study.

To obtain an order of magnitude assessment of the effect of tube diameter on sound propagation a calculation is given for the mixture of liquid and vapor hydrogen contained in a narrow tube of 3/16 in. diameter. The frequencies necessary to lower the sound velocity 5 % for tubes of this diameter are obtained for several pressures. The data required to make these calculations is given in Table F-I.

Values of the critical quality q_c are used to calculate γ_0 so that the effects of phase change on sound propagation may be neglected. The ratio of the specific heats at low frequency, γ_0 in equation F.2 is calculated from

TABLE F-1

EFFECT OF TUBE WALLS ON KINEMATIC VISCOSITY OF VAPOR

P (lb/in ² abs)	T (°R)	q_c	C_{pg} (BTU/lb °R)	ρ_g (lb/ft ³)	μ_g (10 ⁻⁶ lb/sec ft)	k_g (10 ⁻⁶ BTU/sec ft °R)
14.7	36	0.375	2.60	0.084	0.735	2.70
48.	45	0.435	2.98	0.251	0.904	3.22
120.	54	0.450	3.36	0.684	1.07	3.67

C_{pfo} (BTU/lb °R)	ν_g (10 ⁻⁶ ft ² /sec)	ν'_g (10 ⁻⁶ ft ² /sec)	γ_o
2.32	8.73	10.90	1.194
2.80	3.60	4.44	1.214
3.45	1.56	1.87	1.216

$$\gamma_o = \frac{q_c \gamma_\infty + \frac{(1 - q_c)}{C_{vg}} C_{pfo}}{q_c + \frac{(1 - q_c)}{C_{vg}} C_{pfo}} \quad (F.4)$$

Equation F.4 has been derived in Section IV-B. Values of k_g , C_{pg} , C_{pfo} , μ_g , and ν_g for saturated hydrogen vapor were obtained from Ref. 21. Substituting this data in equation F.2 gives the corrected kinematic viscosity ν'_g from which the corrected sound velocity can be derived. Rewriting equation F.1 in the form:

$$\frac{\Delta c}{c} = \frac{1}{2r_T} \sqrt{\frac{2\nu'_g}{\omega}} \quad \text{where } \Delta c = \text{sound velocity change, } (c - c')$$

A 5 % decrease in velocity due to the tube effect gives the frequency f , as

$$f = \frac{100 \nu'_g}{A} \quad (F.5)$$

where $A = \pi r_T^2$ = cross-sectional area of tube. For a tube of 3/16 in. diameter, $A = \pi (1/128)^2 \text{ ft}^2 = 1.92 \times 10^{-4} \text{ ft}^2$. At 14.7 psia, $\nu'_g = 1.09 \times 10^{-5} \text{ ft}^2/\text{sec}$, then from equation F.5, $f \sim 6.0 \text{ cycles/sec}$. At 48 psia, $\nu'_g = 4.44 \times 10^{-6} \text{ ft}^2/\text{sec}$, then, $f \sim 2.0 \text{ cycles/sec}$. At 120 psia, $\nu'_g = 1.87 \times 10^{-6} \text{ ft}^2/\text{sec}$, then, $f \sim 1.0 \text{ cycles/sec}$.

It is to be noted that a frequency of 6.0 cycles/sec would be required to lower the sound velocity 5 % in the liquid hydrogen-vapor mixture of quality 0.375 at atmospheric pressure. This value is considerably below the frequency of 30 cycles/sec calculated in Section IV-B to yield the equilibrium sound velocity in the mixture under the same conditions.

It may be concluded, therefore, that the effect of tubes of 3/16 in. diameter on the low frequency equilibrium sound velocity is generally very small.

APPENDIX G

DERIVATION OF THE FORMULA USED TO CALCULATE THE HIGH FREQUENCY SOUND VELOCITY

By definition, the sound velocity in a fluid is

$$c = \sqrt{\left(\frac{\partial p}{\partial \rho}\right)_S}$$

where S denotes isentropic conditions. Alternatively this may be written in terms of the specific volume V , of a gas as

$$c^2 = -V^2 \left(\frac{\partial p}{\partial V}\right)_S \quad (G.1)$$

Enthalpy per unit mass of gas is

$$H = E + pV$$

$$dH = TdS + Vdp$$

E is the internal energy per unit mass of gas. Thus for an isentropic process, where $dS = 0$,

$$\left(\frac{\partial H}{\partial p}\right)_S = V \quad (G.2)$$

Using the first law of thermodynamics,

$$TdS = dE + pdV = 0$$

Therefore,

$$\left(\frac{\partial E}{\partial V}\right)_S = -p \quad (G.3)$$

Expressing equation G.1 in terms of H and E, and substituting equations G.2 and G.3 into G.1,

$$c^2 = -v^2 \left(\frac{\partial p}{\partial H}\right)_S \left(\frac{\partial H}{\partial V}\right)_S = -v^2 \left(\frac{\partial p}{\partial H}\right)_S \left(\frac{\partial H}{\partial E}\right)_S \left(\frac{\partial E}{\partial V}\right)_S$$

Therefore,

$$c^2 = \frac{p}{\rho} \left(\frac{\partial H}{\partial E}\right)_S \quad (G.4)$$

Now,

$$\left(\frac{\partial H}{\partial E}\right)_S = \frac{H}{E} + E \left[\frac{\partial(H/E)}{\partial E} \right]_S$$

Then,

$$c^2 = \frac{p}{\rho} \frac{H}{E} + \frac{pE}{\rho} \left[\frac{\partial(H/E)}{\partial E} \right]_S$$

or

$$c^2 = \frac{p}{\rho} \frac{H}{E} \left[1 + \frac{E^2}{H} \left[\frac{\partial(H/E)}{\partial E} \right]_S \right] \quad (G.5)$$

The above expression G.5 for the sound velocity c , as a function of H , E , p , and ρ is used to calculate the high frequency propagation velocity, c_∞ in the liquid hydrogen-vapor mixture. This is discussed in Section II-D.

APPENDIX H

LITERATURE ON BOILING HEAT TRANSFER AND TWO PHASE FLOW

NOMENCLATURE FOR APPENDIX H

A	=	area
C_p	=	specific heat at constant pressure
G	=	mass velocity
g	=	acceleration due to gravity
h	=	heat transfer rate
H_{fg}	=	latent heat of vaporization
k	=	thermal conductivity
N_{Nu}	=	Nusselt number
N_{Re}	=	Reynolds number
N_{Pr}	=	Prandtl number
\dot{Q}	=	heat flow rate
T	=	temperature
T_s	=	saturation temperature
ρ	=	density
X_{ti}	=	Lockhart-Martinelli parameter for turbulent turbulent flow
x	=	quality $G_g / (G_g + G_f)$
σ	=	surface tension
μ	=	dynamic viscosity

SUBSCRIPTS

f	=	liquid
g	=	vapor or gas
t	=	total
TP	=	two-phase
SPL	=	single-phase-liquid

APPENDIX H

LITERATURE ON BOILING HEAT TRANSFER AND TWO PHASE FLOW

1) INTRODUCTION

Boiling is the process of heat addition to a fluid resulting in a change of phase from liquid to vapor. Boiling heat transfer may occur in systems:

- a) where only natural convective forces operate. This process is known as pool boiling and may be further sub-divided into nucleate and film boiling
- b) where forced convective forces are imposed which result in the flow of fluid along a tube or channel. Due to evaporation the fluid is a mixture of liquid and its vapor at the saturation condition. This is described as one-component two-phase flow. The flow of a mixture of a liquid and some other gas or vapor is described as two-component two-phase flow.

It is evident from the volume of published material that substantial research effort has been invested in studies of boiling heat transfer and the characteristics of two-phase flow. To a great extent, the heat transfer work has been concentrated on pool boiling, particularly in the nucleate range. Two-phase flow studies have been mainly directed to the prediction of pressure drop, friction factors and choking or critical mass flow. On grounds of convenience and the direct applicability of results much of the work on heat transfer has been carried out using water. Similarly, with two-phase flow, the studies have been made mainly with mixtures of water and steam or water and air.

Single-component two-phase flow is generally more complicated both experimentally and analytically than two-component two-phase flow. In addition to momentum and energy transfer there exists the possibility, with single-component two-phase flow, of mass transfer at the vapor-liquid interface with consequent changes in the phase velocities and the density along a flow section.

Data on boiling heat transfer and the two-phase flow characteristics of cryogenic fluids and systems are steadily accumulating but the volume of data available at this time is too limited and too specialized to allow for its effective use to accurately predict the performance of systems in general.

2) STATUS OF THE PROBLEM

In a recent (1962) comprehensive review Zuber and Fried¹ have critically examined the use of available data for predicting the rates of heat transfer to liquid hydrogen in particular and other fluids in general when a change of phase takes place. Both pool boiling and two-phase flow systems were considered. Their conclusions are so pertinent as to be worth quoting here in entirety:

a) Nucleate Pool Boiling

"The proposed correlations for nucleate pool boiling do not take into account the conditions of the heating surface. Consequently these equations are not general and cannot predict the heat transfer rates for any solid-liquid combinations.

For a 'smooth' surface and for a given solid-liquid combination, the equation proposed by Rohsenow² can be used for predicting the heat transfer rates to liquid hydrogen at various pressures

when the value of a constant (for a particular solid-liquid combination) is determined from one set of experimental conditions. An equally satisfactory agreement was obtained using an equation proposed by Labountzov.³

Quantitative experimental data pertaining to the effect of surface conditions on the heat transfer rates in nucleate boiling are very scarce."

b) Forced Convection with a Change of Phase

"Experimental data indicate that the heat transfer coefficient in forced convection with a change of phase depends on the two-phase flow patterns.

Reliable correlation for predicting the two-phase heat transfer coefficients are not available. The correlation schemes available in the literature cannot be used for predicting the two-phase heat transfer coefficient to liquid hydrogen in forced flow.

An understanding of the two-phase flow patterns will be required before successful correlation of two-phase heat transfer coefficients can be made."

c) Critical Heat Flux Density

"The critical heat flux density to liquid hydrogen in pool boiling can be predicted from equations available in the literature.

No general equations that would permit the reliable prediction of the critical heat flux in forced convection are available. Experimental data indicate that in forced convection the

critical heat flux can be induced by several mechanisms."

d) Effect of Reduced Gravity

"The vapor generation is unaffected by a reduction in the gravitational field whereas the vapor removal depends on the nature of the force field. Both problems can be analyzed in terms of information available in the literature."

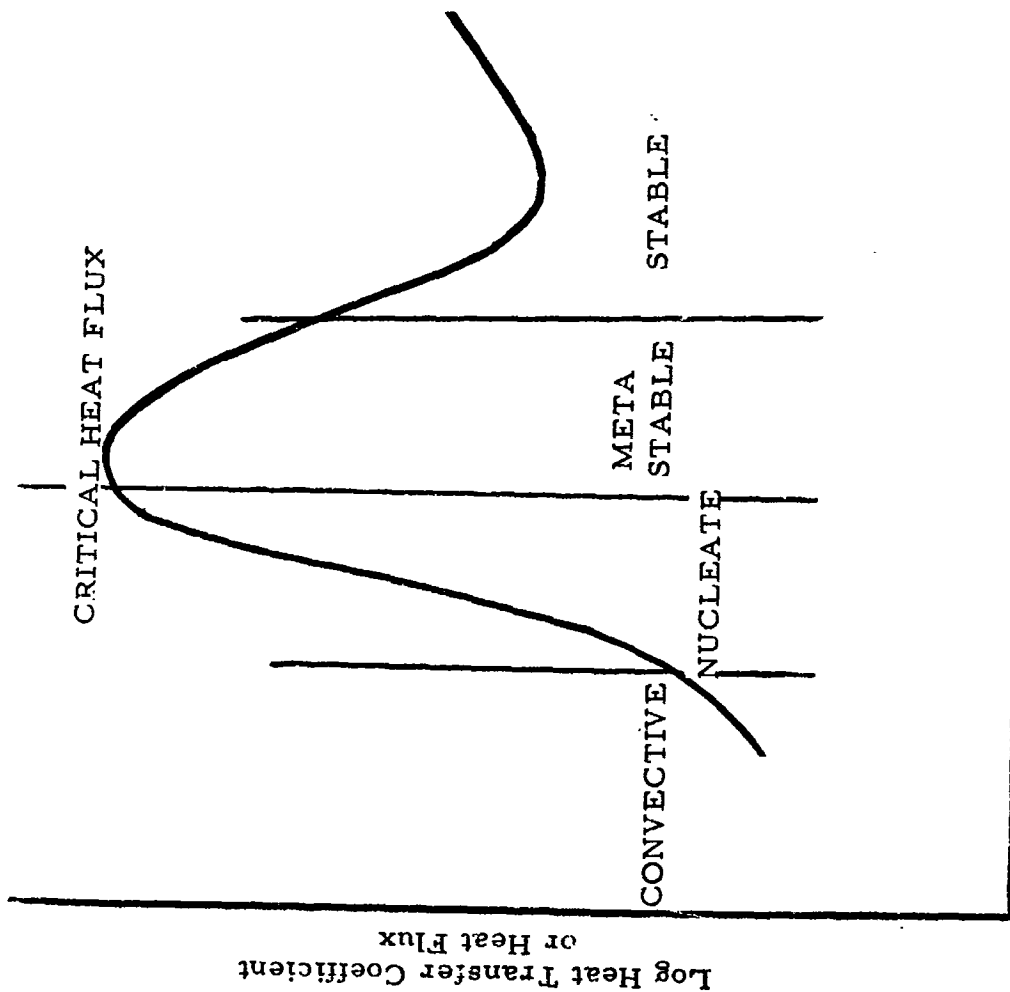
An independent survey of the literature, including that available subsequent to the critical review quoted above, does not reveal justification for any substantial revision of these conclusions.

The mechanism of pool boiling is sufficiently understood except for the effect of the surface finish of the solid heater or container. Much more analytical and experimental work remains to be done before a similar understanding of any two-phase flow system is completely established.

3) GENERAL DISCUSSION

a) Pool Boiling

Pool boiling occurs when heat is supplied so as to evaporate a liquid without the imposition of forced convective forces. Four distinct regions may be recognized in which the boiling exhibits different characteristics, as first recognized by Nukiyama⁴. These regimes depend on the temperature difference between the liquid and the solid heater surface and they may be defined as the convective, nucleate, meta-stable and stable film boiling regions as shown in Fig. H-1. As the heater surface temperature rises in a pool of unsaturated liquid natural convective currents are established. These circulate liquid, some of which evaporates at the free surface. A further increase in heater temperature



Log Temp. Difference Between Wall and Fluid

Fig. H-1 POOL BOILING CHARACTERISTIC VARIATION
IN HEAT TRANSFER COEFFICIENT OR HEAT FLUX
WITH TEMPERATURE DIFFERENCE BETWEEN
WALL AND FLUID

results in the formation of small vapor bubbles on the heater surface which grow to a critical size, depart and then condense before reaching the free surface. This is the phenomenon of partial boiling, as it is so called.

As the temperature difference increases more and larger vapor bubbles form which rise to the surface, break through it and join the vapor above the liquid. This is the region of nucleate boiling and is characterized by increase in both the heat flux and the heat transfer coefficient with increase in the temperature difference up to a maximum value called 'the critical heat flux'.

If more heat is supplied to the heater an unstable film of vapor forms on the solid surface. Large bubbles form on the outer surface of the film and the film itself collapses and reforms rapidly. The presence of the film reduces the heat transfer coefficient, an effect which consequently reduces the heat flux to the liquid. This causes an increase in the heater temperature thus increasing the difference between it and the liquid temperature and thereby accentuating the formation of the vapor film. This cumulative process proceeds until the vapor film becomes stable and continuous with a low heat flux and a large difference in temperature between the heated surface and the liquid. Eventually, unless the heater is first burned out, the influence of radiation from the very hot heater surface becomes significant and the heat flux once more increases. Once the stable film is established the vapor bubbles form at the outer edges of the vapor film and the metal surface has little effect.

The region of nucleate boiling is of greatest interest because this is where the maximum heat transfer coefficients and heat fluxes can be obtained. Experimental data has shown that the condition of the surface

has a substantial effect on these quantities because both depend not only on the temperature difference but also on the number of bubbles produced. The bubble population density depends on the nucleation characteristics of the surface, an important factor of which is the size of the surface irregularities. Jakob and Fritz⁵ investigated boiling on rough and smooth heating surfaces and found that the heat flux of the rough surface was greater than that of the smooth, but no satisfactory correlation of the effect of surface irregularities appears to have been produced. It may be mentioned that the relationship between surface roughness and nucleation site density is being further investigated in the Heat Transfer Laboratory of the Illinois Institute of Technology.⁶ This study substantiates the early findings of Jakob and Fritz. Kezios and co-workers are also investigating the frequency spectrum of nucleation sites.

Some two dozen equations have been proposed to correlate data in the nucleate boiling region. Most are limited to the range and conditions in which the experiments were conducted but a few have been found to correlate the experimental results for a number of liquids and liquid-solid combinations.

One equation proposed by Rohsenow² for 'smooth' surface is of the form

$$\frac{h}{k_f} \left[\frac{\sigma}{g(\rho_f - \rho_g)} \right]^{1/2} = \frac{1}{C} \left[\frac{\dot{Q}/A}{\mu_f H_{fg}} \left[\frac{\sigma}{g(\rho_f - \rho_g)} \right]^{1/2} \right]^{2/3} N_{Pr}^{-0.7} \quad (H-1)$$

The constant C has different values for different surface-liquid combinations and must be determined from experimental results available for a given surface.

Another equation recommended for use by Zuber and Fried¹ when the constant C cannot be determined is that proposed by Labountzov:³

$$\frac{h}{k_f} \frac{C_p \rho_f}{(\rho_g H_{fg})^2} \sigma T_s = 0.125 N_{Re}^{0.65} N_{Pr}^{1/3} \quad (H-2)$$

For $N_{Re} > 10^{-2}$, and

$$\frac{h}{k_f} \frac{C_p \rho_f}{(\rho_g H_{fg})^2} \sigma T_s = 0.0625 N_{Re}^{0.5} N_{Pr}^{1/3} \quad (H-3)$$

For $N_{Re} < 10^{-2}$ where

$$N_{Re} = \frac{\rho_f}{\rho_g} \frac{\dot{Q}/A}{\mu_f H_{fg}} \frac{C_p \rho_f \sigma T_s}{(\rho_g H_{fg})^2} \quad (H-4)$$

For the critical heat flux in pool boiling Zuber and Fried¹ recommend the use of the following approximate equation:

$$\frac{(\dot{Q}/A)_{crit}}{\rho_g H_{fg}} \left[\frac{\rho_g^2}{\sigma_g (\rho_f - \rho_g)} \right]^{1/4} \simeq \pi/24 \quad (H-5)$$

b) Some Aspects of Two-Phase Flow

In general two-phase flow has been classified as:

- a) one component - a mixture of liquid and its vapor
- b) two component - a mixture of liquid and a gas of different composition.

Other more complex mixtures may exist such as a liquid and its vapor at saturation conditions with a gas of different composition. These however do not appear to have been classified or to have received any significant study.

Many of the characteristics of one component and two component flow appear to be similar. One component flow is the more complicated of the two types both analytically and experimentally. This is because in addition to momentum and energy transfers there may also be mass transfer between phases at the liquid vapor interface along any flow section.

A flow equation including these various degrees of freedom requires knowledge of an accurate flow model incorporating the possibilities of different phase velocities (slip) and variation in density because of a change in the quality along the flow section. No satisfactory equalities of this type have yet been proposed and essentially no work has been done for the case where the flow patterns are changing. The mass, momentum and energy transfers at the liquid-vapor interface are all rate processes which require time to attain their equilibrium values. Although of obvious importance very little is known about these transfer rates under flow conditions but many instances of metastable flow have been reported.

Much of the work on two phase flow has been directed to the identification of the various flow patterns that can exist, the prediction of two phase pressure drop during isothermal flow and the determination of criteria for choking or critical mass flow.

Flow Patterns

Martinelli et al⁷ have identified four basic types of flow:

- (i) Viscous liquid and viscous vapor
- (ii) Viscous liquid and turbulent vapor
- (iii) Turbulent liquid and viscous vapor
- (iv) Turbulent liquid and turbulent vapor.

They have also suggested the classification of flow in terms of a Reynolds number.

A comparison of flow patterns observed by other investigators has been made by Alves.⁸ He listed the following sequence of flow patterns in a horizontal pipe as the gas phase mass velocity is increased.

- (i) Pure liquid
- (ii) Bubble flow (bubbles move along the upper part of the pipe at about the same velocity as the liquid)
- (iii) Plug flow (alternate plugs of gas and liquid)
- (iv) Stratified flow (vapor flowing above the liquid)
- (v) Wavy flow (vapor above a wavy liquid surface)
- (vi) Slug flow (periodic frothy slugs pass through the pipe at a greater velocity than the average liquid velocity)
- (vii) Annular flow (liquid flows in a film around the inside wall of the pipe and the gas flows at a higher velocity as a central core)

- (viii) Mist or spray flow (gas with liquid entrainment flowing in a pipe with wetted walls sometimes called 'fog flow')
- (ix) Pure gas

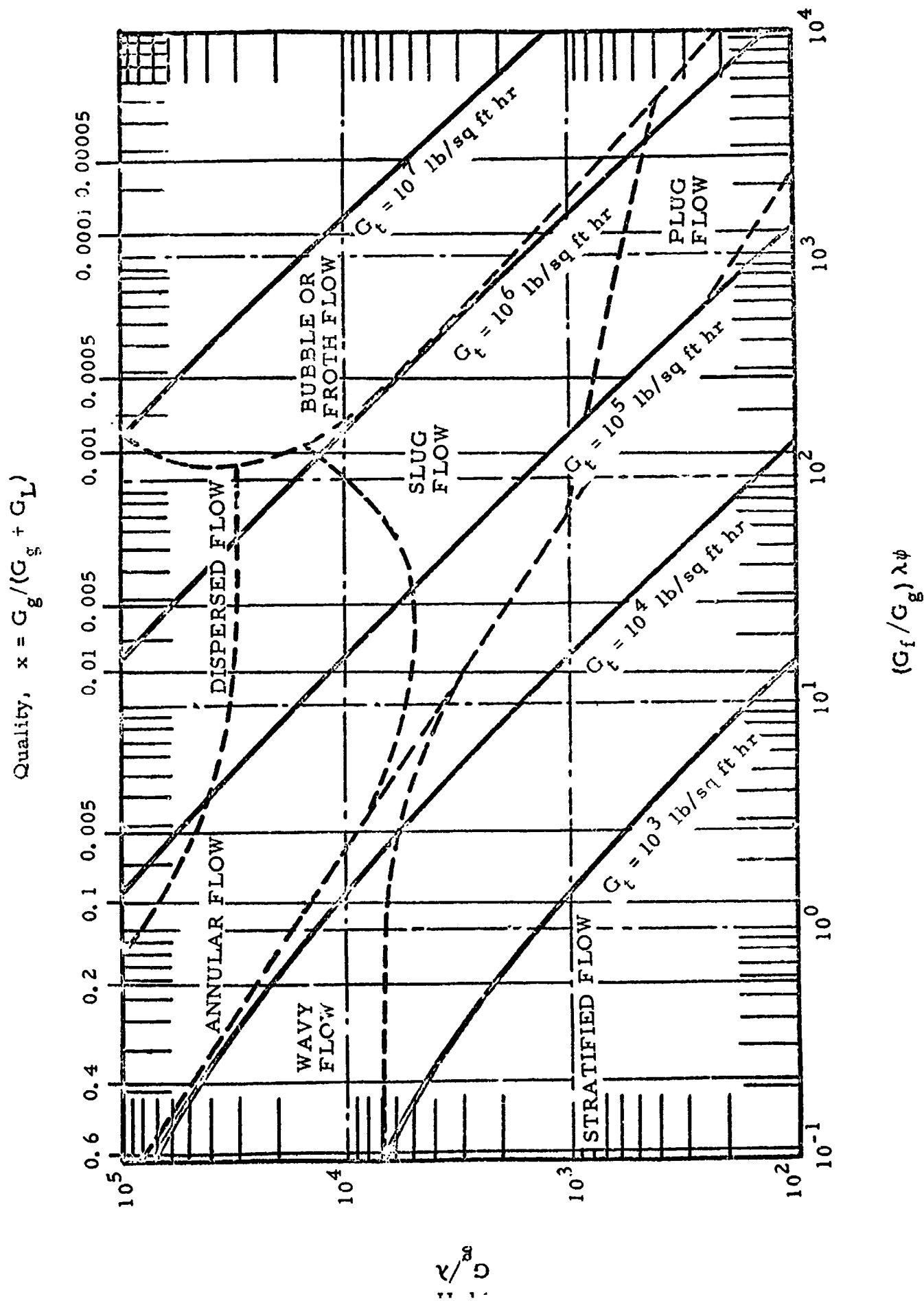
In a one component system in which boiling occurs the ratio of liquid to vapor changes with distance from the entrance of the pipe and therefore the flow patterns change. Given sufficient heat flux or length of pipe the whole spectrum of flow patterns listed above will exist until at sufficiently high qualities mist, fog, or spray flow develops.

Correlations of flow patterns in two phase flow have been presented in chart form by Baker,⁹ Krasiakova,¹⁰ and by Lunde.¹¹ Baker's chart was prepared specifically for the flow of two component oil and gas mixtures in oil pipe lines from the data of Jenkins,¹² Gazley,¹³ Alves,⁸ and Kosterin.¹⁴ Later the chart was used by Ishii et al¹⁵ for steam water mixtures, by Leonhard and McMordie¹⁶ for Freon 12 and by Bronson et al¹⁷ for liquid hydrogen. Fair agreement was noted between the types of flow observed and those predicted by the Baker chart.

The Baker chart has been used here for a study of the effect of the total mass flow rate and saturation temperature on the flow patterns of hydrogen for isothermal flow at the saturation condition. The results are presented in Figs. H-2 to H-5. The ordinate G_g/λ and $(G_f/G_g)\lambda\psi$ were used by Baker following a suggestion by Holmes¹⁸ where λ and ψ were defined as follows:

$$\lambda = \left[(\rho_g/0.075)(\rho_f/62.5) \right]^{1/2} \quad (H-6)$$

and



$$(G_f / G_g) \lambda \psi$$

Fig. H-2 FLOW REGIMES FOR HYDROGEN AT DIFFERENT RATES OF FLOW
AND AT THE SATURATION CONDITIONS OF 25°R

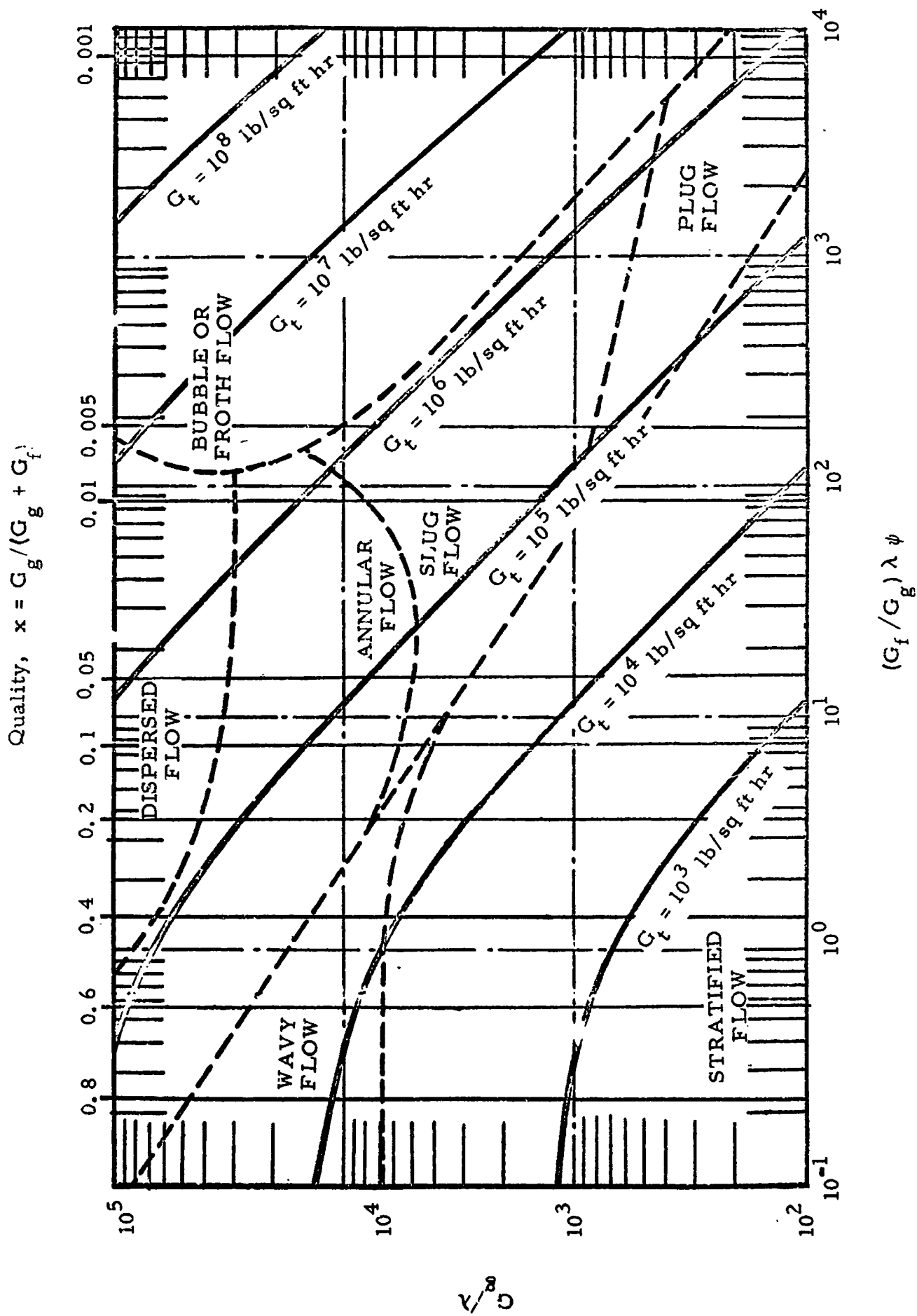


Fig. H-3 FLOW REGIMES FOR HYDROGEN AT DIFFERENT RATES OF FLOW
AND AT THE SATURATION CONDITIONS OF 54°R

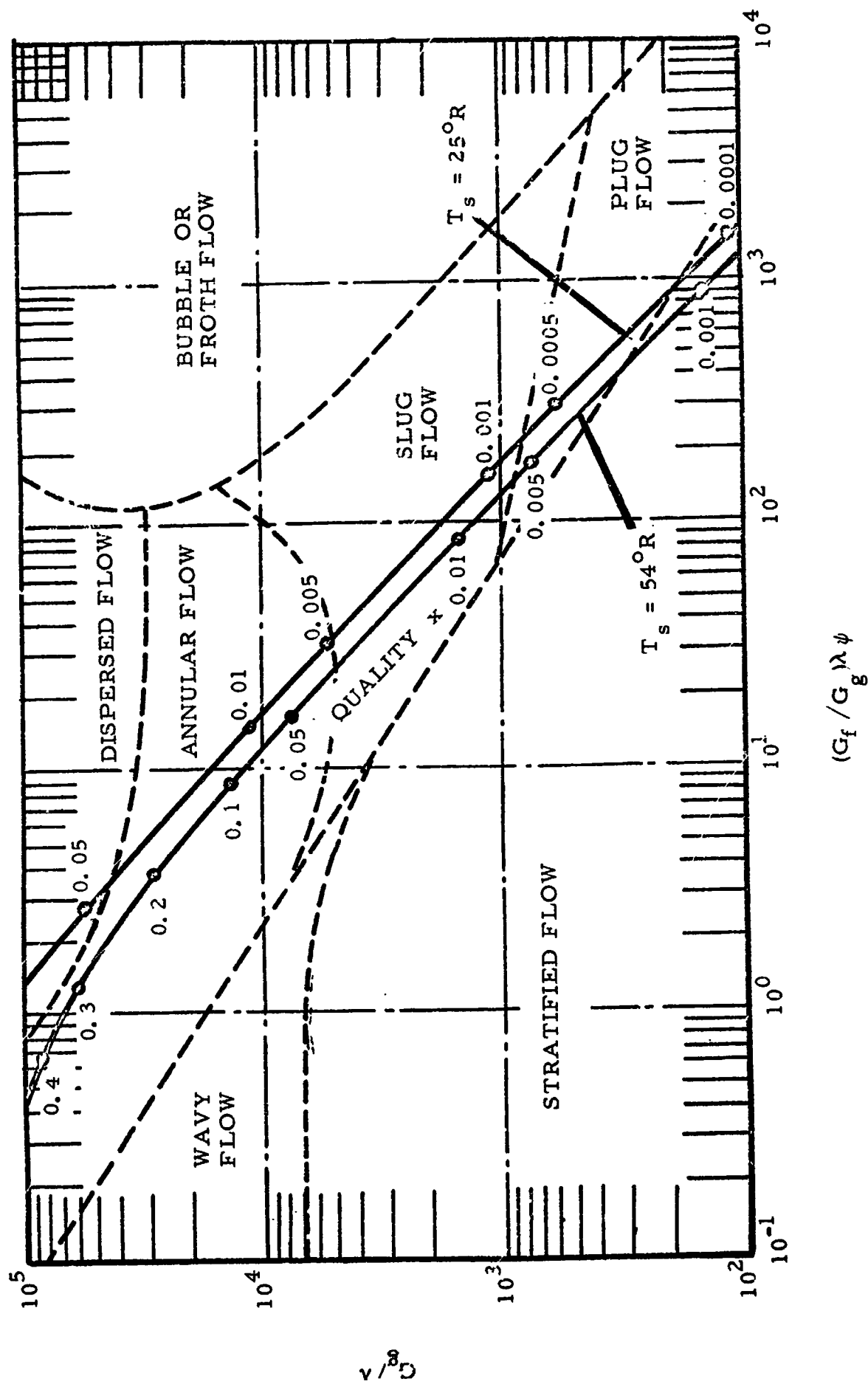


Fig. H-4 COMPARISON OF THE FLOW REGIMES OF HYDROGEN AT SATURATION
CONDITIONS OF $25^\circ R$ AND $54^\circ R$

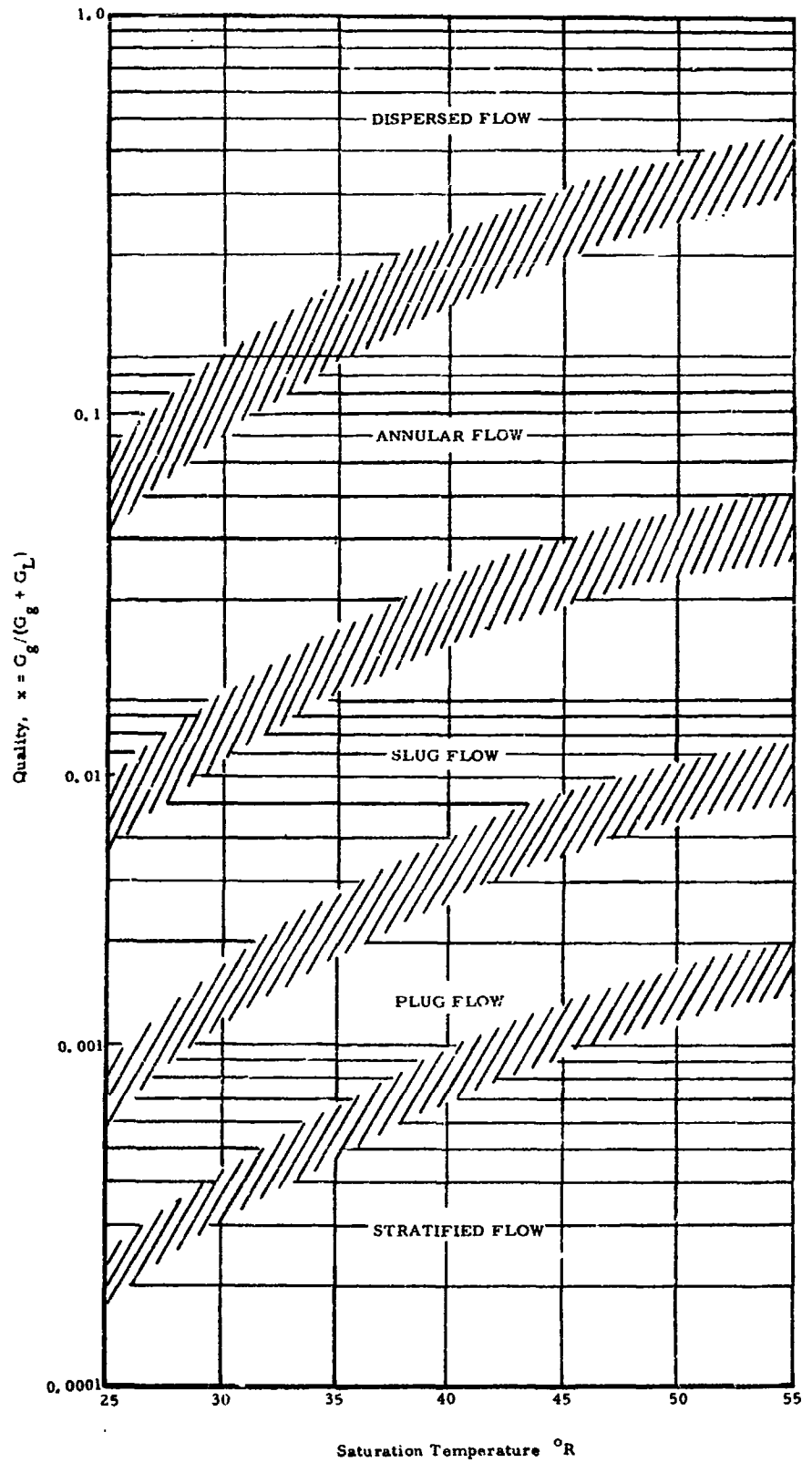


Fig. H-5 POSSIBLE FLOW REGIMES OF LIQUID HYDROGEN AS A FUNCTION OF THE QUALITY AND SATURATION TEMPERATURE MASS FLOW RATE = 10^5 LB/SQ FT HR

$$\psi = (73/V) \mu_f (62.5/\rho_f)^2^{1/3} \quad (H-7)$$

In Fig. H-2 a series of curves are presented for hydrogen flow rates ranging from 10^2 to 10^7 lb ft⁻² hr⁻¹. The quality of the mixture, defined as $G_g/(G_g + G_f)$ is shown at the principal points. The curves ascend from right to left, that is as the mass of fluid in the vapor phase increases. The transition of the flow patterns is clearly shown. The eventual change to the dispersed or fog flow occurs at different values of the quality depending on the flow rate. Figure H-2 was prepared for flow at the saturation conditions corresponding to 25°R and Fig. H-3 for saturation conditions at 54°R. In Fig. H-4 the two curves for the 100,000 lb ft⁻² hr⁻¹ flow rate at temperatures of 25°R and 54°R are compared. Although closely adjacent and parallel for most of their length there is a considerable difference in the location of specific values of the quality as shown. From this diagram and other similar plots for different saturation conditions, Fig. H-5 was prepared. This shows the effect of quality and saturation temperature on flow pattern for a total mass flow rate of 100,000 lb ft⁻² hr⁻¹. One important result which should be noted is the relatively low quality at which the hydrogen assumes the dispersed flow regime.

Other diagrams for different rates of mass flow may be prepared. The shapes of the curves obtained are similar but their location is different as might be expected from Figs. H-2 and H-3.

At present there is insufficient experimental data to confirm or deny the validity of the use of Baker's chart for such predictions.

c) Critical Mass Flow

When the flow at the discharge of a constant area or converging area device is such that a reduction in the downstream pressure will not increase the mass rate of flow the condition is referred to as choked, critical, or mass limiting flow. It can occur in every fluid regarded as a compressible fluid.

Critical mass flow for the pure gas phase is well understood and theoretical solutions for some ideal flow cases do exist. Recently (1963) Smith¹⁹ has prepared a choking two-phase flow literature summary and he supplemented this with design charts for a number of cryogenic and other fluids. The idealized solutions provide upper and lower limits for actual flow cases and reasonable agreement with experimental results may be observed.

d) Two Phase Heat Transfer

Two phase heat transfer processes are not well understood. The subject was reviewed by Collier²⁰ and since then other publications have become available. Various methods and correlations have been proposed for predicting the heat transfer rates. Rohsenow²¹ proposed a super-position method considering the heat flux to be made up of a boiling flux and a convective flux. In other cases, the use of pool boiling equations above have been proposed. It has become clear however that in fact several modes of heat transfer prevail as progressive vaporization takes place along a duct. A typical characteristic of the local evaporating heat transfer coefficient versus exit quality for several mass flow rates is shown in Fig. H-6. Zuber and Fried¹ have described the three regions thought to prevail:

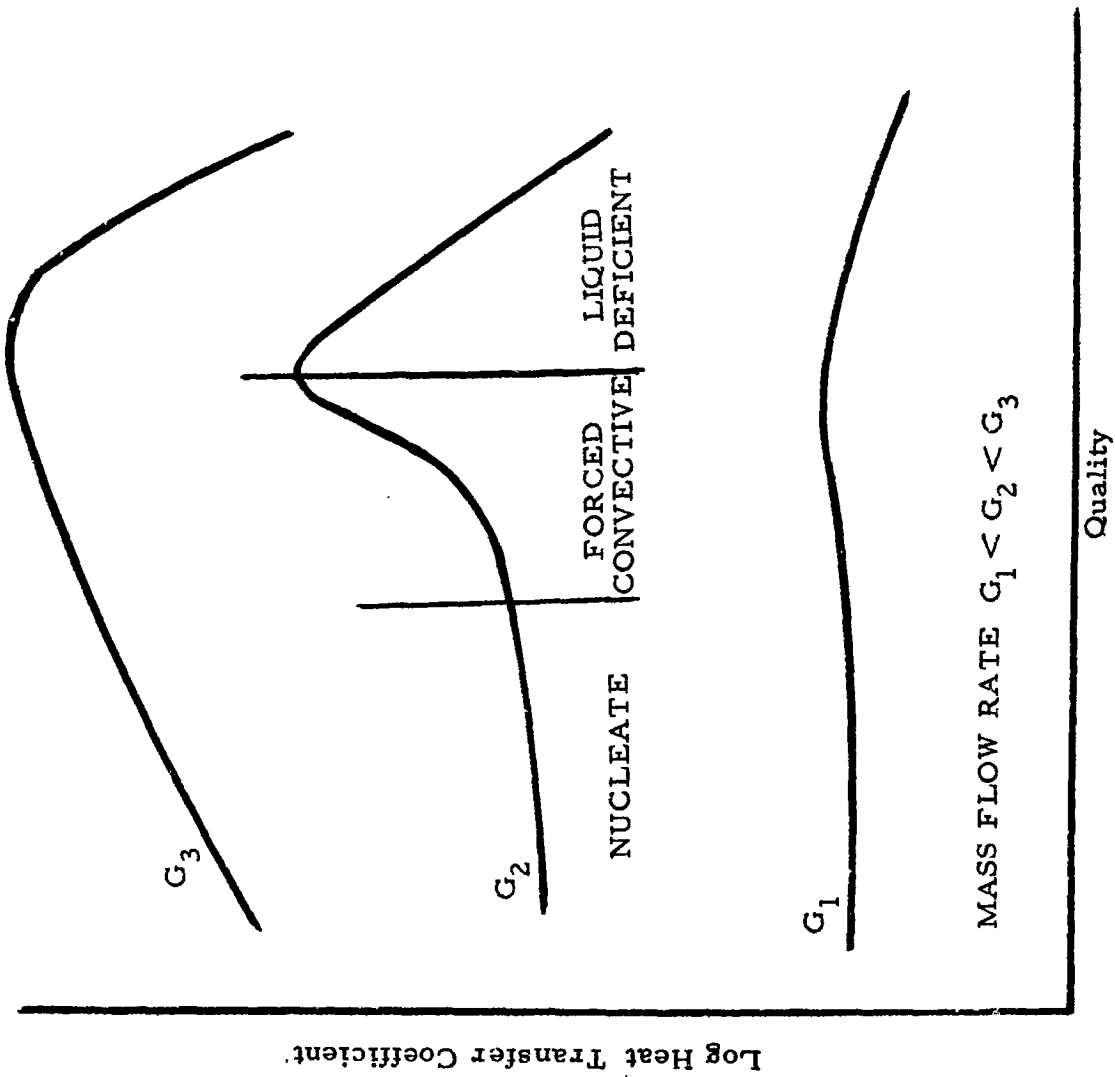


Fig. H-6 TYPICAL ONE COMPONENT TWO PHASE FLOW

"Region 1 is the nucleate boiling region in which the heat transfer coefficient is independent of quality. In this region, the vapor formation occurs at the heating surface in the form of bubbles that grow, detach and subsequently become dispersed in the flowing liquid. It is thought that in this region the heat transfer is governed by the mechanism of nucleate boiling.

Region 2 is the forced convective region in which the heat transfer coefficient increases with quality. As the quality increases along the duct, the increased velocity of the two-phase mixture induced by the vaporization process suppresses the nucleate boiling process, and beyond this point the heat transfer becomes governed by the forced convection process. The actual flow pattern of the two-phase mixture is not known. Some researchers believe that only a liquid film is in contact with the solid surface. Others believe that the liquid is in the dispersed phase that is continuously being deposited and re-entrained from the heating surface.

Region 3 is the liquid deficient region in which the heat transfer coefficient decreases with increasing quality. In this region, the liquid film no longer wets the surface. The heat transfer is no longer due to a highly conducting liquid film but to a poorly conducting gas as a consequence of which the heat transfer coefficient sharply decreases."

For correlating data in Region 1, equations have been used which were originally proposed for nucleate pool boiling, including the equation of Rohsenow quoted above.

Sterman et al²² correlated data for water and ethanol using a relation of the form:

$$\frac{(N_{Nu})_{TP}}{(N_{Nu})_{SPL}} = 6150 \left[\frac{\dot{Q}/A}{\rho_g H_{fg} \mu_f} \left(\frac{\rho_g}{\rho_f} \right)^{1.45} \left(\frac{H_{fg}}{C_p T_s} \right)^{1/3} \right]^{0.7} \quad (H-8)$$

where the single phase Nusselt modulus was based on liquid properties and the two phase Nusselt modulus was given by:

$$(N_{Nu})_{TP} = \frac{h_{TP}}{k_f} \left[\frac{\sigma}{g (\rho_f - \rho_g)} \right]^{1/2} \quad (H-9)$$

In Region 2 most correlations are based on the Lockhart-Martinelli⁷ parameter X_{tt} defined by

$$\frac{1}{X_{tt}} = \left(\frac{x}{1-x} \right)^{0.9} \left(\frac{\rho_f}{\rho_g} \right)^{0.5} \left(\frac{\mu_g}{\mu_f} \right)^{0.1} \quad (H-10)$$

and are of the form

$$\frac{h_{TP}}{h_{SPL}} = \text{const} \left(\frac{1}{X_{tt}} \right)^m \quad (H-11)$$

Wide variation in the value of the constant and the index 'm' have been reported and no reliable method of prediction is available. Experimental boiling heat transfer coefficients for hydrogen have been reported by Mulford et al,²³ Class et al,²⁴ Malkov et al,²⁵ Brickwedde,²⁶ Weil et al,²⁷ Drayer et al,²⁸ and by Graham et al.²⁹ There were considerable differences in the experimental conditions and apparatus used so that a general correlation of these results is not possible.

Parker and Grosh³⁰ in a study of the heat transfer to a mist flow of steam measured very high heat transfer coefficients for annular-mist

flow. At higher qualities the coefficients decreased with a diminution of the liquid film. At a critical value of the tube wall temperature a drastic reduction in the heat transfer coefficient was observed probably due to the onset of the liquid deficiency described above.

There is therefore a vital need for much further basic research on heat transfer effects in two phase flow. Measurements are required of the local values of heat transfer coefficients, quality and differential phase velocities. Further studies of the flow patterns in two-phase flow are required. Some effort should be made to assess the significance of the physical characteristics of the fluid, the conditions of the surface, the flow rate and the heat flux in determining the points at which the flow patterns change. In other words, it is essential to the general understanding of two-phase flow that suitable criteria be established to allow accurate identification and prediction of the flow regimes.

REFERENCES

- H-1 Zuber, N. and E. Fried, "Two-Phase Flow and Boiling Heat Transfer to Cryogenic Liquids", A.R.S. Journal, p. 1332, 1962.
- H-2 Rohsenow, W., "A Method of Correlating Heat Transfer for Surface Boiling of Liquids", Trans. A.S.M.E., Vol. 74, p. 969, 1952.
- H-3 Labountzov, D.A., "Generalized Correlation for Nucleate Boiling", Teploenergetika, Vol. 7, No. 5, p. 76, 1960.
- H-4 Nukiyama, S., J. Soc. Mech Eng (Japan), 37, p. 367, 1934.
- H-5 Jakob, M., "Heat Transfer", J. Wiley and Sons, p. 622, 1949.
- H-6 Kezios, S.P., Private Communication, IIT Heat Transfer Laboratory, 1963.
- H-7 a) Martinelli, R.C., L.M. Boelter, T.H. Taylor, E.G. Thomsen, and E.H. Morrin, "Isothermal Pressure Drop for Two Phase Two Component Flow in a Horizontal Pipe," Trans. A.S.M.E. Vol. 66, No. 2, p. 139, 1944.
- b) Martinelli, R.C., J.A. Putnam, and R.W. Lockhart, "Two Phase Two Component Flow in the Viscous Region", Ibid. Vol. 42, p. 681, 1946.
- H-8 Alves, G.F., "Co-Current Liquid-Gas Flow in a Pipeline Contractor", A.I.Ch.E., 1953.
- H-9 Baker, O., "Simultaneous Flow of Oil and Gas", Oil and Gas Journal, Vol. 53, p. 185, 1954.
- H-10 Krasiakova, L.I., Zhurnal Technicheskoi Fiziki, Vol. 24, p. 2285, 1954.
- H-11 Lunde, K.E., "Heat Transfer and Pressure Drop in Two Phase Flow", Chem. Eng. Prog. Symp. Series, Vol. 57, No. 32, p. 104, 1958.
- H-12 Jenkins, R., "Two Phase Two Component Flow of Air and Water", M.Sc. Thesis, Univ. of Delaware, 1947.
- H-13 Gazley, C., "Co-Current Gas Liquid Flow III. Interfacial Shear and Stability", Ht. Trans. and Fl. Mechs. Inst., Berkeley, Calif., 1949.

- H-14 Kosterin, S., "An Investigation of the Influence of the Diameter and Inclination of a Tube on the Hydraulic Resistance and Flow Structure of Gas-Liquid Mixtures", *Izvest. Akad. Nauk, SSSR. Otdel Tekh Nauk*, No. 12, 1949.
- H-15 Isbin, H.S., H. R. Moen, R.O. Wickey, D.R. Mosher, and H.C. Larson, "Two Phase Steam Water Pressure Drops", *A. I. Chem. Eng. Conf.*, Chicago, 1958.
- H-16 Leonhard, K.E., and R.K. McMordie, "The Non-Adiabatic Flow of an Evaporating Cryogenic Fluid through a Horizontal Tube", *Adv. in Cryogenic Eng.*, Vol. 6, p. 481, 1961.
- H-17 Bronson, J.C., F.J. Edeskuty, J.H. Fretwett, E.F. Hammel, W.E. Keller, K.L. Meier, A.F. Schuck, and W.L. Willis, "Problems in the Cool-down of Cryogenic Equipment", *Adv. in Cryogenic Eng.*, Vol. 7, p. 138, 1962.
- H-18 Holmes, K., "Flooding Velocities in Empty Vertical Tubes", *Perrys Chem. Eng. Handbook*, 3rd Ed., McGraw-Hill, p. 686.
- H-19 Smith, R.V., "Choking Two Phase Flow Literature Summary and Idealized Design Solutions for Hydrogen, Nitrogen, Oxygen, and Refrigerants 12 and 11", *Nat. Bur. Stands. Tech. Note*, No. 179, 1963.
- H-20 Collier, J.G., "A Review of Two Phase Heat Transfer (1935-1957)", *A.E.R.E., CE/R 2496*, Harwell, England, 1958.
- H-21 Rohsenow, W., "Heat Transfer with Evaporation", *Chem. Eng. Prog. Symp. Series*, p. 101, 1952.
- H-22 a) Stermann, L.A., "Investigation of Heat Transfer to Liquids Boiling Inside Pipes", *Zhur, Tekh. Fiz.*, Vol. 24, p. 2047, 1954.
- b) Stermann, L.S., V.G. Morozov, and S.A. Kovalev, "Investigation of Heat Transfer to Water and Ethanol Boiling Inside Pipes", *Inzh. Fiz. Zhur*, Vol. 2, No. 10, p. 40, 1959.
- H-23 Mulford, R.N., J. Nigon, J. Dash, and W. Keller, "Heat Exchange Between a Copper Surface and Liquid Hydrogen and Nitrogen", *A.E.C. Rept. L.A.*, -1416, 1962.
- H-24 Class, C.R., J.R. DeHaan, M. Piccone, and R.B. Cost, "Boiling Heat Transfer to Liquid Hydrogen from a Flat Surface", *Adv. in Cryogenic Eng.*, Vol. 5, p. 254, 1960.
- H-25 Malkov, M.P., A.G. Zeldovitch, A.B. Fradkov, and I.B. Danilov, 2nd U.N. Conf. on Peaceful Uses of Atomic Energy, Vol. 4, p. 491, 1958 Proc.

- H-26 Brickwedde, F.G., "Production of Heavy Water" (ed. Maloney, J.O., G.F. Quinn, and H.S. Ray), McGraw-Hill, New York, p. 91, 1955.
- H-27 Weil, L. and A. Lacase, "Procès-Verbaux et Résumés des Communications", Société Française de Physique, No. 9, p. 890, 1951.
- H-28 Drayer, D.E., and K.D. Timmerhaus, Adv. in Cryogenic Eng., Vol. 7, p. 401, 1962.
- H-29 Graham, R.W., R.C. Hendricks, Y. Y. Hsu, and R. Friedman, Adv. in Cryogenic Eng., Vol. 6, p. 517, 1961.
- H-30 Parker, J.D., and R.J. Grosh, "Heat Transfer to a Mist Flow", Argonne Nat. Lab., AEC Rand D Rept. ANL-6291, 1961.